



UNIVERSITAT POLITÈCNICA
DE CATALUNYA
BARCELONATECH



MASTER THESIS

Balloons as a tool for Mars exploration

David Rodellar Barranco

SUPERVISED BY

Enric Pastor Llorens

Universitat Politècnica de Catalunya
Master in Aerospace Science & Technology

November 2015

Balloons as a tool for Mars exploration

BY

David Rodellar Barranco

DIPLOMA THESIS FOR DEGREE

Master in Aerospace Science and Technology

AT

Universitat Politècnica de Catalunya

SUPERVISED BY:

Enric Pastor Llorens

Arquitectura de Computadors

ABSTRACT

The last Mars exploration missions, such as Curiosity, Opportunity and Spirit by NASA have proved that autonomous vehicles are suited for Mars surface exploration and are becoming an important part of it. These mobile laboratories are designed to navigate autonomously using the information provided by the on-board sensors to find the best path to achieve the desired destination. Considering the limited lifetime of these vehicles, increasing their mobility and improving the information of the terrain around them can help to increase their scientific performance, being the use of balloons capable to lift instruments into the Mars atmosphere one of the possible solutions.

Despite satellite images of Mars surface have improved their quality since the arrival to the planet orbit of the Mars Reconnaissance Orbiter with the High Resolution Imaging Science Experiment instrument, the information available is not enough to decide the path of the mobile laboratories and therefore they are equipped with sensors which allows them to compute the optimal path. However, those sensors are limited by the line of view available from their positions, which limit the information they gather usually to the immediate terrain, not allowing a full path optimization, and missing possible interesting spots if they are not in the line of sight.

The mobility of the rovers is based on wheels, which can suffer damage due to the terrain they are rolling over or can become stuck as it happened with MER-A, being critical to know the characteristics of the terrain they move over. Even with careful planning, there are zones that being scientifically relevant are unreachable due to the limitations of this type locomotion.

This Master thesis will try to study the opportunities that balloons can provide in the Martian exploration, focusing on improving the image acquisition methods to help the navigation and studying the viability of using balloons for other tasks.

The main objectives of this work are to study the viability of using balloons on Mars, consider the benefits they will suppose in scientific missions and consider the interaction with other elements as for example a home base or a rover. To fulfill this objectives part of the existing literature on the matter will be reviewed and complemented with additional information, and calculations will be performed to corroborate the viability of balloons usage in Mars atmosphere. Finally, a mission proposal will be drafted to expose part of the possibilities of a balloon mission to Mars.

Table of Contents

INTRODUCTION	1
CHAPTER 1 MARS	5
1.1. The planet.....	5
1.2. The surface.....	6
1.3. The atmosphere.....	7
1.3.1. Atmospheric model	8
CHAPTER 2 BALLOONS	11
2.1. General characteristics.....	11
2.2. Types of balloons	11
2.2.1. Hot air balloon	12
2.2.2. Gas Balloon	12
2.2.3. Rozière balloon	12
2.3. Balloon movement.....	13
2.4. Suitable balloons for Mars.....	13
2.4.1. Zero pressure gas balloon.....	13
2.4.2. Super-pressure balloon.....	14
2.4.3. Solar heated balloons	14
CHAPTER 3 INITIAL STUDY OF A BALLOON MISSION TO MARS.....	17
3.1. Mission basics	17
3.1.1. Balloon	18
3.1.2. Deployment.....	19
3.2. Payload.....	19
3.2.1. Energy system	19
3.2.1.1. Autonomous energy sources	19

3.2.1.2. Tethered energy sources	22
3.2.2. Communications, telemetry, data handling and processing systems.....	23
3.2.3. Navigation and attitude control systems	23
3.2.4. Thermal control systems	24
3.2.5. Structure	24
3.2.6. Scientific instruments	25
3.2.6.1. Cameras	25
3.2.6.2. Magnetometer	26
3.2.6.3. Seismic sensors	26
3.2.6.4. Atmospheric sensors	26
3.2.6.5. Subsurface sounding	26
3.2.7. Ground sector	27
CHAPTER 4 PROPOSAL OF A PIGGYBACK BALLOON MISSION	29
4.1. Basket	30
4.1.1. Scientific payload	30
4.1.1.1. Cameras	30
4.1.1.2. Atmospheric sensors	34
4.1.1.3. Magnetometers	38
4.1.2. Systems Payload.....	38
4.1.2.1. Attitude system.....	38
4.1.2.2. Data handling, processing and telemetry	40
4.1.2.3. Communication system.....	41
4.1.2.4. Thermal control	42
4.1.2.5. Energy system	42
4.1.3. Structure design	44
4.2. Tether cable.....	52
4.3. Balloon	52

4.3.1. Balloon dimensions.....	53
4.4. Rover equipment	60
4.5. Deployment	61
4.6. Mission Operation	61
4.7. Balloon lifespan.....	63
CHAPTER 5 FURTHER DEVELOPMENTS.....	67
CHAPTER 6 CONCLUSIONS	69
CHAPTER 7 REFERENCES	71
ANNEX I: ATMOSPHERIC MODEL VALUES	79
ANNEX II: MARS SOLAR FLUX	81
ANNEX III: BALLOON BUOYANCY	85
ANNEX IV: BALLOON LIFESPAN	91

List of Figures

Figure Introduction 0-1 Relation of missions to Mars according to their configuration and their success [1]..... 1

Figure Introduction 0-2 Models of rovers for Mars exploration: (a) Prop-M rover, (b) Sojourner, MER and MSL rover and (c) ExoMars rover..... 2

Figure Introduction 0-3 (a) Ares Martian airplane, (b) Magnus; a proposed balloon for Mars and (c), an helicopter proposed to scout the path of the NASA 2020's rover. 3

Figure 1-1 Composite image created by NASA to ease the size comparison between Earth and Mars..... 5

Figure 1-2 Artistic representation of the Earth global magnetic field and the local remnants magnetic fields in Mars [78]. 6

Figure 1-3 “McMurdo” Mars Panorama taken by NASA’s Mars Exploration Rover Spirit. 6

Figure 1-4 Topographic map obtained from the data of the Mars Global Surveyor IAS altimeter by Maria Zuber [79]. 7

Figure 1-5 Pressure (a) and temperature (b) values measured by Curiosity’s REMS instrument at landing site [9]. 8

Figure 1-6 Part of REMS instrument during its preparation on Earth (a) and once in Mars (b). 8

Figure 1-7 Temperature values obtained with the atmospheric model. 9

Figure 1-8 Pressure values obtained with the atmospheric model. 10

Figure 1-9 Density values obtained with the atmospheric model..... 10

Figure 2-1 Diagram of the forces in a balloon accordingly to equation 2.1..... 11

Figure 2-2 (a) Hot air balloon, (b) gas balloon and (c) Rozière balloon. 12

Figure 2-3 Super-pressure pumpkin balloon during a test on ground [15]. 14

Figure 2-4 Solar heated balloon on Earth..... 15

Figure 3-1 Super-pressure pumpkin balloon during a successful flight test on Earth [80]. 18

Figure 3-2 Maximum solar flux in Wh/m² in Mars surface during an orbital period. 20

Figure 3-3 Mean solar flux per day in Mars upper atmosphere during an orbit [10].	21
Figure 3-4 Variation of the solar flux in a 20° latitude position in Mars during a sol for different orbital positions.	21
Figure 3-5 Prototype of POF by Lasermotive [32] powering a quadcopter.	22
Figure 4-1 MSL HAZCAM and NAVCAM during preparation (left 2 HAZCAM, right 2 NAVCAM).	30
Figure 4-2 Baseline configuration of the Exomars PanCam [38].	31
Figure 4-3 Representation of the PanCam mounted on ExoMars [54].	32
Figure 4-4 REMS sensors on the Curiosity mast.	34
Figure 4-5 DREAMS instrument for the ExoMars 2016 mission [57].	34
Figure 4-6 Design details and operational principle of the Hot-wire anemometer.	35
Figure 4-7 Relative Humidity Sensor before being placed in the boom.	36
Figure 4-8 Pressure Sensor, the intake of atmosphere is the white pipe.	37
Figure 4-9 Sun sensor from Sinclair Interplanetary.	39
Figure 4-10 QRS11 MEMS gyroscope.	40
Figure 4-11 Information flow diagram considered for this proposal.	41
Figure 4-12 Energy system scheme.	42
Figure 4-13 Bottom view of the design proposed for the basket, with most of the scientific instruments in sight.	44
Figure 4-14 Representation of the basket with a simplified model of the NASA Curiosity rover and a human figure to provide a scale.	45
Figure 4-15 Bottom half of the basket with the instruments in storage position (superior image) and in deployed position (lower image).	45
Figure 4-16 Upper view of the interior of the basket with the disposition of the electronics and sensor calculated to maintain equilibrium.	46
Figure 4-17 View from below of the basket with the instruments located on it.	46
Figure 4-18 Upper, lower and side views of the basket.	47
Figure 4-19 Upper, lower and side views of the basket with the hidden elements represented by dashed lines.	48

Figure 4-20 Horizontal (a) and vertical (b) simplified field of view of the panoramic cameras.	49
Figure 4-21 Detail (a) and general view (b) of the panoramic cameras FOV. The delimited zone is the terrain covered, and the coloured zones without limits correspond to the over the horizon FOV.	49
Figure 4-22 Sun sensor vertical FOV (a) and 3d representation of the Sun Sensor sky coverage (b).....	50
Figure 4-23 Detail of the camera with the ring of filters, the magnification system and the two axis gimbal support.	50
Figure 4-24 Union between the tether cable, the basket and the balloon.	51
Figure 4-25 Semi-axis distribution on a spheroid.	54
Figure 4-26 Mass distribution for a super-pressure balloon with a neutral buoyancy altitude of 500 m.	56
Figure 4-27 Mass distribution for a super-pressure balloon with a neutral buoyancy altitude of 750 m.	57
Figure 4-28 Detail of the mass and diameter for the values close to the obtained for the balloon here presented for 500 m (a) and 750 m (b).	57
Figure 4-29 Representation of the Deployed balloon with the basket and the NASA Curiosity rover and a human figure for scale.	59
Figure 4-30 Representation of the balloon and the basket floating in the Mars atmosphere.	62
Figure 4-31 Lift capabilities of the balloon and the lift necessary to keep the balloon floating (total mass lifted).	64
Figure 4-32 Pressure inside the balloon and atmospheric pressure during the balloon lifespan.	64
Figure 4-33 Balloon volume during its lifespan, notice the volume reduction once the gas in the interior reaches the atmospheric pressure.	65

List of tables

- Table 4.1 MSL HAZCAM specifications 32
- Table 4.2 MSL NAVCAM specifications. 33
- Table 4.3 ExoMars WAC specifications..... 33
- Table 4.4 ExoMars HRC specifications. 33
- Table 4.5 Wind sensor specifications. 35
- Table 4.6 Relative Humidity Sensor specifications..... 36
- Table 4.7 Pressure Sensor specifications. 37
- Table 4.8 MSMO specifications. 38
- Table 4.9 Solar Sensor specifications. 39
- Table 4.10 Solar Sensor specifications. 40
- Table 4.11 Approximate power consumption of the elements in the basket. 43
- Table 4.12 Basket structural elements mass..... 51
- Table 4.13 Mass approximation for the different elements in the basket and the basket itself.
..... 53
- Table 4.14 Main characteristics of the different elements of the balloon. 58
- Table 4.15 Free lift force at the moment of the balloon release..... 60
- Table 4.16 Free lift force at the operation altitude of the balloon. 60
- Table I.0.1 Values obtained using the atmospheric model in 1.3.1 and used for Figure 1.7,
Figure 1.8 and Figure 1.9. 79
- Table II.0.1 Values of solar flux at the Martian upper atmosphere during a day for different
orbital positions used in Figure 3.3. 82
- Table II.0.2 Values of maximum solar flux (Wh/m²) at Marts upper atmosphere in different
latitudes at different orbital moments used for in Figure 3.2. 83
- Table III.0.1 Balloon properties for a neutral buoyancy altitude of 750 m..... 87
- Table III.0.2 Balloon properties for a neutral buoyancy altitude of 500 m..... 89

Table IV.1 Lifespan calculations for the balloon. 93

INTRODUCTION

From the beginning of the space exploration Mars has drawn the attention of scientific and general public. These last years the interest for the planet has grown and enterprises both from space agencies and private initiatives are studying and developing methods to be the first ones to lead a manned mission to Mars. Before and after a human being makes the first step on the Mars surface, robotic missions will lead the way.

Since the arrival of man on the Moon, Mars has been seen as the next big challenge for a manned mission. To this day a total of 43 missions have been launched to study the planet, but only 18 have succeed on its main objective (two more missions are considered a partial failure as the lander included in the mission failed while the orbiter succeeds). While a rate of success below the 50% can be considered low the last missions seems to have changed the trend and 80% of the last 10 missions are considered a complete success. Among them one has proved that even a contained budget can provide successful results in a mission to the "Great Galactic Ghoul", the Indian Mars Orbiter Mission.

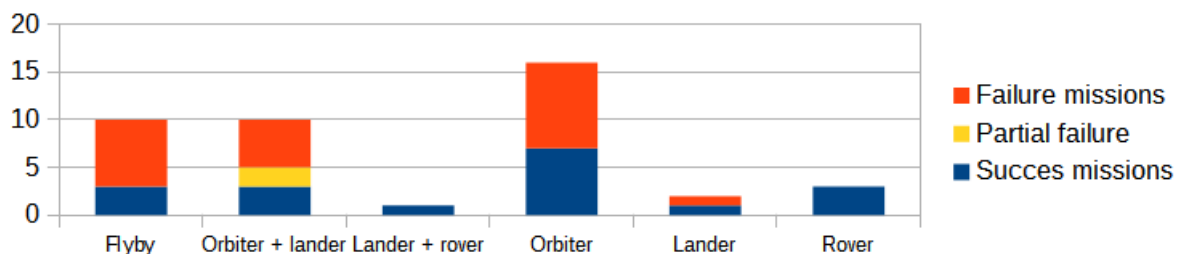


Figure Introduction 0-1 Relation of missions to Mars according to their configuration and their success [1].

Up to the present day the missions sent to study Mars can be classified into three main groups, flyby missions, orbiters and atmospheric missions (which include landers and rovers), being some missions a combination of different configurations (as for example orbiters and landers in the same mission). The first missions to Mars consisted on flybys due to the limitations existing on those days, nevertheless it was possible to obtain information about the Mars atmosphere and get the first close images from the planet. Ten years after the first successful mission a spacecraft achieved to orbit the planet but failed to deploy the lander that travelled with it, similar to what happened to its sister ship months later (MARS 2 and MARS 3). It was four years after the first spacecraft orbiting the planet that a lander achieved to perform its scientific mission on the planet surface (the Viking 1 lander) and it took 21 years after that until the first mobile laboratory rolled over the Mars surface, the Mars Pathfinder rover [1].

In 2015 there are seven active missions in Mars, five orbiters and two rovers, being one of them an impressive achievement in space exploration as it has overwhelmingly surpass its expected capabilities. Each type of mission has its pros and cons, and are

designed according to them. For example, orbiters can obtain information from any place in the planet, but the level of detail is limited to the sensibility and capabilities of the sensors used, while a lander can obtain very precise information about a specific location without providing a context information of the surrounding areas. Likewise, the rovers might be able to obtain the same level of detail of a lander while being able to move and therefore study an area and not just a spot, but the complexity of all the systems involved is increased, as well as the cost to develop and manufacture it.

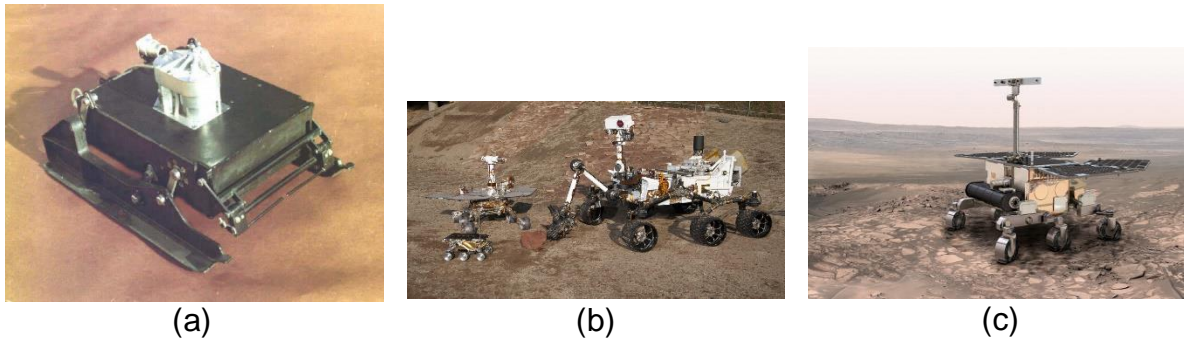


Figure Introduction 0-2 Models of rovers for Mars exploration: (a) Prop-M rover, (b) Sojourner, MER and MSL rover and (c) ExoMars rover.

Since the first missions to the surface of other celestial bodies, space agencies have tried to provide mobility to the scientific instruments to increase the range of locations studied but in the case of the Mars surface has been only recently when this has been achieved. The complexity of the rovers sent to Mars have made them capable to gather a lot of scientific information and in some cases exceed amazingly their live expectancy in more than 3500% [2][3]. The success of this probe configuration to study great areas of a planet surface has occasioned the development of other rovers, such as the ESA ExoMars rover [4] or the NASA 2020 rover, expected to be launched in the near future.

Like other vehicles, rovers have limitations and there are some scientific missions that might be performed better by other type of vehicles. From studying the atmosphere, gathering information of wide areas or even visiting places of difficult access, aerial vehicles can become a good platform to study Mars.

The use of aerial vehicles on Mars have been proposed several times, and from small helicopters to scout the terrain ahead [5] of a rover to a full aerial vehicle such as the ARES proposal [6]. The use of balloons (in the form of aerostats) for this kind of mission provides certain benefits over the other options, as it is not necessary to use part of the energy just to stay in the air. The energy consumption used to move this type of airship is lower, and the probability to damage the payload due to a hard landing is small if no catastrophic fail occurs, it has however drawbacks as well, as for example the limitation on the weight they are able to carry on Mars. Several uses have been considered for balloons on Mars, from using balloons instead of parachutes for soft-landing probes to using the atmospheric circulating patterns to study large areas of the planet [7]. But Mars has proven not an easy target for space missions and therefore

sending a mission based in a configuration not proven yet in the destination might not be the best approach.

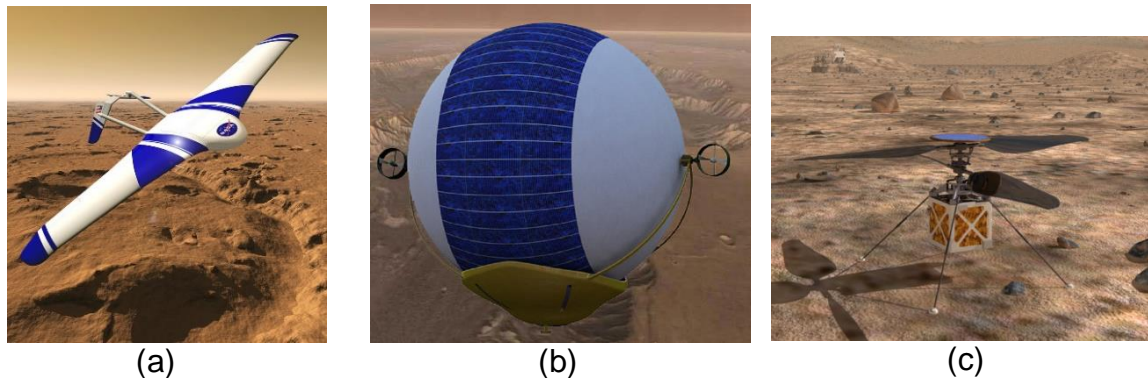


Figure Introduction 0-3 (a) Ares Martian airplane, (b) Magnus; a proposed balloon for Mars and (c), an helicopter proposed to scout the path of the NASA 2020's rover.

The information used by the Martian rovers to navigate through the surface comes either from the rover own sensors or the information gathered by the satellites orbiting the planet. Despite the great improvements in the information the satellites are capable to obtain is not enough accurate to base entirely the rover navigation on it, but it is used to decide future goals for the rover. Rovers use cameras located strategically on their surface to study the terrain and obtain information of their surroundings. The main navigation cameras are located in a mast as it is the highest point in the rover structure and it allows to see further away and collect more information thanks to its position. Despite being the best place in the rover to do so the information gathered might not be enough accurate as terrain elevations or rocks could hide behind them information of areas that could be important for the rover, being interesting places to study or dangerous zones that could force to recalculate the planned route of the rover.

Nowadays this situation is not as important as it could be in the future, as the areas where the rovers land are relatively flat, but in the future when the rovers design allow them to enter into more difficult locations developments aimed to help them in this situations could prove of great help as a more concise knowledge of the surroundings will be necessary. A possible solution for this situation is to elevate the observation point of the navigation cameras, and to do so using a tethered balloon as a platform to situate those cameras is a possible approach, helping locate interesting locations not seen from ground level, avoid dangerous zones and collect information impossible to obtain from the ground.

Sending a tethered balloon as a piggyback mission in one of the future rovers will not only help to fulfil the rover main mission more efficiently and increase the scientific return of the rover mission but help test the technologies involved in the use of balloons in Mars. Allowing in the future successful balloon standalone missions with a smaller risk as the technologies will be already tested and lower cost, as several developments in this kind of piggy back mission could help to reduce the cost of bigger missions.

Chapter 1

MARS

1.1. The planet

Mars is the fourth planet in the solar system, located between Earth and Jupiter (with the asteroid belt located between this last one and Mars), has a mean distance to the sun of 1.5 Astronomical Units and has two moons of small diameter: Phobos and Deimos. It has a day length of 24 hours and 37 minutes (period of time named sol) and a year of 687 Earth days long and due to the eccentricity of the orbit the length of some of the seasons is proportionally longer than the equivalent on Earth. The rotational axis of the planet forms an angle of 25.19° with the orbital plane, almost identical to the inclination of Earth. The radius of the planet is 3396 km (approximately half the Earth radius), and it's about 71% as dense as Earth, being the gravity on the surface of 3.711 m/s^2 . Despite the studies performed it is not yet certain if the internal structure Mars is similar to the one existing on Earth or it differs being solid or liquid.



Figure 1-1 Composite image created by NASA to ease the size comparison between Earth and Mars.

1.2. The surface

The inexistence of a global magnetic field comparable to the one existing on Earth and the atmospheric properties provoke that an important part of the radiation that Earth is shielded against arrives to Mars surface. This is an important constrain in the design on the space mission to operate in the planet surface, as for example the materials must be resistant or be coated against the UV degradation, and the electronics must be capable to work in an environment with elevated levels of cosmic radiation, among other design constrains.

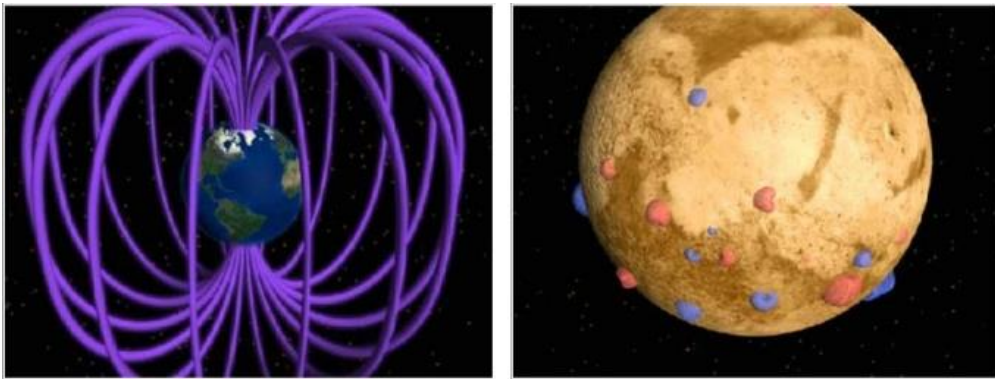


Figure 1-2 Artistic representation of the Earth global magnetic field and the local remnant magnetic fields in Mars [80].

The Mars surface is considered to consist mostly in basalt, covered by a layer of iron oxide dust, with icecaps in the poles formed by the deposition of slabs of CO₂ ice. It has been considered that in the rockiest zones on Mars 1% of the surface is covered in rocks of at least 0.5 m high [8]. The topography of Mars contains basically mountains, canyons, volcanoes, dry lakes and craters, with the highest point at Olympus Mons, and the lowest point located at the bottom of the Hellas impact basin, with a difference of almost 30 km of height.



Figure 1-3 “McMurdo” Mars Panorama taken by NASA’s Mars Exploration Rover Spirit.

There is a big difference between the northern and the southern hemisphere, being the northern hemisphere characterized by plains flattened as results of the lava flow from the existing volcanoes, while the southern higher mean altitude has preserved the remaining craters from ancient impacts on the surface and other old geological structures.

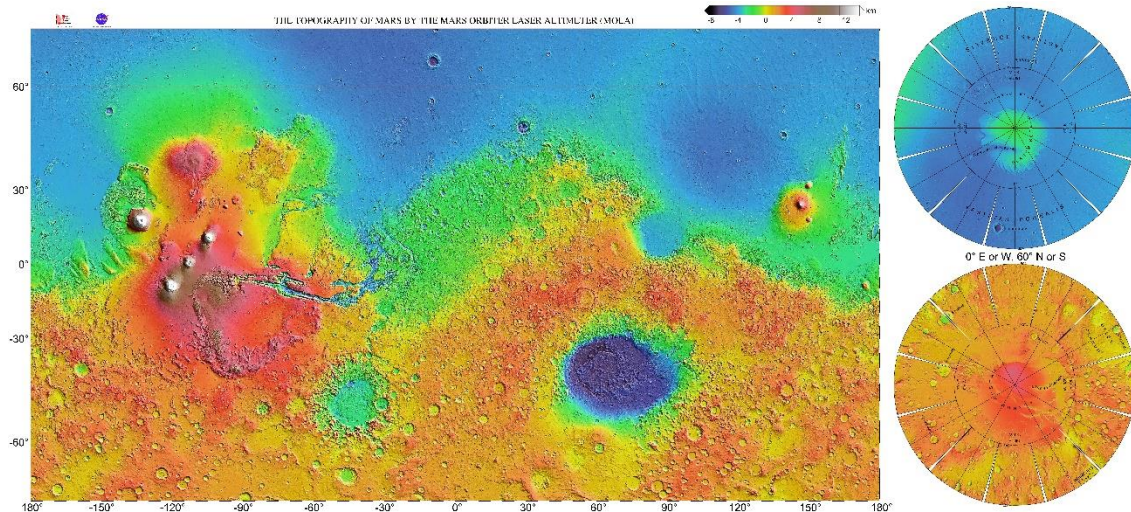


Figure 1-4 Topographic map obtained from the data of the Mars Global Surveyor IAS altimeter by Maria Zuber [81].

1.3. The atmosphere

The Mars atmosphere is composed in great measure of Carbon Dioxide (95,32%), with other elements such as Nitrogen (2,7%), Argon (1,6%), Oxygen (0,13%), Carbon monoxide (0,08%) and smaller traces of Water, Nitrogen Oxide, Neon, Hydrogen-Deuterium-Oxygen, Krypton and Xenon. The pressure of this gases in the mean radius is 690 Pa with a variation of approximately 40% depending on the season. There is a great variation in the atmospheric temperature, depending in altitude, latitude and time, being possible to achieve temperatures of 293 K at noon in the equator and a minimum temperature of 120 K at the poles, actual temperature measurements obtained by the Vikings landers indicate that the temperature variation in the same place can approximate to 100 K [9].

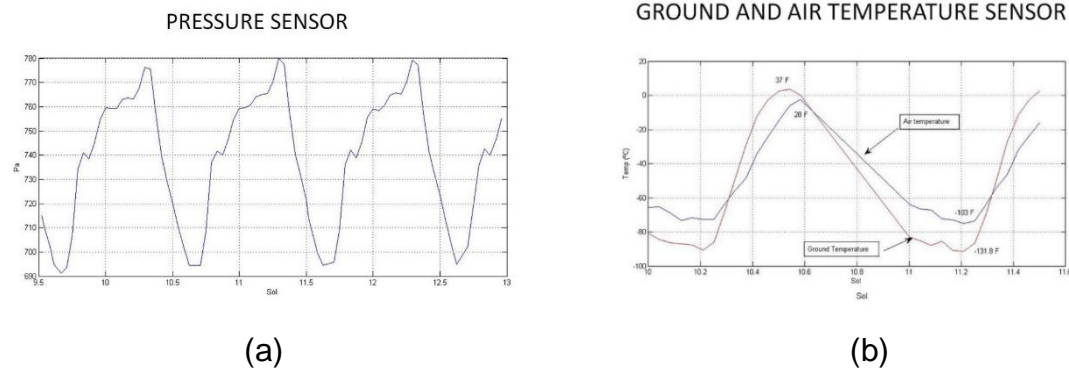


Figure 1-5 Pressure (a) and temperature (b) values measured by Curiosity's REMS instrument at landing site [10].

The information gathered by the Viking landers show that the existing winds in the surface are seasonal, with measured winds of 2 to 7 m/s in summer, 5 to 10 m/s in fall and with peaks during extreme conditions up to 17 to 30 m/s. During this extreme conditions and due to the geology of the planet dust storms can be formed and be local as well as global [11]. The values of the wind were taken within the boundary layer near the surface and therefore above it the wind speeds can approach 50 m/s [12]. However the reduced atmospheric density in comparison to Earth make the effects of this winds less severe [13]. The wind REMS instrument on Curiosity should had provided more accurate information about the winds existing in the surface, but due to malfunctioning of the sensors it's not been possible obtain the scientific information expected [10].

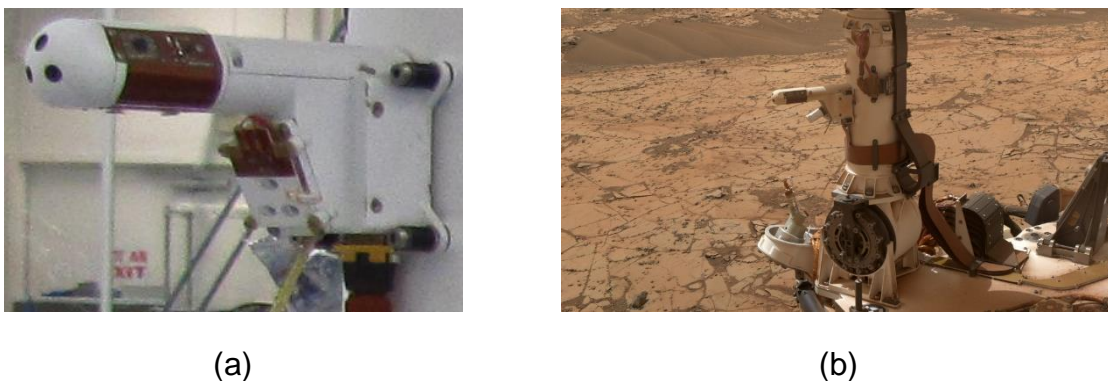


Figure 1-6 Part of REMS instrument during its preparation on Earth (a) and once in Mars (b).

1.3.1. Atmospheric model

Using the information gathered with the instruments of the scientific missions sent to Mars, several mathematical models have been computed, being the most advanced

of them the MARS GLOBAL REFERENCE ATMOSPHERIC MODEL (Mars-GRAM), which provide a full range of possibilities to simulate Mars atmosphere. For the calculations in this Master thesis, a simpler model confectioned by NASA (JPL) with mission data for a latitude of -20° has been used, from just above the surface to an altitude up to 10 km [12].

$$\rho = 0.014694 - 0.001145h + 4.6638 \times 10^{-5}h^{-2} - 9.7737 \times 10^{-7}h^3 \quad (1.1)$$

$$T = 238.78 - 34.488h + 35.133h^2 - 15.96h^3 + 3.7315h^4 - 0.047352h^5 + 0.030962h^6 - 0.000817h^7 \quad (1.2)$$

With the values of density (1.1), temperature (1.2), and the gas constant for the Mars atmosphere ($R_{\text{Mars atmosphere}} = 0,18892 \text{ J}/(\text{g}\cdot\text{K})$) and using the ideal gas law (1.3), in the molar form (1.4), the pressure value for the different altitudes can be obtained.

$$PV = nRT \quad (1.3)$$

$$P = \rho R_{\text{Mars atmosphere}} T \quad (1.4)$$

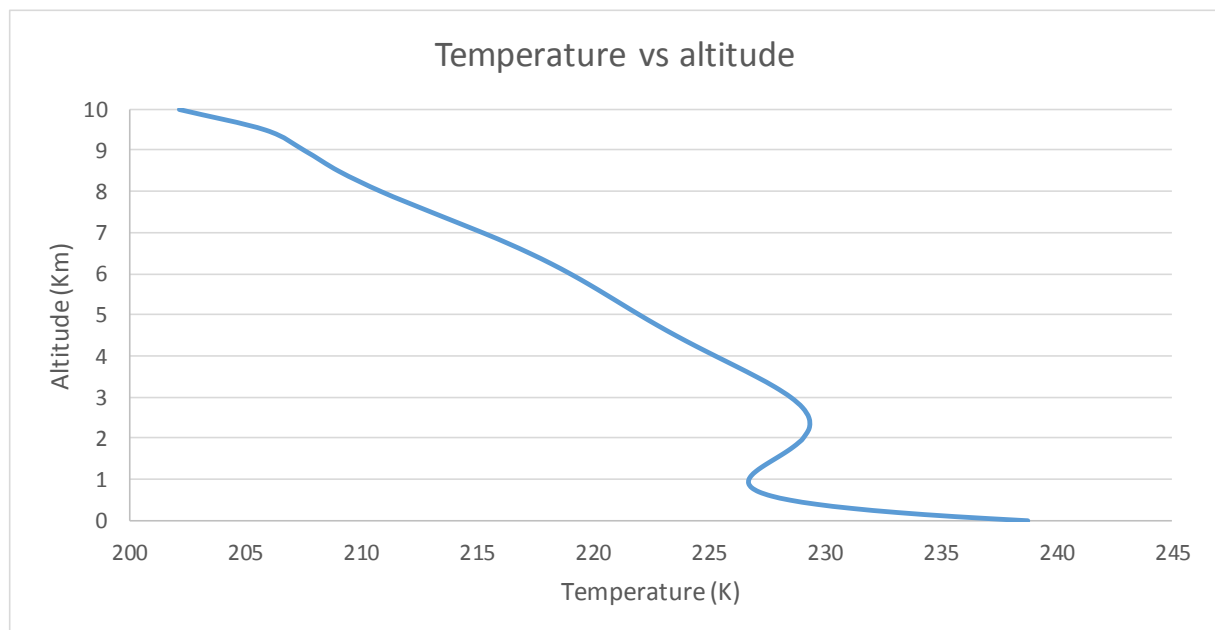


Figure 1-7 Temperature values obtained with the atmospheric model.

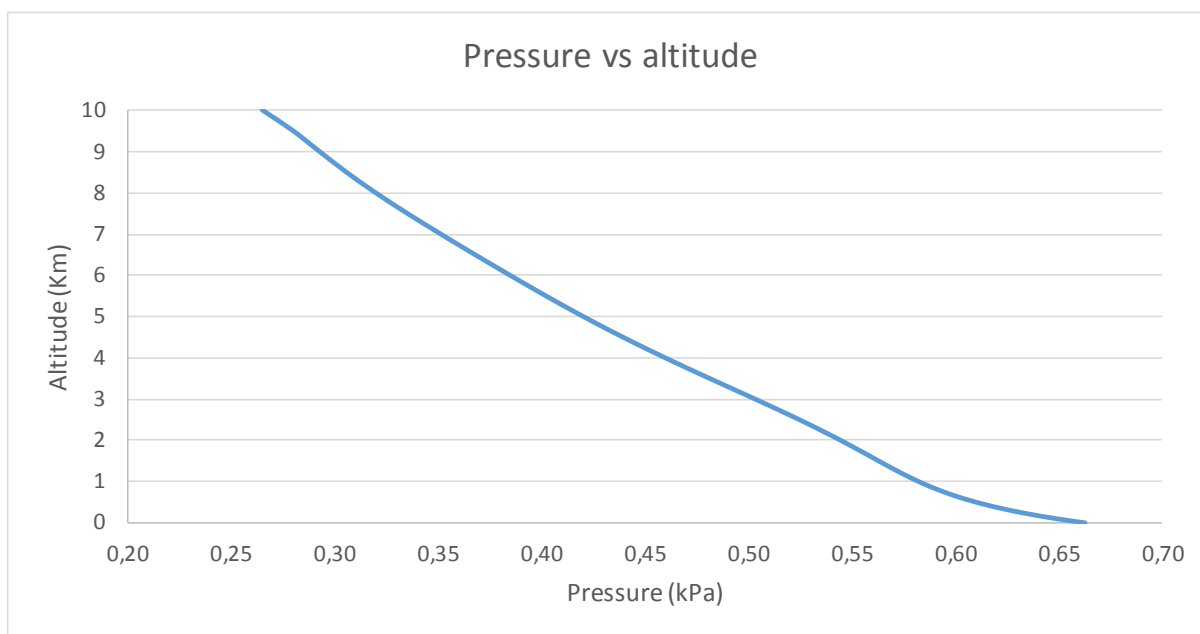


Figure 1-8 Pressure values obtained with the atmospheric model.

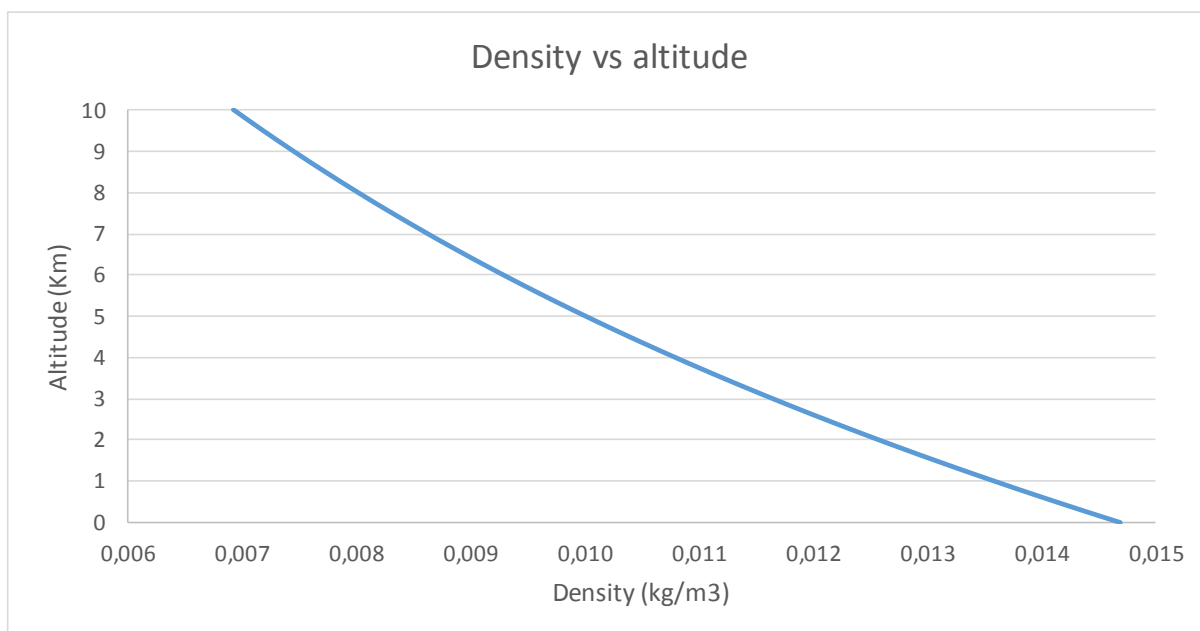


Figure 1-9 Density values obtained with the atmospheric model.

Chapter 2

BALLOONS

2.1. General characteristics

A balloon is a flexible container which can be filled with a gas with different properties than the atmosphere surrounding it, achieving buoyancy, as the Archimedes principle states: “Any object, wholly or partially immersed in a fluid, is buoyed up by a force equal to the weight of the fluid displaced by the object”.

$$Mg = \rho_a gV - mg - m_{gas}g \quad (2.1)$$

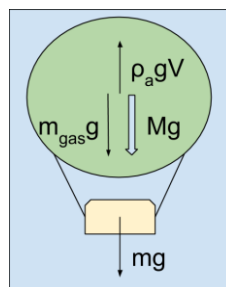


Figure 2-1 Diagram of the forces in a balloon accordingly to equation 2.1.

In an equilibrium case, the equation (2.1)[14] shows the vertical equilibrium of forces, being M the mass of the balloon envelope, V the volume of the balloon, m the mass of the payload, m_{gas} the mass of the filling gas, g the gravitational acceleration and ρ_a the density of the atmosphere. In order to achieve buoyancy control on a balloon two methods can be used, act on the properties of the contained gas ($m_{gas}g$) or modify the payload mass (mg) by changing the ballast.

2.2. Types of balloons

There are several methods to achieve buoyancy in balloons by modifying the contained gas properties in comparison of the surrounding, each one demanding a different design for the balloon in order to obtain the best performance, involving design parameters such as materials, shape, etc.

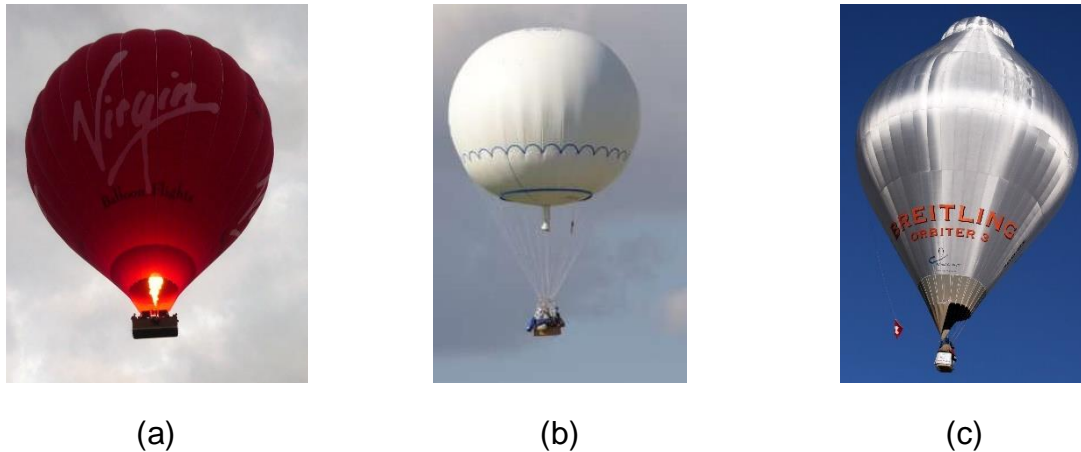


Figure 2-2 (a) Hot air balloon, (b) gas balloon and (c) Rozière balloon.

2.2.1. Hot air balloon

The hot air balloons or Montgolfier balloons are based in the Charles's law or law of volumes that describes the direct relation between a gas volume and its temperature, suffering an expansion when the temperature is increased. Usually gas obtained directly from the atmosphere is heated inside the balloon in order to increase its volume and therefore reducing its density to increase the balloon buoyancy. As this kind of balloons use the same gas inside as the one in the atmosphere around them, they are not very affected by pinholes or small leaks of gas, as it is replaced fast enough.

2.2.2. Gas Balloon

These balloons are based on filling them with gases with lower densities than the atmosphere, being sensitive to pinholes and leaks. Usually at the moment of release they are not fully deployed, achieving their final shape when they are at the desired altitude. Habitual gases used for this kind of balloon are Hydrogen or Helium, but other gases can be used if they are lighter than the atmosphere around them.

2.2.3. Rozière balloon

A Rozière balloon is a hybrid balloon that combines the two previous types of balloons in separate chambers. This balloons have been used on Earth to achieve different records on circumnavigating the Earth, due to the capability to control buoyancy with less fuel consumption than traditional hot air balloons.

2.3. Balloon movement

As balloons do not achieve flight from aerodynamic forces resulting from the movement through a fluid, they don't need to move or have moving parts to obtain buoyancy as other aerial vehicles need. Considering this, the movement of a balloon can be described as:

- Tethered / captured: In this case the balloon is physically connected to a base in the ground, remaining its area of movement limited by the length of the cable. This cables can serve as well to provide energy and data transfer to and from the balloon instruments.
- Controlled flight: In this other case the balloon is equipped with the necessary means to control its movement, being its range of movement limited by the energy, the communications to base and the durability of the balloon itself.
- Free flight: The balloon is driven by the existing winds. Despite a small quantity of control in the direction can be achieved by controlling the buoyancy of the balloon, moving it to a different wind layer, the movement is basically based on the zonal winds.

2.4. Suitable balloons for Mars

Balloons have already been used in space missions, in 1985 the Vega missions program released two balloons in the Venus atmosphere and gathered information about the atmosphere. Despite the atmospheric conditions on Mars make it more difficult to use balloons than in other scenarios, there have been several proposals to use balloons in scientific missions on Mars, both as a moving platform for the scientific instruments or as an alternative to parachutes [15].

Depending in the type of mission and its latitude several systems are possible, the conditions on Mars atmosphere allows to use hot air balloons, both with heat sources or by solar-heated balloons. Gas balloons are possible as well and have been under development by NASA to determine the most adequate technology to manufacture them in order to survive the Martian environment.

2.4.1. Zero pressure gas balloon

It is possible to use zero pressure gas balloons filled with Helium or Hydrogen in Mars but the limitations of this type of balloons suppose a drawback for all the possible uses. As the buoyancy control is achieved by venting the inside gas when there is an excess of altitude or releasing ballast to gain altitude the duration of the flight is limited and affected by the atmospheric conditions. This kind of balloon is less demanding for

material strength, allowing to use on its fabrication light-weight films and impregnated fabrics [16].

2.4.2. Super-pressure balloon

Martian gas balloons are also possible using super-pressure balloons filled with helium or hydrogen, being this second gas more problematic due to the problematics related to its transportation and handling. Once a super-pressure balloon reaches the neutral buoyancy altitude the excess of helium pressurizes the balloon, making unnecessary the use of ballast, maintaining the altitude despite day and night changes and achieving longer flight durations and more stable vertical positioning. This balloons demand stronger materials with low permeability to provide a long flight [17][18].

As the gas contained in the balloon must be transported with the spaceship its quantity is limited and any pinhole or leak can become catastrophic for the balloon. NASA has been developing this type of balloons with very successful results, achieving long duration flights in Antarctica at altitudes where the pressure is similar to the existing on the Mars surface [19][20]. The filling gas can be Helium or Hydrogen, which provides a 24% extra efficiency in the lift, but increases the problems of containment and leaks.



Figure 2-3 Super-pressure pumpkin balloon during a test on ground [16].

2.4.3. Solar heated balloons

Solar Montgolfier balloons have been proposed several times as a good alternative to super-pressure balloons to be used on Mars. This type of balloons uses the sun energy to heat the gas inside being able to produce an increment of temperature of 78K to the atmospheric gas inside the envelope when the surrounding atmosphere is at 220K. As the filling gas inside is the same as in the atmosphere these balloons are not strongly sensitive to leaks, being the gas fast refilled and saving the problems of carrying the gas from Earth.

Due to the buoyancy of the balloon depends directly of the solar energy gathered from the daylight, the season and latitude of the release will affect the type of mission capable to perform. This can force the balloon to land during the nights if they are long

enough to cool down the gas, and making it possible that during one of those nights the balloon became deflated enough to avoid it to inflate again once the sun dawn and heat it. This type of balloon allows to control the buoyancy by releasing part of the filling gas and therefore forcing new gas inside, reducing the temperature and consequently increasing the density and reducing the buoyancy, which provide the possibility to perform several soft landings, opening the opportunity to collect samples from different places or to deploy a net of sensors. Several test have been performed in the Earth atmosphere in conditions similar to the existing in the deployment on Mars proving the viability of applying this principles to balloons aimed to explore Mars [8][21][22][23][24].

Other methods to heat the gas might be possible, such as electric resistant or using the heat generated by a RTG to inflate a balloon, but these methods might be to complex and heavy for the conditions existing on Mars.



Figure 2-4 Solar heated balloon on Earth.

Chapter 3

Initial study of a balloon mission to Mars

The technologies involved in the use of balloons in Mars have been tested already on Earth, but a good opportunity to prove these technologies in real conditions is to test them through a low budget piggyback mission, serving as a technology demonstrator [25]. In this type of mission, the objective is to prove new technologies or apply new methods to existing methodologies, therefore the scientific objectives are not the only ones, but a supporting feature of the test of new technologies.

With these concepts in consideration and to prove the possible utility of balloons as tools for Martian exploration the mission proposed for this balloon mission to Mars will be to serve as an accessory for a rover, providing only additional elements and not critical. This will avoid any problem with the main objectives of the rover mission and allow the rover to continue performing its main mission once the balloon has lost its buoyancy capabilities.

3.1. Mission basics

Recently NASA has proposed a small autonomous helicopter to scout the terrain at a safe distance of the rover (to prevent accidents) in advance for the daily moves of the next 2020's Mars rover, exposing how critical is to improve the knowledge of the terrain the rover will face. The helicopter is expected to have approximately 3 minutes of autonomy, being able to fly up to 100 meters of altitude and having a ground track of 600 meter [5]. With a similar objective but without the limitations that imply using a rotatory-wing aircraft (low mass and critical moments during landing and taking off) the use of a tethered balloon can provide the necessary information for a safe movement of the rover besides hosting other scientific payload. Another recent development with a similar goal is the Prandtl-m proposal which prototype is scheduled to be tested soon. It has been developed to be included as a ballast in the aero shell in the next NASA rover mission to Mars inside a CubeSat structure and deployed during the descend on the planet, gathering information and taking detailed images of the surface [26].

The objectives for this mission are quite similar to the expected in those two proposals. The tethered balloon will deploy once the rover is on the surface providing information of the surrounding areas to the rover it is linked to, host other scientific payload and test the durability and performance of a super-pressure balloon on Mars.

3.1.1. Balloon

The studies indicate that one of the optimal configurations for a balloon on Mars is a pumpkin super-pressure balloon [20]. Despite other configurations are capable to operate in Mars as well, like solar Montgolfier, zero pressure gas balloons or spherical super-pressure balloons their performance is not expected to be as good as the super-pressure pumpkin balloon. Solar Montgolfier suffer from great altitude variation due to the lack of energy gathering during the night existing the possibility that in one of altitude variations the tethering cable might become wrap with something leaving the balloon stranded. Zero pressure gas balloons depend on the ballast release or gas vent to maintain the desired altitude, decreasing the life expectancy of the balloon.

The reason of choosing a pumpkin shape super-pressure balloon instead of a spherical one is that in the spherical one the envelope material should resist both the stress produced due to the difference of pressure between the inside and the outside and the stress produced by the loads the balloon is carrying. In a pumpkin shaped balloon, the envelope material only has to resist the stress produced by the difference of pressure (horizontal loads) while the payload loads (vertical loads) are supported by the vertical fibres around the balloon that give it its lobed shape.

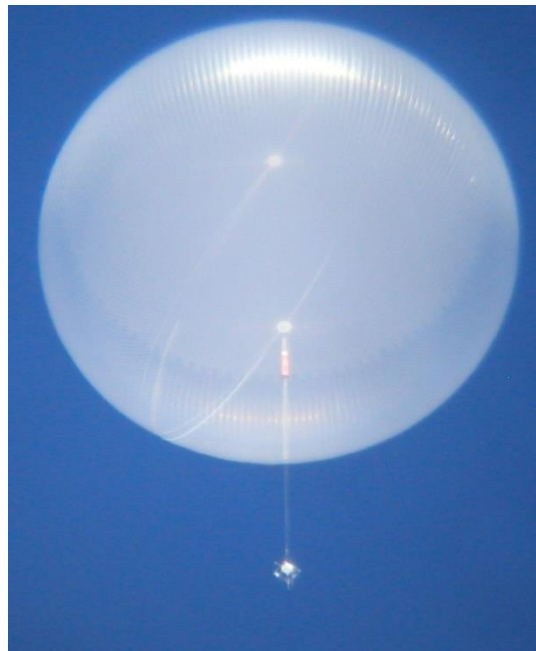


Figure 3-1 Super-pressure pumpkin balloon during a successful flight test on Earth [82].

The material for the balloon skin has to be taken into consideration as well, having been proposed the use of uniform polyethylene bilaminates or co-extruded linear low density polyethylene, and using PBO (Zylon) for the tendons [15][27][28]. The material to be used as tether and to connect the balloon to the payload need to present high strength characteristics and be resistant to the Martian environment, such as a high UV radiation, Zylon or Kevlar can be considered for this purpose but will need protection against the environment [29].

3.1.2. Deployment

Almost all the current studies for Mars balloons are focused nowadays in a deployment during the entry into the planet atmosphere because this studies work on the premises of a solo mission for the balloon. Deploying a balloon during the entry on the planet has some clear advantages, such as reducing the mass of the entry vehicle, as a lander won't be necessary, but also implies exposing the balloon envelope to loads not existing in a regular inflation due to the deceleration and inflation occurring at the same time [16][21][30].

In this mission proposal the balloon is expected to work as the sidekick of a rover and consequently the deployment system has to be adequate for this situation. This implies that the deployment will occur in the planet surface and it will need enough clearance to avoid any incident with the surroundings or the rover itself.

3.2. Payload

3.2.1. Energy system

Several systems can be considered to provide the energy necessary for the operation of the different systems on the balloon, each one with its benefits and drawbacks. Two main approaches can be established, an autonomous source of energy aboard the balloon or providing the energy from the rover through the tethering.

3.2.1.1. *Autonomous energy sources*

Solar energy has already been used to provide energy to several spacecraft on the Martian surface, but present several problems being the first one, and most important in this mission configuration the mass it represents. The energy demand of the different systems on the balloon will stablish if this is a possible option, being the energy demand directly proportional to the size (and mass) of the solar cells. This fact has an impact in the total mass and therefore in the final volume of the balloon needed.

With an estimated efficiency of 29% [31] in the solar cells used nowadays for small satellites it would represent a maximum production of approximately 200 Wh/m^2 at the maximum production moment in the best production season in the upper part of the Martian atmosphere, as can be seen in Figure 3-2. The production value is inferior in lower altitudes if a 15% solar attenuation is considered due to the thickness of the atmosphere [12]. This value is only valid to solar cells perfectly aligned for an optimal performance, but as the energy converted varies as a function of the cosines of the incident light and the surface of the cell [32], the energy gathered would be smaller, even without considering the degradation the solar cells suffer with time. In Figure 3-3

can be observed the average solar insolation at Mars upper atmosphere for different latitudes during a planet orbit around the sun.

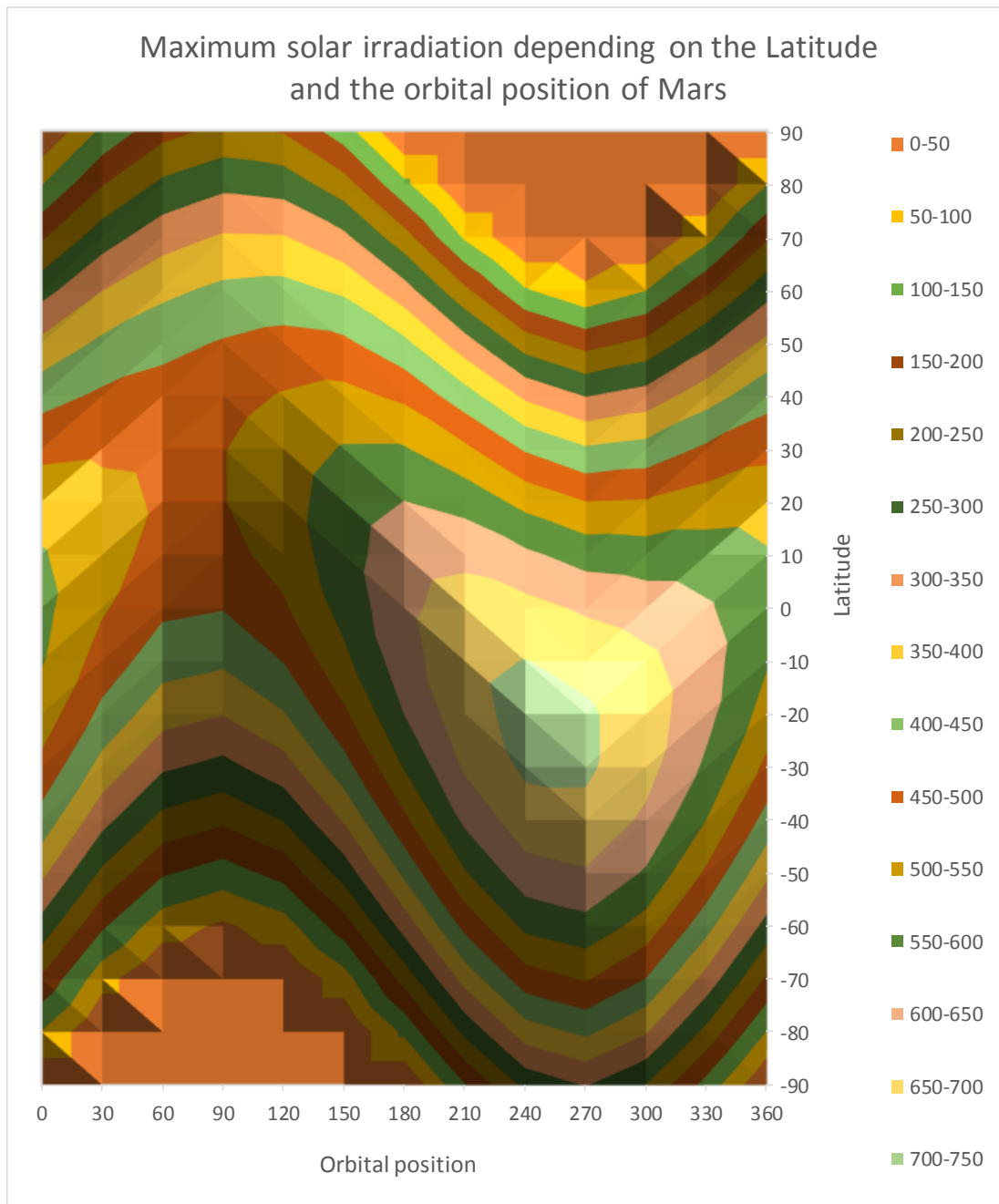


Figure 3-2 Maximum solar flux in Wh/m² in Mars surface during an orbital period.

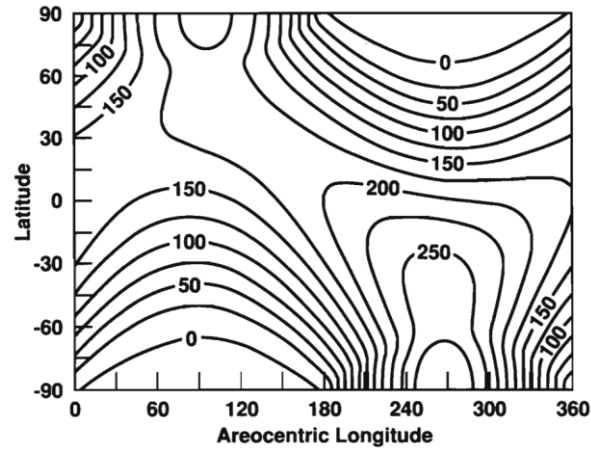


Figure 3-3 Mean solar flux per day in Mars upper atmosphere during an orbit [11].

As can be seen in Figure 3-4 the energy available during a sol in Mars is not constant and achieves a maximum in the midday (the start of the plot in Figure 3-4) then descending until it becomes zero during the night to increasing again with the sunrise. This force to implement a battery system in any spacecraft using solar cells in Mars, not even to perform scientific activities during the night, but to provide enough energy to keep the critical systems working, and to dimension the solar cells not only for the operations of the moment, but to gather enough energy to survive the night as well. Further information about the solar flux graphics shown in Figure 3-2 and Figure 3-4 is available in ANNEX II: Mars solar flux.

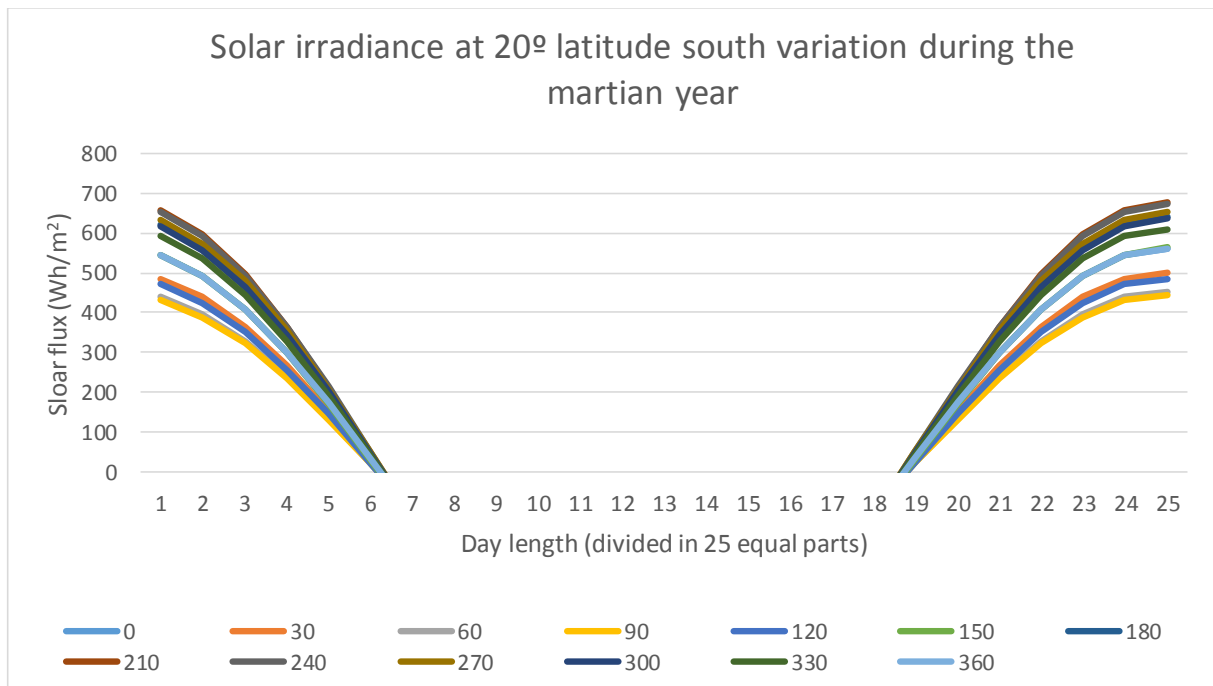


Figure 3-4 Variation of the solar flux in a 20° latitude position in Mars during a sol for different orbital positions.

The use of other energy sources might be possible, such as radioactive generators [12] but at the moment the lightest Radioactive Thermal Generator (RTG) is the one implemented in Curiosity, with a mass of 44 kg and a power generation of 125 W [31] it might be considered inadequate for a balloon based mission.

Batteries could be an option if the length of the mission is small enough, but long missions wouldn't be possible without charging systems. Even in that case, the operational temperature is limited, and the aging in the batteries imply a voltage decay with time. Therefore as a result of the loss of efficiency of batteries with time is necessary to dimension the battery to provide the necessary energy at the end of the mission, which suppose the use of batteries capable to store more energy than the necessary at the start of the mission [12].

3.2.1.2. Tethered energy sources

In this case the energy is not produced on the balloon but somewhere and transferred to the balloon. The limiting factor on the method to transfer the energy is the range of the transferring method. The most used method to provide electrical energy nowadays is by a conducting cable, such as copper cable, but the weight it might suppose make some alternatives quite interesting for a tethered balloon.

Power Over Fibre (POF) is nowadays capable to transfer up to 70 watts (DC) to a distance of 500 m, with a receptor capable of transforming the laser light into electrical energy while using the same optic fibre to transfer data to the other end with a receptor device of approximately 150 g [33]. This method is based in using optic fibre between the energy source and the place where the energy will be used, with a laser diode to transform the electrical energy into light and a photovoltaic cell to transform it back [34], this transformation generates heat that needs to be dissipated. One of the benefits of using this kind of power supply is that provides a complete electrical isolation between the ends of the tether [35].



Figure 3-5 Prototype of POF by Lasermotive [33] powering a quadcopter.

Wireless energy transfer is an option as well, but the necessity of an accurate tracking and pointing systems might increase the complexity and weight of the systems above the capabilities of a small tethered balloon.

3.2.2. Communications, telemetry, data handling and processing systems

To lighten as much as possible the balloon, a possible solution is to not process any data in the balloon and send the direct raw data from the instruments to the rover. This approach limits the possibilities of autonomous energy sources as the balloon will become an extension of the rover, without capability of working by its own. As it might be interesting regarding the mass saving in the balloon it limits in great measure its utility.

The other side of this situation is to include all the necessary to process and store the information gathered on-board before transmitting it to the rovers, but it will imply a greater energy consumption and a higher part of the mass available dedicated to systems instead of instruments.

It is clear that neither of the options above exposed is an optimal solution and that a balance between processing the information on-board and sending it to the rover is necessary, but the right configuration will depend on the scientific payload and consequently on the amount of data generated.

Despite it is possible to implement a basic movement capability to the balloon by using propellers or other methods, the basic functionality of the balloon can be achieved without it, with the saving in mass that it supposes. Therefore, the telemetry the balloon might generate should be minimal, the status of the different elements of the payload while other relevant information might be included by the information gathered by the scientific payload.

Regarding the data transfer between the balloon and the rover the same existing problem as with the energy transfer can be observed. Systems using radio or laser communication are possible but imply the inclusion of guidance systems that might be too complex for a lightweight balloon. Consequently using the tethering to include a cable for data transmission can be a good solution, especially when nowadays it is possible to transmit data by the same methods used to transfer energy (by electrical wire or by optic fibre [33]).

3.2.3. Navigation and attitude control systems

In the case the balloon is on a free flight configuration limited by the tethering cable a navigation system will be focused basically to identify in which direction the rover is located to determine the balloon positioning and help to interpret the information

collected for the rover navigation and provide a context to the rest of the information obtained.

As exposed in the previous section, despite it's possible to provide the balloon with actuators to modify its position inside the range provided by the tethering cable, the inclusion of this systems is linked with an increase of the complexity of the balloons systems and its weight. Depending on the purpose of the instruments included in the balloon this might be necessary and additional navigation systems should be required to assure a safe flight of the balloon.

Despite the nature of the balloon and the basket to remain on its natural position some conditions might alter it (such extreme wind). Those conditions will possibly imply the loss of the balloon as well, therefore implementing an attitude control system might be irrelevant, if those conditions are achieved the balloon could have been already destroyed. To determine the attitude several instruments can be used, such as star trackers, sun sensors, gyroscopes, accelerometers, angular rate sensors or even use the images acquired by cameras of the terrain to determine its position and orientation [31][36][37][16].

3.2.4. Thermal control systems

As the environment in Mars is not suitable for the correct operation of the different electronic equipment that will be part of the payload thermal control is necessary to assure a correct performance of the different instruments and systems. The thermal control system will be in charge of preserving a temperature inside of the basket allowing the correct performance of the system while extracting the necessary amount of heat generated by the different electronic equipment to prevent overheating in the systems.

Different methods used together for missions on Mars include Multi-Layer Insulation (MLI), silica aerogel insulation (which requires less installation time and provide an 11% mass reduction with the same performance than MLI [31]), gold paint as passive systems and heaters, radiators, heat pipes and thermostats as active temperature control.

3.2.5. Structure

As the rest of the elements that are part of the balloon payload, the structure containing them should be as light as possible being capable as well to isolate the payload from the balloon, as spherical or ellipsoidal balloons tend to turn due to the action of the wind and a stable platform is preferable to perform scientific studies. The structure might avoid as well the access of the dust existing in the Martian atmosphere to the interior to prevent any possible damage to the instruments located in there. The structure must be capable as well to conduct electricity, as radiation can induce potential charge accumulation in the electronics.

Despite aluminium has good properties, its density is not optimal and other options such as composites based on cyanate resin might have a better performance for the function in study. Metal laser sintering is a possibility as well, but a poor material strength and problems with outgassing due to the porous nature of the material are drawbacks for its use in this kind of scenario [31].

3.2.6. Scientific instruments

The characteristics of balloons make them capable to perform a great variety of scientific tasks, some of them not possible otherwise. Aerial vehicles in Mars are considered a good platform to include scientific equipment capable to improve the quality of the information that until now has been gathered only by satellites in orbit, despite reducing the area of study. In the case of balloons, another benefit can be the capability of deploying sensors of big volume that for other aerial vehicles might be impossible due to the aerodynamic forces present during flight [16].

3.2.6.1. Cameras

The information acquired by cameras studying the overflying areas can be used to improve the planning of future missions identifying interesting spots or dangerous areas. The highest spatial resolution images from Mars have been taken by the HiRISE instrument situated on the Mars Reconnaissance Orbiter and have a spatial resolution of 30 cm per pixel [38], not enough though to be used as the base of the navigation of an autonomous vehicle on the surface. Therefore, closer images would improve the information a rover will dispose to set a save path or discover interesting zones to perform scientific test.

Despite the navigation purpose might be one of the main uses of the imaging of the ground from a tethered balloon, won't be the only one. The possibility to include a wheel of filters such in the future ExoMars rover PANCAM [39] or the existing in the Beagle 2 [40] can provide useful information in different fields, such as geology or weather. For example, it is possible to study the Aeolian processes by studying the images taken [41], put in context the images taken from orbit, perform atmospheric studies by observing the clouds appearing in the images or the dust particles in suspension by comparing the quality of the light in the sky.

3.2.6.2. Magnetometer

Although Mars doesn't have a global magnetic field, the existence of strong remanent magnetism in specific zones will allow if studied to test the hypothesis of the Mars magnetic field decay. To do so a magnetometer positioned in a balloon will provide information that satellites at their altitudes are not capable to obtain. Among other objectives this could help determinate the magnetism of Martian rocks or investigate the leakage of the solar wind induced magnetosphere using the correlation between the data obtained in orbit and in a balloon observer [42][43].

3.2.6.3. Seismic sensors

The use of non-tethered balloons is usually considered in order to gather data from a position not available but to airships, but the deployment of a net of seismic sensors using balloons capable of control the buoyancy and depositing sensors on the ground is another possible use for balloons on Mars [22].

3.2.6.4. Atmospheric sensors

To study in detail the Mars atmosphere and detect the atmospheric signature originated from localized subsurface biological or geological activity is possible to use a tuneable laser spectroscopy. Being more flexible than a mass spectroscopy (by being able to specificity different isotopomers in a simpler way) and providing faster response than a mass spectrometer a tuneable laser spectroscopy has been long used on Earth in aerial platforms. The detection of methane could be possible with this kind of sensor, and could help localize local sources of it with more accuracy than nowadays, being the presence of methane of irregular concentrations on the Mars atmosphere a possible indicator of the existence of biological activity on the planet [23][44].

Instruments capable to measure wind speed, direction, temperature and other properties that characterize an atmosphere might be useful to compare the information that has already been obtained and will be obtained in the surface. Instruments similar to REMS might be used to obtain that information.

3.2.6.5. Subsurface sounding

The nature of a balloon probe provides the possibility of deploying big and lightweight structures that otherwise would be impossible or highly difficult to deploy on the surface [25][45]. This structures could be used to search for subterranean deposits of water in a level of detail impossible from orbit [23].

3.2.7. Ground sector

To assure the correct performance of the balloon several systems will be necessary on the rover, some related with the systems named in the previous sections such as the power or communications systems. Another element necessary in the rover will be a structure to fix the tethering cable connecting to the balloon and to cut the tether cable when the buoyancy force of the balloon is not enough to keep it floating, allowing the rover to continue its normal operations without the danger of being tangled with it or damaged by the balloon, its payload or envelope.

Chapter 4

Proposal of a piggyback balloon mission

Balloons have not been used yet on Mars, therefore the risk that supposed to send a whole mission depending on untested technologies might be admissible, but not and optimal solution. Consequently, including some of those technologies as a complementary part in an existing mission, without being critical to its development can help improve the results of a future mission based completely in balloon technology.

One of the possible scenarios where a balloon piggyback mission can be useful is as a sidekick in a rover mission. Nowadays the rovers rely on optical systems (such as stereo cameras) and satellite images to navigate in Mars. Satellite images are first used to identify possible interesting locations where to direct the rover, and then using the optical systems located in the rover a more accurate identification of locations is made, with all this information the ground team prepares a step by step process to move the rover from one location to another [46]. If the conditions are good enough the rover is capable to drive autonomously as well using the information gathered by its sensor to calculate a route and follow it [47].

The information gathered by a rover to its navigation come from several sensors around it, from cameras aiming to the front and the rear (Hazcam) and several cameras in a mast to study the surroundings. The cameras located in the mast are limited by the height of it, for this reason the information they are capable of obtain is limited to the immediate surroundings that are captured in the line of sight of the sensors. Despite the satellite imagery has hugely improved the information that provides is only capable to provide general information of the whereabouts of the rover and although it can help decide future objectives for the rover is not usable for navigation. For this reason, a piggyback mission with a balloon capable of provide information of the surroundings areas to the rover can help improve its navigation capabilities and avoid dangerous zones. It might be capable as well to detect scientific interesting spots that otherwise wouldn't be notice by being out of the line of sight and at the same time prove the technologies for further advanced missions based on balloons on Mars.

As a piggyback mission its main focus is to provide as many information possible to improve the rover navigation, while obtaining other valuable information impossible to acquire from surface and test some of the technologies involved in balloon missions on Mars, all of this in a contained mass and volume to not penalize the rover main mission.

4.1. Basket

In a balloon the platform where the payload is located is commonly named basket. It is responsible to allocate all the different elements of the payload while serving as a link between the balloon and the rover and providing a survival environment to the electronics of the payload. In this mission it will be equipped as well with a mechanism capable to isolate the scientific payload from the natural movement of the balloon.

4.1.1. Scientific payload

Among the different instruments which can provide valuable data for this type of mission, cameras will be the key element to acquire information for the rover navigation. Other scientific instruments will be included as well, taking in consideration their mass and volume, such as atmospheric instruments and magnetometers. It's important to remark that all the values and specifications of the instruments here stated are just an initial approximation and that more adequate equipment probably exist or can be developed for the porpoises here explained.

4.1.1.1. Cameras

Three cameras will be located around the basket based on the Hazcam [48] and Navcams [49] cameras present on the Curiosity rover with a field of view (FOV) of 124° in vertical and 120° horizontally and a definition of 1024×2048 pixels [50][51][52], providing a surrounding image of the surface below and part of the sky. In other words, a panoramic view conformed by the bottom half of an imaginary sphere surrounding the basket.

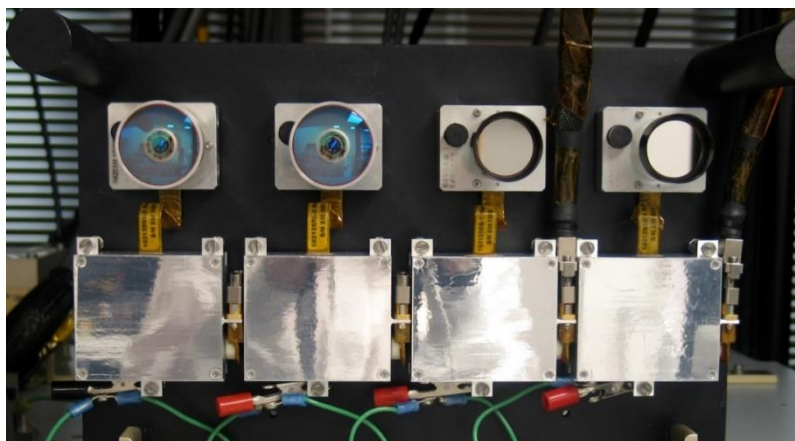


Figure 4-1 MSL HAZCAM and NAVCAM during preparation (left 2 HAZCAM, right 2 NAVCAM).

Besides providing direct visual information of the rover surroundings the images can be processed in order to obtain an elevation model of the surface as exposed in [37]. As the rover won't be stationary for long periods, the rover movement will provide the change in location necessary to obtain these results, and even if the rover does not move the length of the tether and the wind direction and speed will produce a change in the balloon position relatively to the ground that might be enough to produce similar results.

Additionally, another camera will be located focusing the upper part of the basket in order to survey the balloon state, in this case the camera will have a reduced FOV, big enough to frame the balloon and with a lower definition of 1024 x 1024 pixels, as the Hazmat cameras.

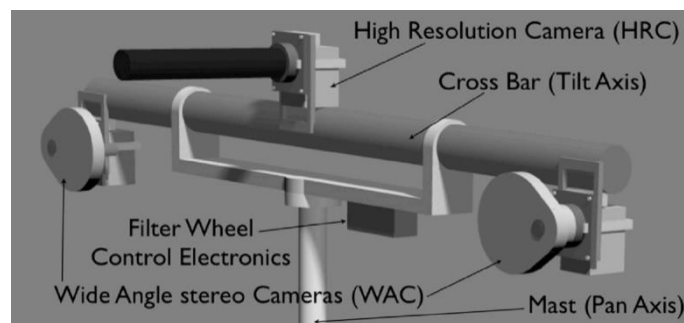


Figure 4-2 Baseline configuration of the Exomars PanCam [39].

A camera in a gimbal will be placed in the lower part of the basket in order to obtain better images of localized elements, using the information provided by the attitude control system and the method described in [37] to aim it correctly. It will have a similar definition as the three cameras used to obtain a panoramic view but with a narrower FOV and enhancing optics to provide enough augmentation. It will be equipped as well with a disk of filters similar to the used in the Beagle 2 [40] and the proposed Wide Angle stereo Cameras (WAC) for the ExoMars rover that will allow to perform different geological estimations about the surface below and characteristics of the High Resolution Camera (HRC) from Exomars as well [39][44][45]. This camera should benefit from the magnification capabilities of the HRC and the filter systems from WAC.

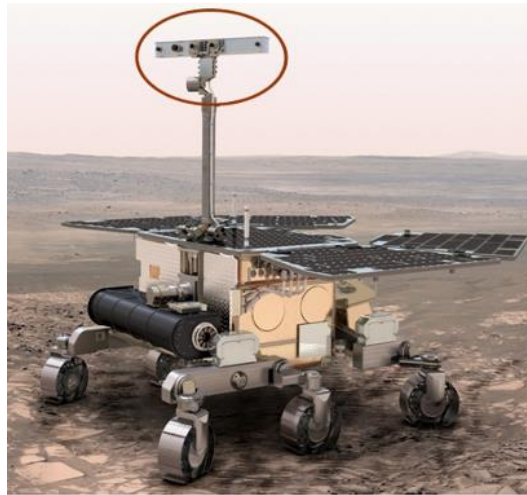


Figure 4-3 Representation of the PanCam mounted on ExoMars [55].

The values used from these cameras are only used for purposes of acquiring information about dimensions, mass and capabilities of cameras suitable to operate in mars, differing in areas such as definition, optics specifications or the mass from the values of a final element suitable to be included in this kind of mission.

HAZARD AVOIDANCE CAMERA (HAZCAM)	
FOV	124°
Definition	1024x1024 pixels
Power	2.15 W
Weight	245 g
Dimensions (electronics)	67x69x34 mm
Dimensions (detector head)	41x51x15 mm

Table 4.1 MSL HAZCAM specifications.

NAVIGATION CAMERA (NAVCAM)	
FOV	45°
Definition	1024x1024 pixels
Power	2.15 W
Weight	220 g
Dimensions (electronics)	67x69x34 mm
Dimensions (detector head)	41x51x15 mm

Table 4.2 MSL NAVCAM specifications.

WAC	
FOV	65°
Definition	1024x1024 pixels
Power	1.5 W
Weight	200 g

Table 4.3 ExoMars WAC specifications.

HRC	
FOV	4.8°
Magnification	~x7 (compared to WAC)
Definition	1024x1024 pixels
Power	0.9 W
Weight	Not available

Table 4.4 ExoMars HRC specifications.

4.1.1.2. Atmospheric sensors

Several atmospheric sensors have been included in missions to Mars, among others the REMS instrument, the sensors to be included in the ExoMars 2016 and ExoMars 2018 to perform atmospheric studies or other sensors developed for other Mars missions.

REMS is the atmospheric sensor package included in the rover Curiosity, including wind, ground temperature, air temperature, relative humidity, pressure and UV radiation. During the time it has been in Mars it has provided relevant information despite the malfunction of the wind sensors [56][10].

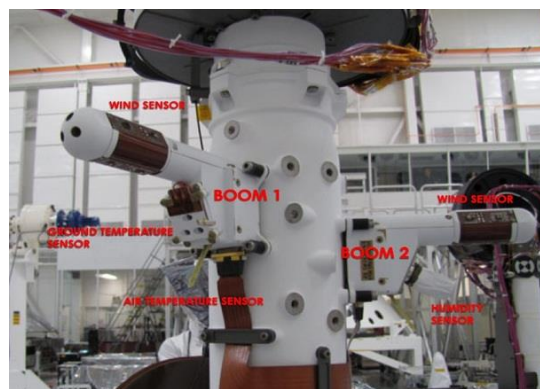


Figure 4-4 REMS sensors on the Curiosity mast.

Dust characterization, Risk assessment and Environment Analyzer on the Martian Surface (DREAMS) is the package of instruments included in the future ExoMars 2016 mission, with a similar number of instruments: thermometer (MarsTem), pressure sensor (DREAMS-P), humidity sensor (DREAMS-H), 2-D wind sensor (MetWind), electric field sensor (MicroARES) and Solar Irradiance Sensor (SIS) [57].

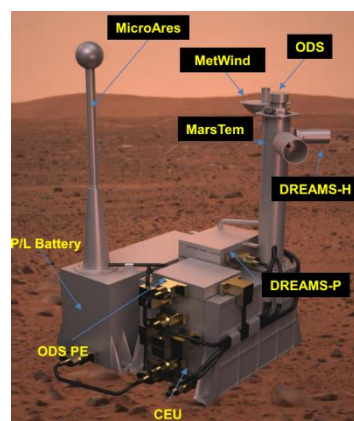


Figure 4-5 DREAMS instrument for the ExoMars 2016 mission [58].

Among all the possible sensors existing or in study to perform atmospheric research in Mars a selection of them has been done being their mass and power consumption key elements on their selection.

Among others a wind sensor located in the basket of a balloon can provide values not affected by the perturbation of the surface in the winds, and allow the comparison in direction and intensity from the values taken at ground level. This type of sensors are based in keeping an element at a stable temperature compared to the air temperature, and then by the energy necessary to keep that temperature extrapolate the existing wind. The sensor chosen is a hot wire temperature sensor as the one proposed in [59], with a contained mass and volume it includes as well air temperature sensors and it determine the wind direction by placing a set of temperature sensors around the hot wire and detecting the change of temperature of the air indicating the leeward of the hot wire. Usually temperature values are obtained by specific sensors, but being the mass one of the defining properties of a balloon every gram is important and this instrument can provide the temperature value as well. In the case of this sensor the operation procedure is explained in Figure 4-6.

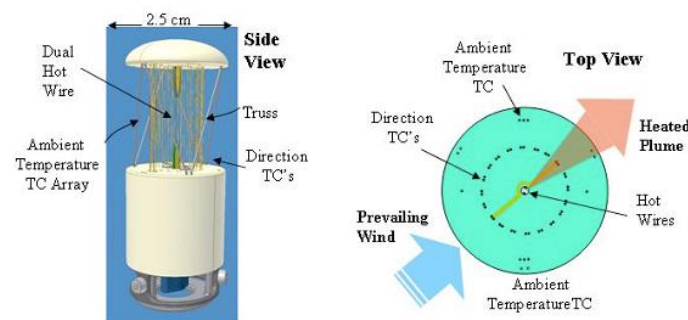


Figure 4-6 Design details and operational principle of the Hot-wire anemometer.

Wind sensor	
Weight (ATS and boom included)	30 g
Dimensions	25x25x75 mm
Bit/Sec	224 bps
Kbits/Sol	1.2 Mbit/sol
Power	300 mW
Range of detection	0 to 100 m/sec
Resolution of the sensor	$\pm 9^\circ$ in horizontal direction
Accuracy	$\sim 10\%$

Table 4.5 Wind sensor specifications.

Mars is not as dry as it might seem, the presence of water vapour in the Mars atmosphere is well documented [60] and a Relative Humidity Sensor (RHS) was included among the different instruments part of REMS. The inclusion of a RHS as a sensor in a balloon could provide interesting information about the water existing in the Martian atmosphere and compare the results obtained by similar instruments in the ground level. The instrument is based in the change of properties of an element as a function of the temperature and the humidity, thus controlling the temperature thoroughly the humidity can be estimated [61][62].

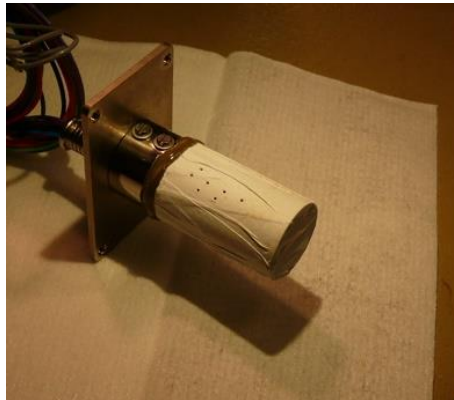


Figure 4-7 Relative Humidity Sensor before being placed in the boom.

RHS	
Weight	13 g
Bit/Sec	208
Kbits/Sol	1433.6
Power	15 mW
Temperature of operation	203 to 323K
Range of detection	from 0 to 100 %RH
Resolution of the sensor	1 %
Accuracy	± 2 % RH in 0 °C ± 4 % RH in -40 °C ± 8 % RH in -70 °C

Table 4.6 Relative Humidity Sensor specifications.

An atmosphere is usually characterized by three elements, its temperature, its pressure and its density, being possible to determine one with the values for the other two (is necessary as well to know some other variables, as the composition of the atmosphere for example). Therefore, including a pressure sensor in the basket will help characterize the atmosphere and serve as an indicator of the altitude of the balloon. This will be achieved by comparing the information with the sensors of the same type that the rover will probably incorporate and the different existing models of the Martian atmosphere providing information about the balloon status and the expected duration of the balloon [63].

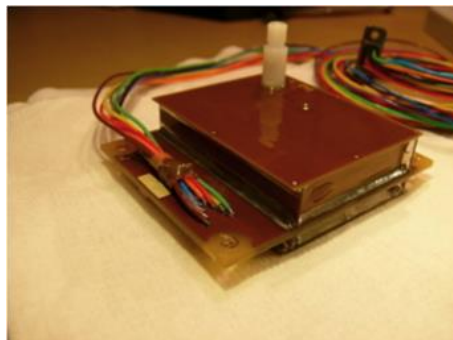


Figure 4-8 Pressure Sensor, the intake of atmosphere is the white pipe.

PS	
Weight	35 g
Bit/Sec	216
Kbits/Sol	1536
Power	15 mW
Temperature of operation	228 to 328 K
Range of detection	4 to 12 hPa
Resolution of the sensor	0.2 Pa
Accuracy	3.5 Pa

Table 4.7 Pressure Sensor specifications.

4.1.1.3. Magnetometers

In the next NASA mission to Mars, InSight [64], one of the instruments is a magnetometer composed by two identical high-sensitivity ($5 \text{ pT}/\sqrt{\text{Hz}}$ at 1 Hz) magnetic field sensors with a weight of approximately 500 g [65]. Its heavy weight, despite being a light magnetometer for the standards of space explorations, makes it not completely fitted for the porpoise of using it on an airborne mission.

A lighter and smaller magnetometer is being developed for the ExoMars mission by the Technical University of Denmark [66] as small and lightweight as a small matchbox named Mars Surface Magnetic Observatory (MSMO). Being the mass a critical element in the design of a balloon mission this one is more adequate for the porpoise of this mission. Not detailed specifications are available about the exact weight, size and power consumption of this magnetometer. For this reason an approximation value will be used adopting the specifications of this magnetometer [67] being the closest that it has been found to the size and weight characteristics indicated in [66] and similar to other existing magnetometers for space applications [68].

MSMO	
Weight	150 g
Power	500 mW
Sensitivity	$5 \text{ pT}/\sqrt{\text{Hz}}$

Table 4.8 MSMO specifications.

4.1.2. Systems Payload

Not being specifically scientific instruments a wide range of other instruments and systems are required to assure the correct operation of the scientific payload and provide information necessary to contextualize the information obtained.

4.1.2.1. Attitude system

Despite the low density of the Mars atmosphere, the wind can have an impact on the balloon attitude as it is studied in [29], and therefore modify the orientation and the attitude of the balloon and the basket. For this reason, it is necessary to include sensors and tools that allow identify where the different sensors of the basket are aiming to obtain a context of the information gathered.

Using the cameras it is possible to detect where the horizon is located, and with that information it's possible to obtain information about the attitude of the basket [69]. Using the cameras as well there are methods in development to generate a surface map and locate the place where the images were taken from [37]. Both methods are optimal for the tethered balloon configuration, as all the computing necessary can be performed in the rover the balloon will be linked to avoiding the increase of mass that any other method will suppose. With the cameras will be possible as well to obtain information of the position of some celestial bodies such as the sun or one of the natural satellites of Mars which orbital mechanics are well known and therefore providing information about the orientation and the attitude of the basket.

Using the same method of observing celestial bodies, sun sensors are elements specifically design to obtain the position of the sun and therefore establish the position and attitude of the object they are attached to. Nowadays exist on the market several sun sensors aimed to be equipped on small satellites that are extremely lightweight in comparison to other alternatives. Considering the mass and the FOV of the instrument, the NanoSSOC-D60 [70] is a good alternative to heavier models to include in the basket. Given its FOV the distribution of the sun sensors will mimic the one of the panoramic cameras.

SOLAR SENSOR NanoSSOC-D60	
Weight	4 g
Dimensions	27.4 x 14 x 5.9 mm
FOV	$\pm 60^\circ$
Type	2 orthogonal axes
Power	10 mW
Temperature of operation	243 to 358K
Accuracy	$< 0.5^\circ$
Sensitivity	$< 0.1^\circ$

Table 4.9 Solar Sensor specifications.



Figure 4-9 Sun sensor from Sinclair Interplanetary.

For the occasions where the sun is not visible it will be necessary to equip the basket with a sensor capable to determine the attitude without it. A gyroscope is a good solution being a MEMS-based gyroscope a solution with not as good precision as other based in different technologies, but out of the requirements they need. The special needs that the equipment has to be able to withstand in space implies that even MEMS gyroscopes, which have been used for years on earth and its size and weight are quite low, when to be used on space those properties are in part lost due the reinforcement necessary to properly work outside Earth [71]. For the purposes of this mission, a suitable gyroscope has been found in the QRS11 from Systron Donner Inertia [72].

QRS11 MEMS gyroscope	
Weight	60 g
Dimensions	Ø 41.275 x 16.383 mm
Range of detection	±100°/sec.
Power	400 mW
Temperature of operation	233 to 353K
Sensitivity	≤0.004°/s

Table 4.10 Solar Sensor specifications.



Figure 4-10 QRS11 MEMS gyroscope.

4.1.2.2. Data handling, processing and telemetry

In order to keep the weight of the basket as low as possible all the data will be processed in the rover, performing the minimal operations as possible in the basket, therefore only the necessary elements to gather the information of the different sensors and send it to the rover will be present on the basket.

The operation procedure of the balloon will start by an order of the main computer in the rover to obtain the information from a determined sensor in the balloon, this order will be given to the balloon controller in the rover which will be in charge of all the communication between the rover and the balloon. Then the balloon controller will send the necessary commands through the POF system to the balloon, where will be received by the balloon computer that will order the sensor controller to initiate the operation of the sensor, then the sensor will provide the data to the balloon computer and the information will flow to the rover. The sensor controller is basically a switch or relay that provide the correct current to the different elements, including the balloon computer, with the difference that the balloon computer switch will be always in the same position closing the energy circuit. Once the observation has finalized, the balloon computer will contact the sensor controller to shut down the sensor.

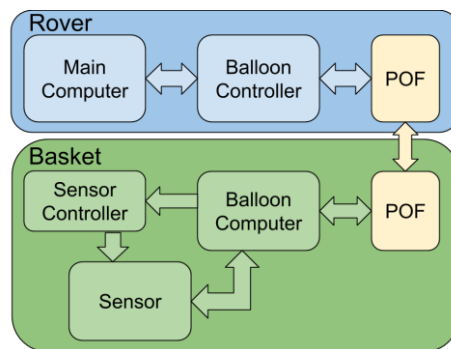


Figure 4-11 Information flow diagram considered for this proposal.

To establish the possible characteristics of the computer present on the basket the values of different COTS (Commercial Off-The-shelf) computer systems for CubeSat [73] have been used as an approximation, being 100g, 90 x 90 x 20 mm and a power consumption of 2 watts an approximation of the actual possible values a computer used for these purposes could have.

4.1.2.3. Communication system

The system chosen to provide energy to the basket is a POF system and the same system can be used to transmit data at a higher rate than copper cable and without being affected by electromagnetic disturbances. For the distance considered in this mission (a maximum of 500 m above the rover position) the system taken as reference is capable of transmit at 1 GHz with negligible signal loss. This transmission speed is more than enough as not all the instruments will be transmitting at the same time and their bandwidth is not as big, since they generate information at a rate of megabits per second and the system is capable to transfer gigabits per second. The flux of information will be greater in the downlink than in the uplink, with the thermal and design consequences it supposes.

4.1.2.4. Thermal control

The chosen POF system for communications and energy is based on transforming the laser light into electrical energy through a photovoltaic panel. This process generates heat, which could be used to keep the interior of the basket at the desired temperature by adjusting the part of the heat generated which will be released in the inside of the basket or released to the atmosphere. It could be possible as well to combine the periods of data transfer with the episodes when the heat is more necessary in the interior of the basket. As no detailed information about the heat produced by the element is not possible to determine if further heaters or radiators will be necessary to maintain a stable temperature inside the basket.

On the other side, silica aerogel will be included in the amount necessary to isolate the interior of the basket from the outside conditions in the required zones, but as stated before no detailed information is available and further studies about the basket configuration and heat flow might be necessary to determine its necessity.

4.1.2.5. Energy system

The method selected to provide electric energy to the basket is the use of Power Over Fibre, which present some benefits over the other methods. This system is lightweight, free from Electromagnetic Interference (EMI) as electrically nonconductive, remaining the basket isolated from the rover if the tether cable is nonconductive as well. With a POF system is possible to integrate the communications in the same system with an elevated bandwidth.

For the purposes of this proposal the specifications of this systems have been taken from the one developed by LaserMotive, the Micro-POF Mark 2, capable to provide a 70 watts DC power out to a maximum of 500 m with a receiver of 150 g while being able to transmit data [33]. As it can be seen in Table 4.11 the required power to operate the different sensors and systems present in the basket is below the capabilities of the Mark 2, and as the POF technology is scalable the final mass requirements may be lower than the generic ones used in this approximation.

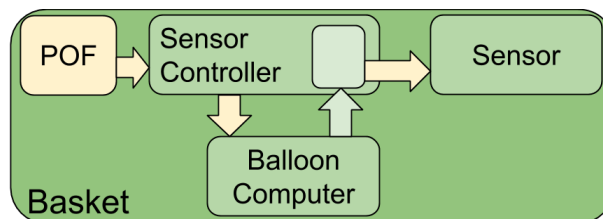


Figure 4-12 Energy system scheme.

The electric energy will arrive to the basket through the POF system, then the sensor controller will redirect the correct amount of energy to the on-board computer, which will command the sensor controller to provide energy to the sensors and the other systems when necessary. Taken as an approximation to the characteristics of the sensors controller the properties of offered COTS power systems for CubeSat [74] the physical characteristics (always considering that the one included in the basket won't be equipped with batteries) can be considered to be 100 g of mass, dimensions of 90 x 90 x 25 mm and 115 mW of power consumption.

Items in the basket	
Panoramic Camera	2.15 W
Panoramic Camera	2.15 W
Panoramic Camera	2.15 W
Balloon Camera	2.15 W
Gimbal Camera	1.5 W
Wind sensor	0.3 W
RHS	0.015 W
PS	0.015 W
Magnetometer	0.5 W
Solar Sensor	0.01W
Solar Sensor	0.01W
Solar Sensor	0.01W
MEMS gyroscope	0.4 W
MEMS gyroscope	0.4 W
Sensor controller	0.115 W
On-board computer	2 W
Thermal control	To be determined
	13.875 W

Table 4.11 Approximate power consumption of the elements in the basket.

4.1.3. Structure design

In order to provide a stable location to the different sensors located in the basket the structure needs to provide static equilibrium to all the elements, as well as having a profile that is not affected negatively by the winds on Mars. The shape chosen to fulfil these requirements is an ellipsoid with the two semi-major axis equal to 200 mm and the semi-minor axis being 50 mm, the resulting volume is an oblate spheroid. For this study case the thickness of the basket has been established in 3 mm to provide only a possible value to the mass required to conform it.

Despite the low density of the Martian atmosphere, the effect of the winds at the flight altitude must be taken in consideration, and the ellipsoid shape can provide a similar response no matter the direction of the wind. Following the same principle, the different instruments over the surface of the ellipsoid must not imply a big impact in the basket behaviour, as well as produce as low interference between them as possible. The general distribution of the different elements located in the exterior of the basket can be seen in Figure 4-13. In Figure 4-15 the storage configuration of the movable elements in the bottom of the basket can be observed and compared with the deployed position. It can be observed as well that the vertical position of the wind sensor provides it with minimal interference with the wind disturbances produced by the other elements (to assure the correct interpretation of the results of the WS further studies in a wind tunnel or CFD simulations are highly necessities).



Figure 4-13 Bottom view of the design proposed for the basket, with most of the scientific instruments in sight.

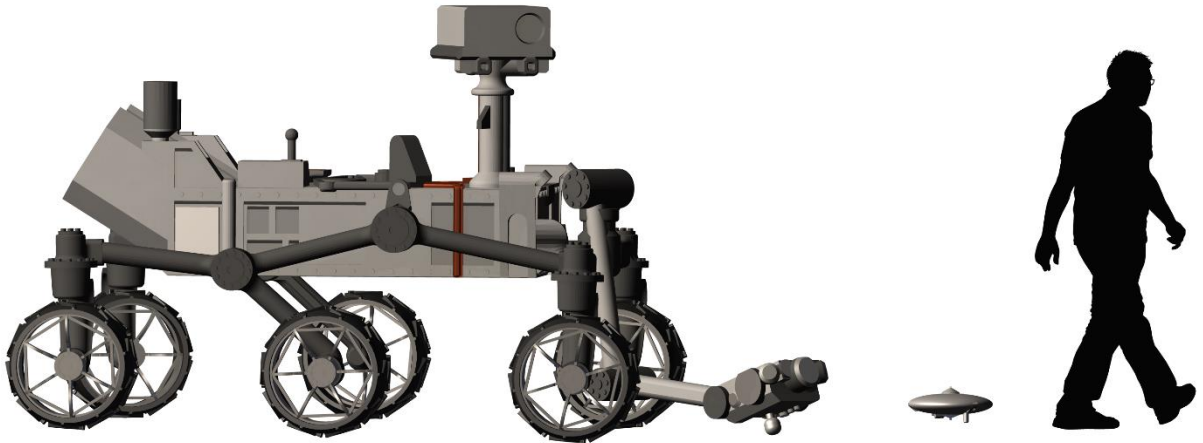


Figure 4-14 Representation of the basket with a simplified model of the NASA Curiosity rover and a human figure to provide a scale.

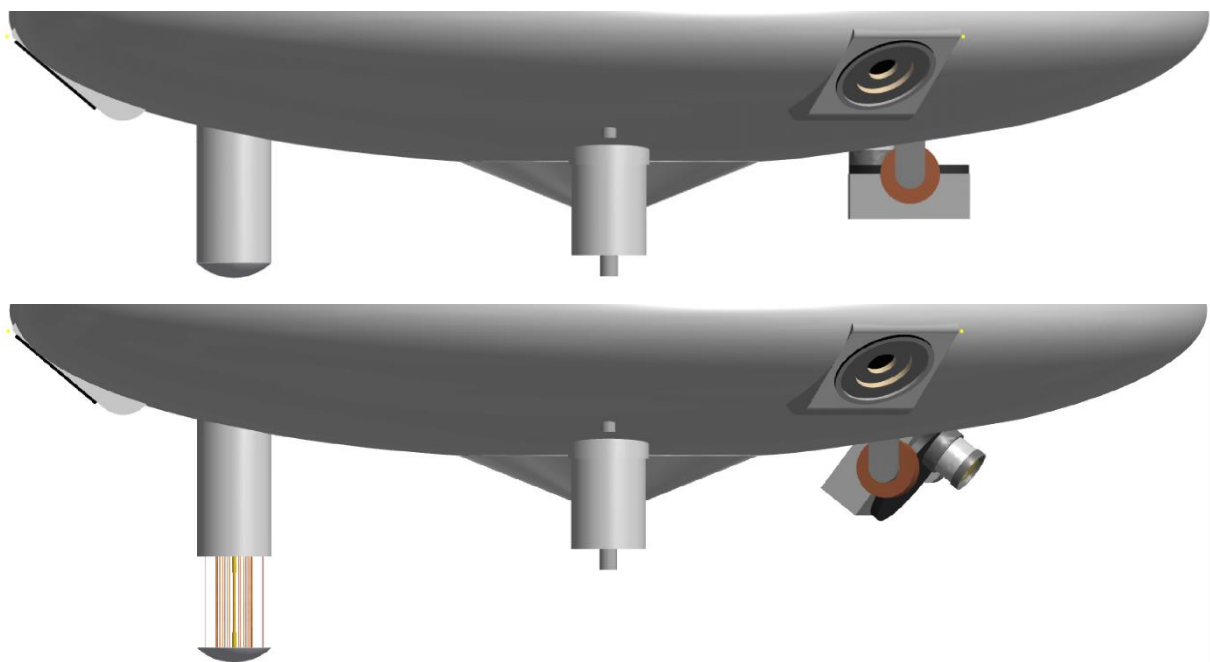


Figure 4-15 Bottom half of the basket with the instruments in storage position (superior image) and in deployed position (lower image).

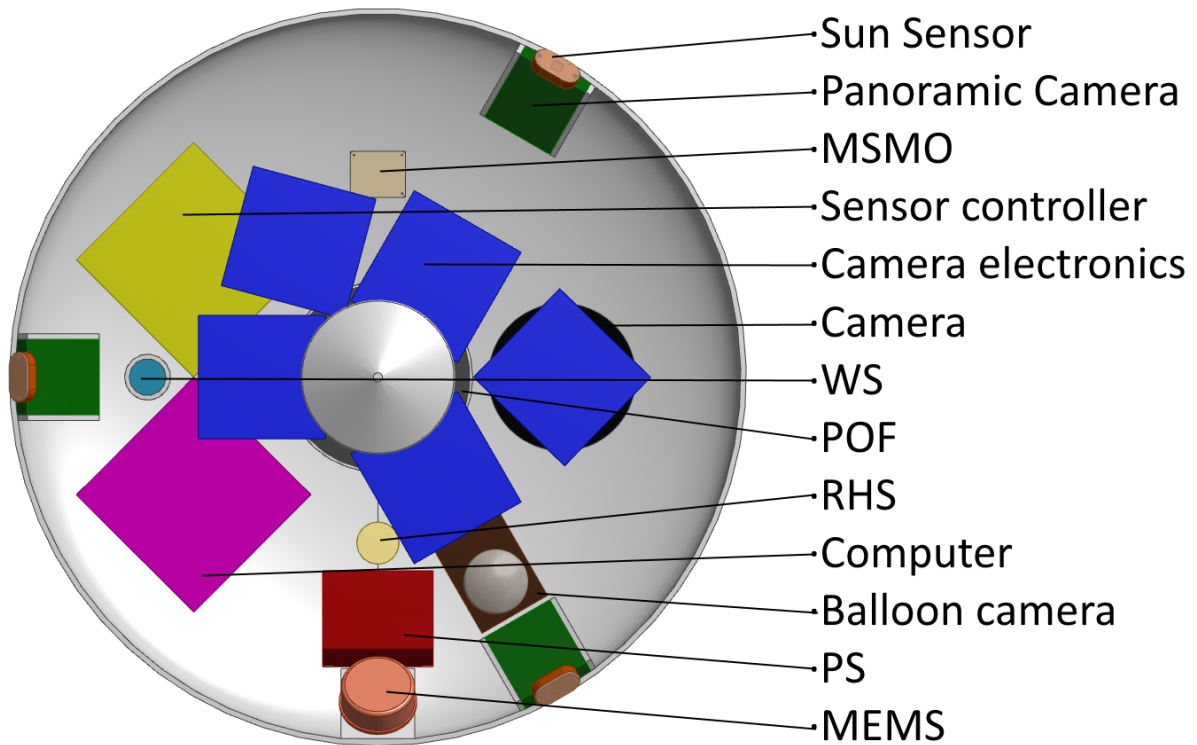


Figure 4-16 Upper view of the interior of the basket with the disposition of the electronics and sensor calculated to maintain equilibrium.

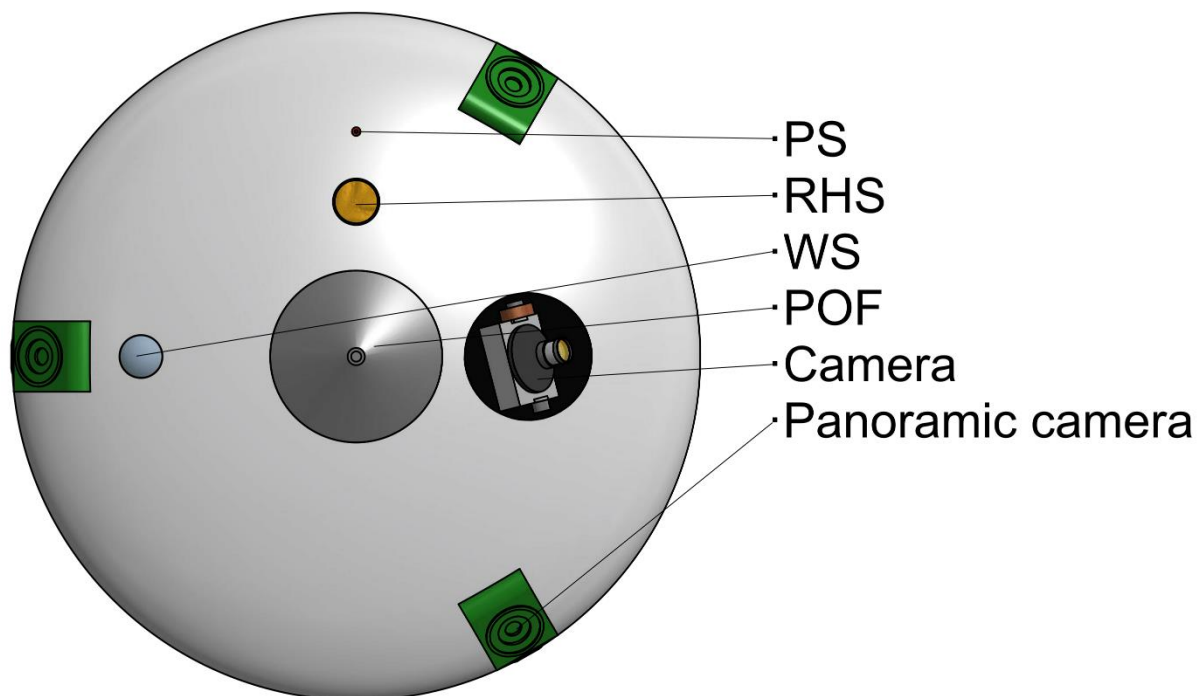


Figure 4-17 View from below of the basket with the instruments located on it.

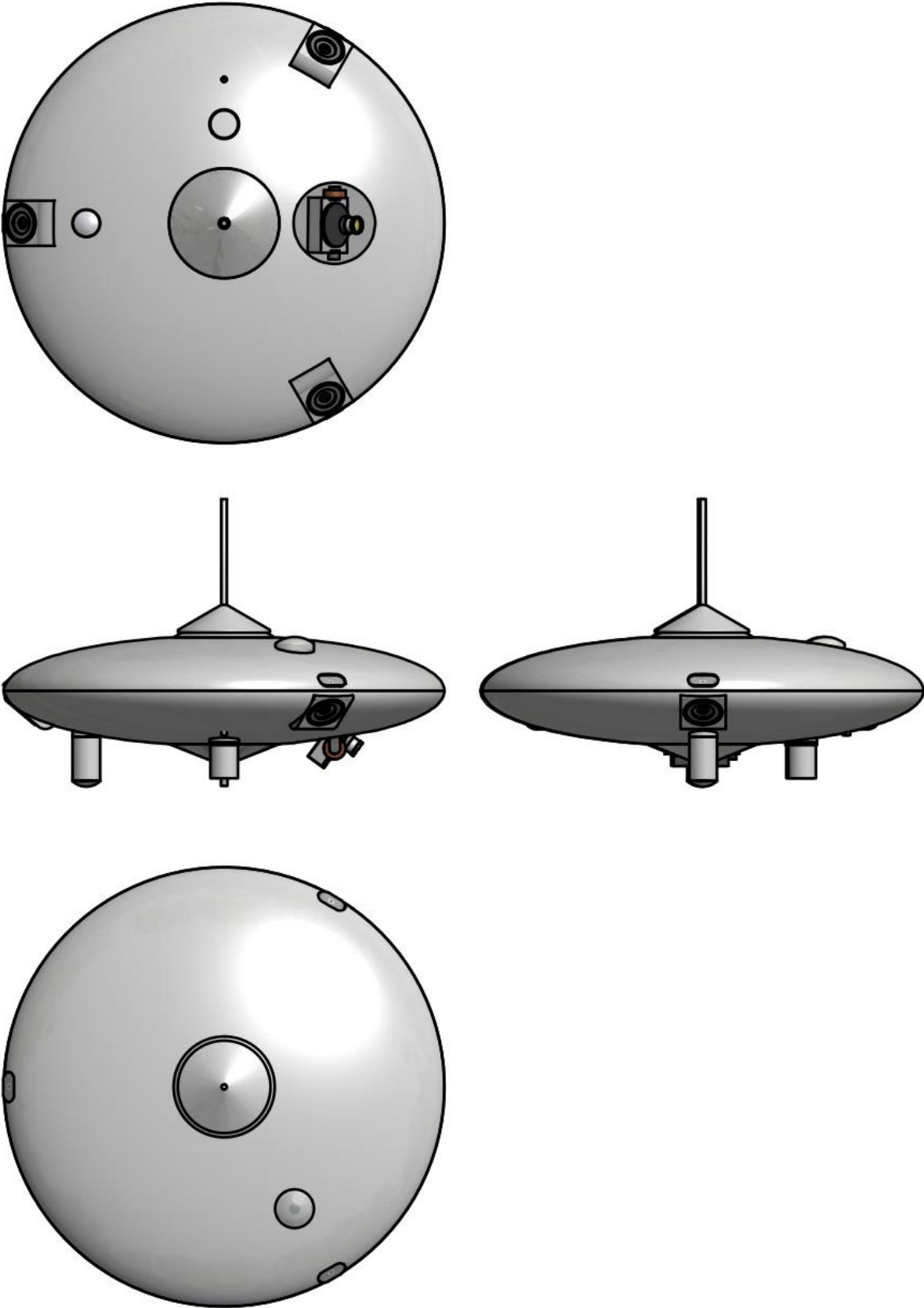


Figure 4-18 Upper, lower and side views of the basket.

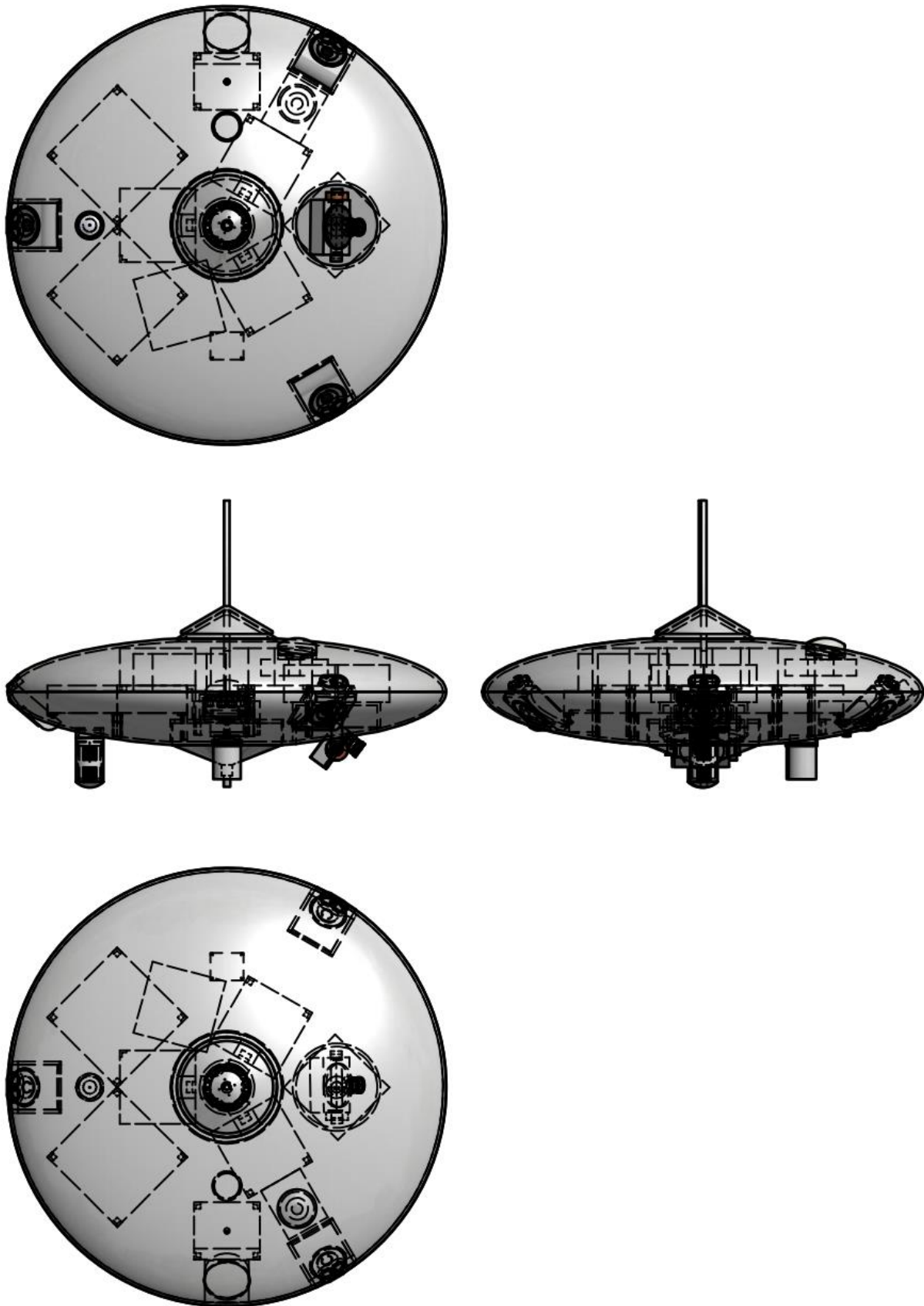


Figure 4-19 Upper, lower and side views of the basket with the hidden elements represented by dashed lines.

The different instruments are located in positions where the static equilibrium of the basket is assured while keeping themselves free of interference with each other and assuring the proper aiming for the different sensors. With this consideration the panoramic cameras are located in the exterior part of the ellipsoid, spaced 120° from each and oriented 40° below the horizontal, providing a complete view of the surface below the basket up to approximately 2,2 km, with a triangular zone with a base of about 645 m where the FOV of the three panoramic cameras are superposed as can be seen in Figure 4-21 a. After this full coverage area, the FOV of the cameras cover each one of them an area of about 57 km in distance with a FOV of 97° [75].

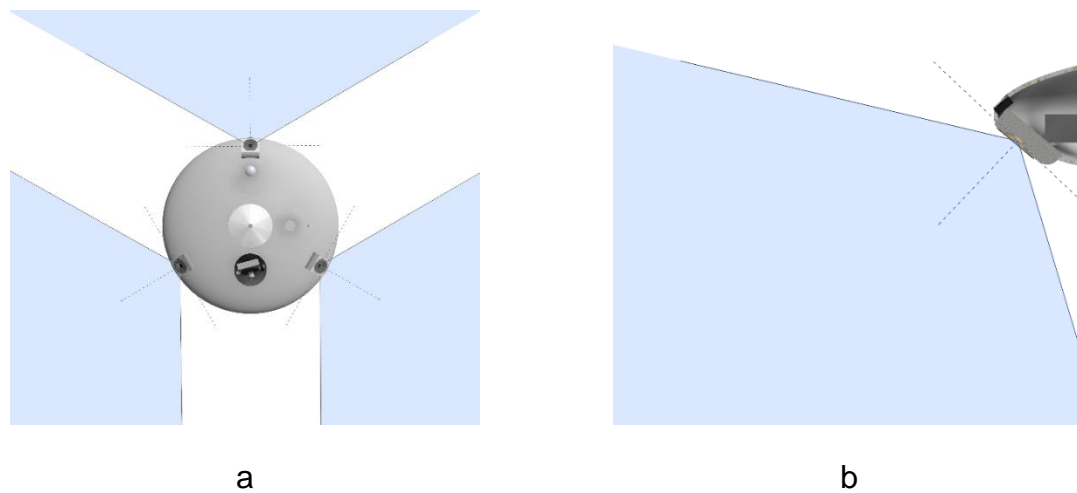


Figure 4-20 Horizontal (a) and vertical (b) simplified field of view of the panoramic cameras.

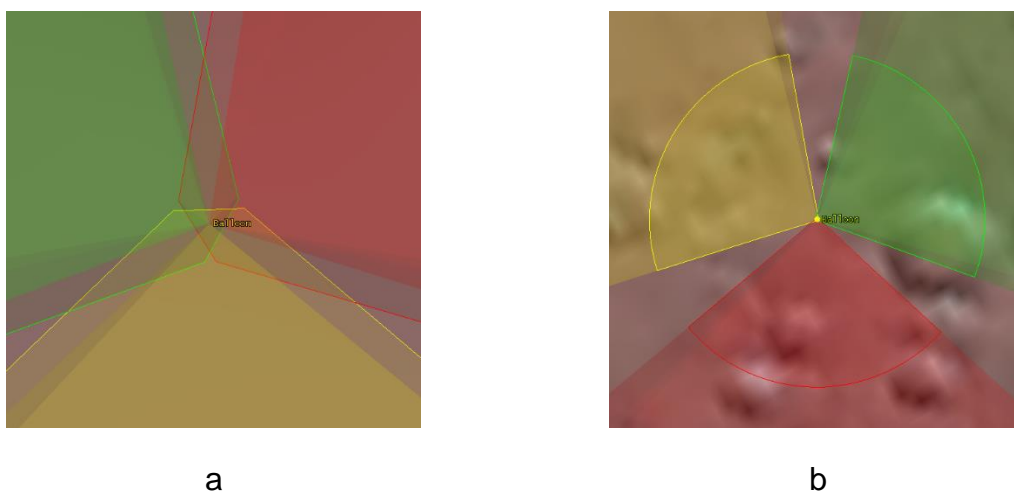


Figure 4-21 Detail (a) and general view (b) of the panoramic cameras FOV. The delimited zone is the terrain covered, and the coloured zones without limits correspond to the over the horizon FOV.

As the sun sensors share the same FOV as the panoramic cameras they have the same horizontal distribution, but the sensor is at 40° with the horizon, covering 10° below the horizon and overlapping some areas with the other sensors above the horizon and only having a small triangular zone from the sky without coverage, as can be seen in Figure 4-22 b.

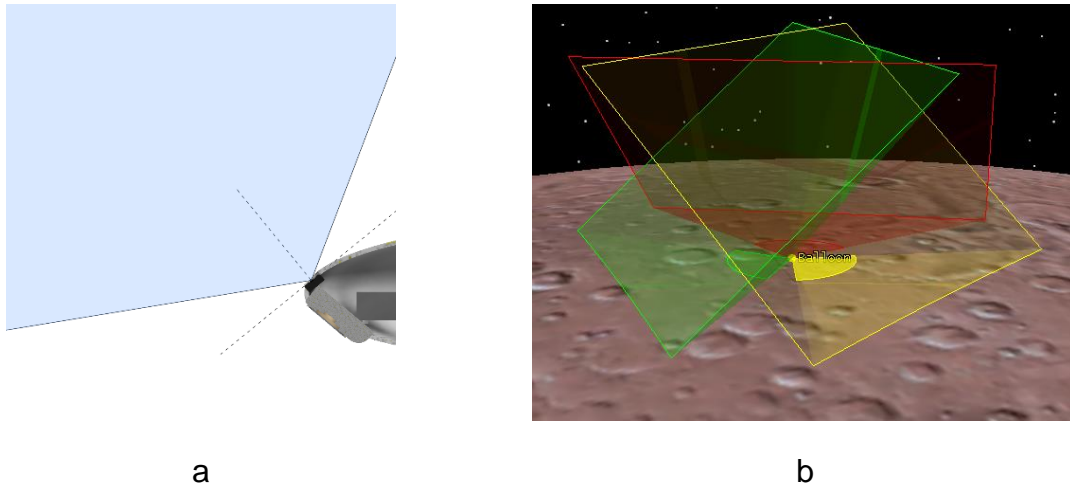


Figure 4-22 Sun sensor vertical FOV (a) and 3d representation of the Sun Sensor sky coverage (b).

The camera equipped with filters and magnification to perform wider range of observation has been located in the bottom of the basket in a gimbal system, allowing it to take pictures in any direction through a two axis rotation system. As seen in Figure 4-15 the camera will be positioned in a storage position until the deployment on Mars, in order to save space and to protect the lens from the impact of small rocks or dust during the landing. As well as the other elements in the balloon the camera will be properly shielded against radiation and the external conditions.

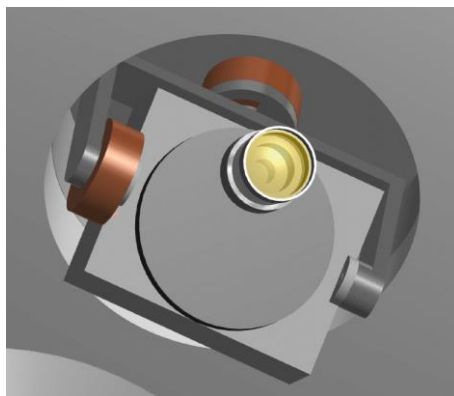


Figure 4-23 Detail of the camera with the ring of filters, the magnification system and the two axis gimbal support.

To provide a proper union between the tether cable, the balloon and the basket, in this last one a mechanism will unite the tether cable and the cables from the balloon. In Figure 4-24 this mechanism is represented in green, being the red element the POF system and the basket structure in blue. The mechanism allows the balloon to rotate freely due to the wind effects, without applying further stress to the tether cable.

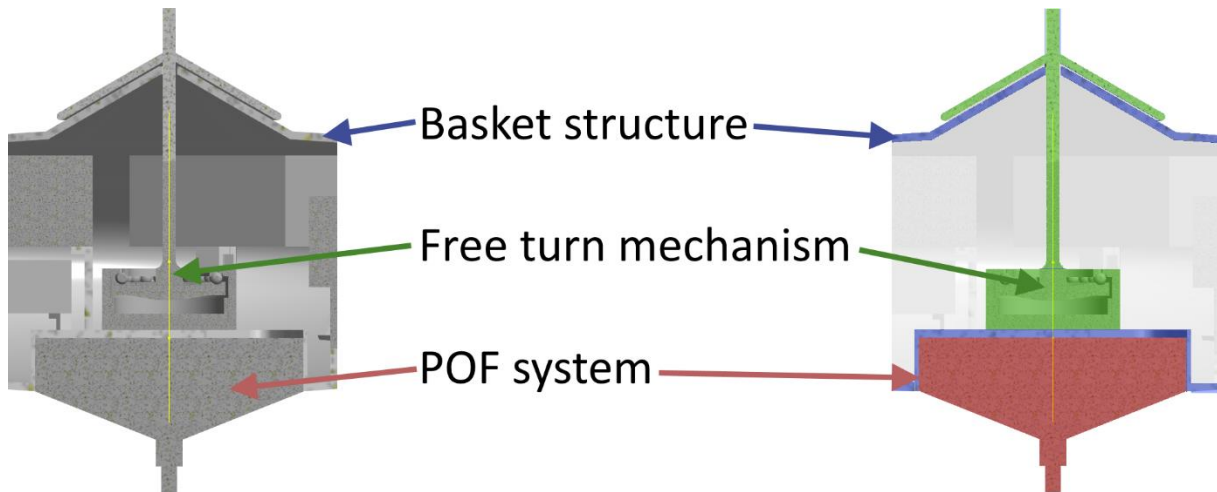


Figure 4-24 Union between the tether cable, the basket and the balloon.

The estimated weight for the basket elements, including the bottom and the upper part of the basket and the union element of the tether cable and the balloon is estimated considering the use of Selective Laser Sintering as a manufacturing process. The material selected for it is Windform[®] XT 2.0 due to the material good properties and behaviour, as for example its good outgassing performance which allow the use of it for space applications. To obtain the mass of the material used the density of the material provided by the material company [76] was introduced in the CAD software for the specific CAD part designed and the software provided the estimated mass included in Table 4.12.

Part	
Basket lower part	404 g
Basket upper part	485 g
Tether union	34 g
Total	923 g

Table 4.12 Basket structural elements mass.

4.2. Tether cable

The main two candidate materials for the tether cable are aramid fibres, Kevlar 49 and Zylon, but as Zylon presents a lower density with similar mechanical characteristics will be the one used for the calculations. Using the values obtained from [29] for the forces a tether cable might suffer of a balloon of similar characteristics, a load of approximately 150 N is the maximum expected due to the wind effects, applying the correspondent safety factor (FS=4 correspondent to human spacecraft [77]) the diameter necessary of tether is obtained. Zylon has a tensile strength of 5800 MPa and a density of 1540 kg/m³ [78]. Using the tensile strength formula 4.1, and isolating the radius of the area the equation 4.2 is obtained and operating the square in the radius 4.2 is finally obtained. Applying the force, the safety factor and the tensile strength to 4.3 the necessary radius of the tether cable is obtained.

$$\sigma = \frac{F \cdot SF}{A} = \frac{F \cdot SF}{\pi \cdot r^2} \quad (4.1)$$

$$r^2 = \frac{F \cdot SF}{\pi \cdot \sigma} \quad (4.2)$$

$$r = \sqrt{\frac{F \cdot SF}{\pi \cdot \sigma}} \quad (4.3)$$

The results indicate that a tether cable of Zylon with a diameter of less than 0,4 mm is capable to resist the loads that can be present in the Mars environment. With this diameter and the altitude where the balloon will be placed (500 m), the volume (0.2 m³), and therefore the mass, of the tether cable can be estimated in 308 g. As the Zylon fibres are sensitive to UV radiation a coating is necessary to resist the Martian conditions, it has been taken in consideration by using a tether diameter greater than the obtained by the calculations. The optic fibre from the POF system will be braided with the tether cable, without being responsible to support the loads.

4.3. Balloon

In order to correctly define the characteristics of the balloon necessary to lift the different elements of the payload, the mass of this elements is crucial. In this mission proposal several elements chosen to be part of the payload were not designed to be airborne, and therefore their mass might not be representative of an element conceived with lightweight as main focus. In conclusion, specifically designed elements for this type of mission could drastically reduce the total mass of the payload, and therefore enable a more compact balloon or maintaining the balloon dimensions improve the duration of its mission or include more instruments.

4.3.1. Balloon dimensions

The first step to correctly establish the dimensions of the balloon capable of lifting the payload is to establish the mass it will be required to lift. The total mass of the basket and of its component can be observed in Table 4.13.

Items in the basket	
Panoramic Camera	245 g
Panoramic Camera	245 g
Panoramic Camera	245 g
Balloon Camera	245 g
Gimbal Camera	~250 g
Wind sensor	30 g
RHS	13 g
PS	35 g
Magnetometer	150 g
Solar Sensor	4 g
Solar Sensor	4 g
Solar Sensor	4 g
MEMS gyroscope	60 g
Communication system	Mass included in the energy system
On board computer	100 g
Sensor controller	100 g
Thermal control	TBD
Energy system	150 g
Structure	923 g
Tether cable	308 g
Total	3111 g

Table 4.13 Mass approximation for the different elements in the basket and the basket itself.

The buoyancy of a balloon can be expressed as in equation 2.1, rearranging the elements of that equation 4.5 is obtained, being m_{He} the helium mass, $m_{envelope}$ the mass of the balloon envelope and $m_{payload}$ the mass of the payload (the basket and the different elements inside), ρ_a is the density of the atmosphere outside the balloon, ρ_{He} is the density of the Helium inside the balloon, g is the gravity and V is the balloon volume.

$$\rho_a \cdot V \cdot g = \rho_{He} \cdot V \cdot g + m_{envelope} \cdot g + m_{payload} \cdot g \quad (4.4)$$

$$\rho_a \cdot V = \rho_{He} \cdot V + m_{envelope} + m_{payload} \quad (4.5)$$

$$V \cdot (\rho_a - \rho_{He}) = m_{envelope} + m_{payload} \quad (4.6)$$

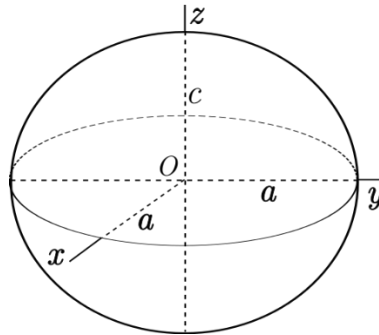


Figure 4-25 Semi-axis distribution on a spheroid.

As the mass of the balloon envelope is at this point unknown and a function of the final volume of balloon necessary to lift everything, this value can be approximated by using equation 4.6 using the known values for the density of the gas inside the balloon, the density of the atmosphere at the desired equilibrium point, the payload mass already obtained and the volume of the balloon. As the mass of the envelope depends on the volume the payload mass can be estimated given a volume value. The dimensions of the balloon have been approximated by obtaining the ratio between diameter and height of super pressure test balloons from photography's contained in [20] and [19] and calculating the average values for the oblate spheroid obtaining the following relation between the semi-axis:

$$a = 1,559055 \cdot c \quad (4.7)$$

$$V = \frac{4}{3} \cdot \pi \cdot a^2 \cdot c \quad (4.8)$$

$$S_{Oblate\ Spheroid} = 2 \cdot \pi \cdot a^2 \cdot \left(1 + \frac{1 - e^2}{2} \cdot \tanh^{-1} e \right) \quad (4.9)$$

$$e^2 = 1 - \frac{c^2}{a^2} \quad (4.10)$$

With the relation of the semi-axis and the volume and surface formulas (4.8 and 4.9) it is possible to establish the relation between the dimensions of the balloon and the payload it will be able to lift. To determine the envelope mass is necessary to calculate the envelope thickness necessary to sustain the difference of pressure that will exist at the operation altitude, being the chosen material Linear Low-Density Polyethylene (LLDPE) with a minimum Young's module of 250 MPa and a density of 911 kg/m³ [79]. Having the balloon pumpkin shape the effort the material will have to sustain will be in the horizontal direction.

To obtain the thickness necessary is necessary to start with equations related with the calculations of pressured vessels. For this is necessary to considerate the balloon cut in half by a vertical plane.

$$P = \Delta P \cdot A_{ellipse} \quad (4.11)$$

$$Horizontal\ Force = \sigma \cdot L_{ellipse} \cdot t_{envelope} \quad (4.12)$$

Being ΔP the pressure difference between the inside and the outside of the balloon, $A_{ellipse}$ the area of the interior of the cut, $L_{ellipse}$ the perimeter of that cut, σ the stress in the material and $t_{envelope}$ the thickness of the envelope. The area and the perimeter can be obtained by the area of an ellipse (4.13) and the Ramanujan approximation for the ellipse perimeter (4.14).

$$A_{ellipse} = \pi \cdot a \cdot c \quad (4.13)$$

$$L_{ellipse} = \pi(3 \cdot (a + c) - \sqrt{(3 \cdot a + c)(a + 3 \cdot c)}) \quad (4.14)$$

$$\Delta P \cdot A_{ellipse} = \sigma \cdot L_{ellipse} \cdot t_{envelope} \quad (4.15)$$

$$t_{envelope} = \frac{\Delta P \cdot A_{ellipse}}{\sigma \cdot L_{ellipse}} \quad (4.16)$$

The neutral buoyancy altitude used for the calculations is actually higher than the actual service altitude, set to be 500 m. This will reduce the effects of the wind in the balloon position allowing a closer position to the vertical of the rover and improving the life expectancy of the balloon at the desired altitude as the extra amount of helium will compensate the permeability of the balloon envelope. Therefore, the altitude value used for the calculations has been established in a value 50% greater, being 750 m of altitude the neutral position for the balloon in design. As can be seen in Figure 4-26 and Figure 4-27 the difference in the capabilities of the balloon are minimal, the values used to represent this figures can be reviewed in ANNEX III: Balloon buoyancy. The value obtained for the envelope mass has been incremented in a 15% to contemplate the pumpkin shape of the balloon, as the close to 90° lobes forming a pumpkin shape suppose approximately an increment of an 11% in the outline in the horizontal plane and consequently an increase of the same magnitude in the surface, volume and mass of the envelope.

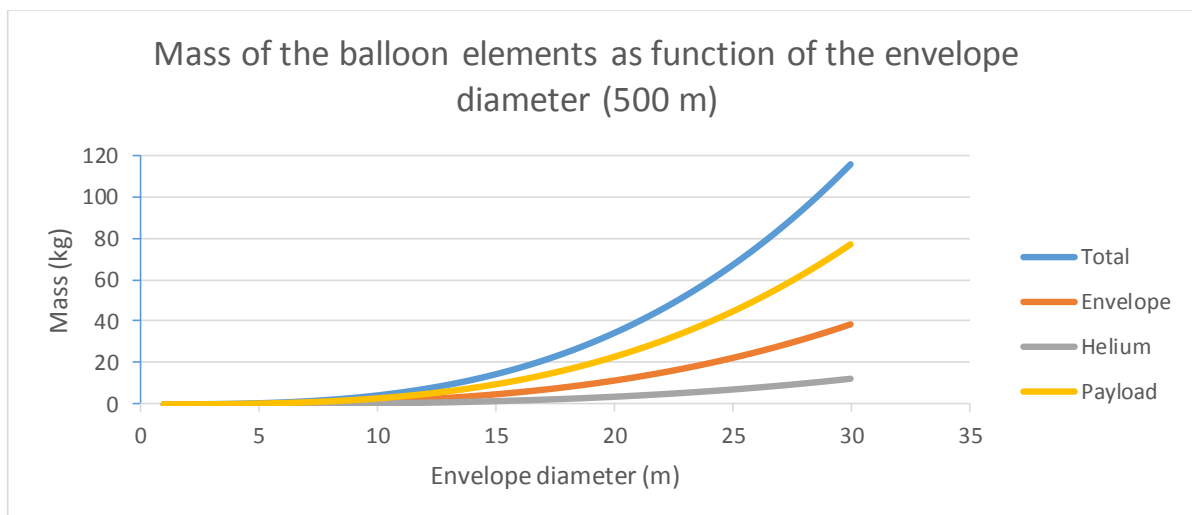


Figure 4-26 Mass distribution for a super-pressure balloon with a neutral buoyancy altitude of 500 m.

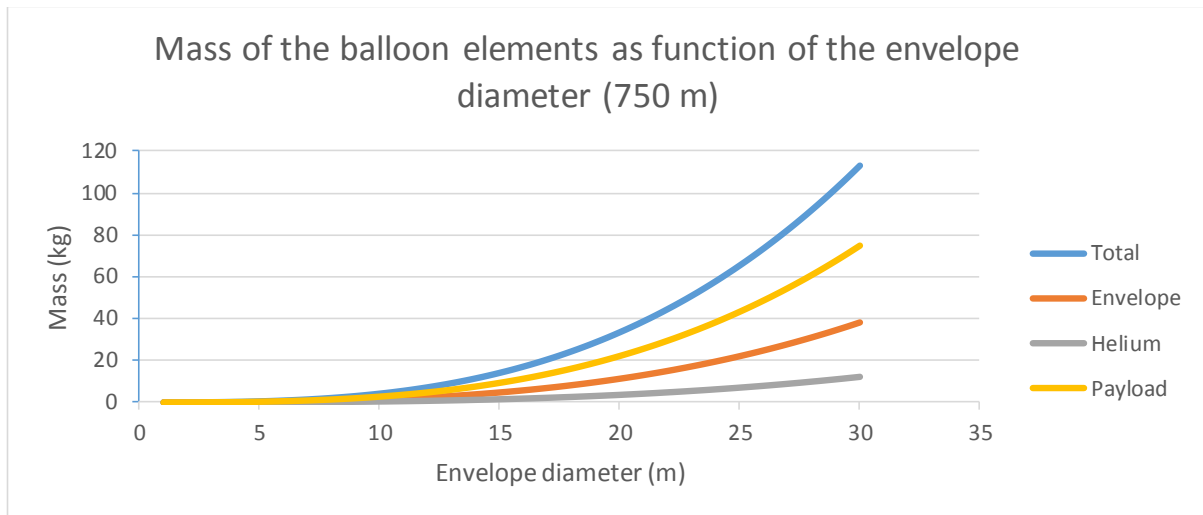


Figure 4-27 Mass distribution for a super-pressure balloon with a neutral buoyancy altitude of 750 m.

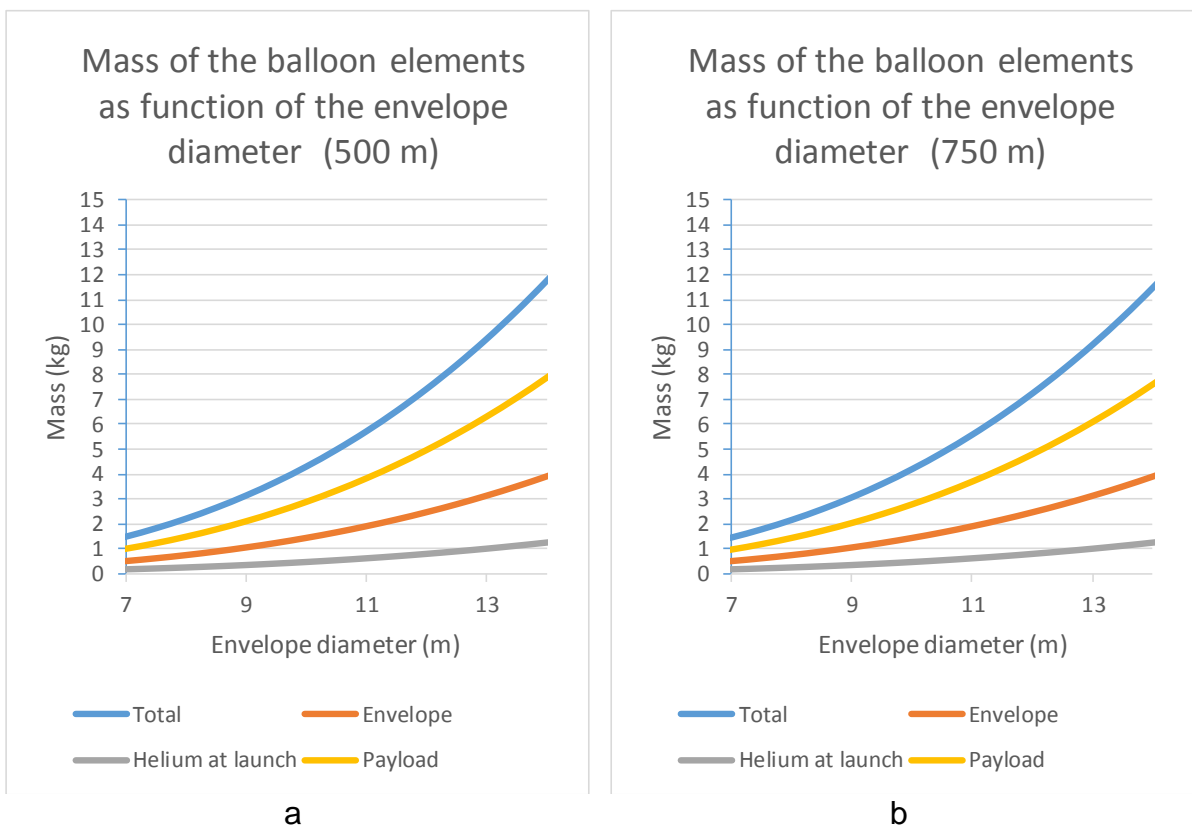


Figure 4-28 Detail of the mass and diameter for the values close to the obtained for the balloon here presented for 500 m (a) and 750 m (b).

From the data in ANNEX III: Balloon buoyancy, considering the mass of the payload and performing some calculations the balloon diameter estimation provides a value between 10 m and 10.5 m, taking the 10.5 m diameter balloon value for the envelope, it will have a mass of 1.63981 kg which will be used to perform posterior calculations.

Using the values gathered in this chapter the volume of the balloon can be obtained by modifying equation 4.6 to isolate the volume parameter obtaining the equation 4.17, the final dimensions and characteristics of the super-pressure balloon are indicated in Table 4.14. One of the considerations for this calculations is that the initial density of the Helium inside of the balloon is affected by the temperature, and therefore this correction has been taken into consideration when performing the computations. The excess of mass due to the smaller envelope necessary from the one used in the calculations will be considered the part of mass due to the tendons and cords necessary to link the basket and the balloon, as well as a possible valve to regulate a possible situation of overpressure of the Helium.

$$V = \frac{m_{envelope} + m_{payload}}{(\rho_a - \rho_{He})} \quad (4.17)$$

Definitive balloon characteristics	
Balloon volume	381,081 m ³
Oblate spheroid a (balloon radius)	5,215 m
Oblate spheroid c	3,345 m
Balloon height	6,690 m
Payload mass (basket, instruments, etc.)	3.111 kg
Balloon envelope mass	1,640 kg
Balloon total mass	4,751 kg
Helium mass	0,509 kg
Envelope thickness	4,93611x10 ⁻⁰⁶ m
Envelope stored volume	0,00154 m ³

Table 4.14 Main characteristics of the different elements of the balloon.



Figure 4-29 Representation of the Deployed balloon with the basket and the NASA Curiosity rover and a human figure for scale.

As the balloon is not in a neutral buoyancy altitude there is an additional term in the forces equilibrium equation. This term is named free lift force and is represented in 4.18 as F_{FL} and can be considered the force responsible to move the balloon towards its neutral position. The values for this force are indicated in Table 4.15 and Table 4.16, being the first one the value for the moment of the release of the balloon and the second one the value of the force at the operating altitude due to choosing a higher neutral buoyancy point to provide more stability to the balloon.

$$V \cdot (\rho_a - \rho_{He}) \cdot g = (m_{envelope} + m_{payload}) \cdot g + F_{FL} \quad (4.18)$$

$$V \cdot (\rho_a - \rho_{He}) \cdot g - (m_{envelope} + m_{payload}) \cdot g = F_{FL} \quad (4.19)$$

Free lift at 0m	
Atmosphere density	0,014694 kg/m ³
Helium density	0,001334611 kg/m ³
Free lift	1,262474733 N

Table 4.15 Free lift force at the moment of the balloon release.

Free lift at 500m	
Atmosphere density	0,014133037 kg/m ³
Helium density	0,001394401 kg/m ³
Free lift	0,384611644 N

Table 4.16 Free lift force at the operation altitude of the balloon.

4.4. Rover equipment

Being the balloon united to a rover and using this connection to obtain energy and transmit information, the rover need to be equipped with several systems to guarantee the correct performance of the balloon. Among other elements the POF system will serve as a communication link between the rover computer and the balloon computer, as well as provide the energy necessary to send it through the fibre towards the basket.

In the usual configuration of nowadays rovers, the highest point of their structure is the mast where the different cameras and other instruments are located. By being the highest point, the most adequate to accommodate the fixing point for the tether that unite the basket and the rover, its position might help to prevent the undesired interaction between the tether and the rover's instruments or mechanisms. At the fixing point will be located a severing mechanism capable to cut the tether when the balloon lose its lifting capabilities or other incidents can make the tether cable a danger for the rover, its instruments or mechanisms.

It can be considered as well that the tank containing the Helium used for the balloon inflation is part of the rover equipment, even if afterwards is detached.

It could be interesting to contemplate the possibility of using the rover robotic arm (if it is equipped with a proper device) to release the rover or his components from the balloon or the tether cable if an incident occurs where one of those ends up interfering with the proper functionality of the rover or its components.

4.5. Deployment

The deployment of the balloon will start once the rover is in the planet surface, in the most adequate moment to prevent that any rover equipment interferes with the inflation process. The balloon envelope will require the proper folding in order to prevent the envelope to fall over the rover or make contact with elements that can puncture or damage it.

The ideal position of the balloon for the deployment is on an elevated surface where no elements could puncture the envelope, being the upper part of the rover the more adequate. The first step in the balloon deployment will be testing the correct performance of the basket systems and in case they don't respond abort the deployment to avoid any possible danger for the rover main mission. Once all the elements located in the upper surface of the rover during the travel from Earth that could be deployed without jeopardising the envelope integrity are at their final position the balloon inflation will start.

Once the balloon is fully inflated it will be released from temporary fixations and a test on the basket systems will be performed while the basket is still fixed to the rover. If the results are positive the basket fixations will be released and the basket and the balloon will start to elevate towards the operational altitude while it raises as well the tether, which will be located in a position where it won't interfere with any other element. With the tether fully deployed the balloon and the basket would be at their operational altitude, and a full diagnosis will be performed to the basket systems to calibrate the systems and assure their correct performance.

4.6. Mission Operation

The normal operation of the different systems will have several elements working continuously in the background such as the gyroscope or the sun sensor to provide an accurate positioning of the basket and their different instruments. This forces elements such as the on board computer, the sensor controller and the POF system to work as well, providing also heat to the interior of the basket to compensate the external temperatures.

Other instruments, such as the wind sensor or the relative humidity sensor will work under scheduled activation to provide a consistent data rate, while cameras will probably proceed with a mixed system, with several control images during the sol and on demand images. As the data flow generated by the cameras is the greatest of all the instruments included in the basket it might be impossible to use them all at once, and therefore their simultaneous use will be limited by the capabilities of the systems in the basket.



Figure 4-30 Representation of the balloon and the basket floating in the Mars atmosphere.

The correct performance of the balloon will be monitored by two main instruments, the camera focusing the balloon to detect changes in its shape or possible punctures and the pressure sensor, which will continuously control the pressure and therefore the altitude of the set. An additional control element can be the inclusion of a sensor detecting the force the balloon is applying to the tether, as the balloon will continuously pull the tether upwards while it is capable to lift the payload.

In case any serious abnormality in the altitude or the good condition of the envelope is detected the severing mechanism existing in the fixing point on the rover will cut the tether to, helped by the wind, prevent the set (balloon, basket and tether) to fall in the proximities of the rover and damage it with an impact or tangling it with the tether cable or the envelope. As the service life of a rover is greater than the expected for a balloon in Mars this mechanism will assure that the primary mission of the rover is not affected by the relatively short life expectancy of this piggyback mission.

In order to increase the safety of the rover it might be possible to include a parachute in the basket in order to reduce its speed and help it to soar away with the wind in case the balloon explodes, to avoid an impact to the rover, but it will imply an increase in the payload mass.

4.7. Balloon lifespan

The gas contained inside a balloon has a natural inclination to scape, leaking through holes or damaged parts or by diffusion through the envelope material.

$$\text{Rate of loss} = \frac{\delta \cdot P \cdot A}{t} \quad (4.20)$$

$$\text{Per cent volume loss per time unit} = \frac{\text{Rate of loss}}{\text{Volume of the balloon}} \quad (4.21)$$

With this two equations is possible to calculate the quantity of Helium the balloon will lose every sol, being δ the permeability of the polyethylene to Helium at 25°C (298K), P the partial pressure of the gas, A the surface of the balloon in contact with the atmosphere and t the thickness of the envelope. The values obtained by this procedure can be reviewed in ANNEX IV: Balloon Lifespan.

The results here obtained are a mere approximation, as values for the permeability for the material used in the envelope at the temperature it will be exposed has not been found and on its place the vale provided in the Table 2 of [17] have been used after the necessary unit conversion. As well the increase in the balloon surface due to the pumpkin shape has not been taken in consideration for this approximation and using instead the surface of the oblate spheroid of same volume. The lifespan here obtained is only valid a first approximation as it does not take into consideration the dynamic conditions of the Mars atmosphere, with cyclic variations in temperature and pressure of the atmosphere in a daily basis. Is it important to remark as well that the envelope material will be exposed to an adverse environment with dust and UV radiation among other things that would probably have an impact in any lifespan expected.

The outcome of the calculations shows that approximately sol 48 will be the last day the balloon will preserve the status of super-pressure balloon. From the release sol to sol 48 the lift capability of the balloon will be increasing as the quantity of Helium inside the balloon will decrease while conserving the same volume, reducing the density of the gas and therefore increasing the lift capability according to equation 4.18. From sol 48 onwards the reduction in Helium mass will entail the balloon volume reduction while it keeps the atmospheric pressure and consequently the lift capability of the balloon until approximately sol 88 when the balloon won't be capable to lift the payload anymore and will start to descend.

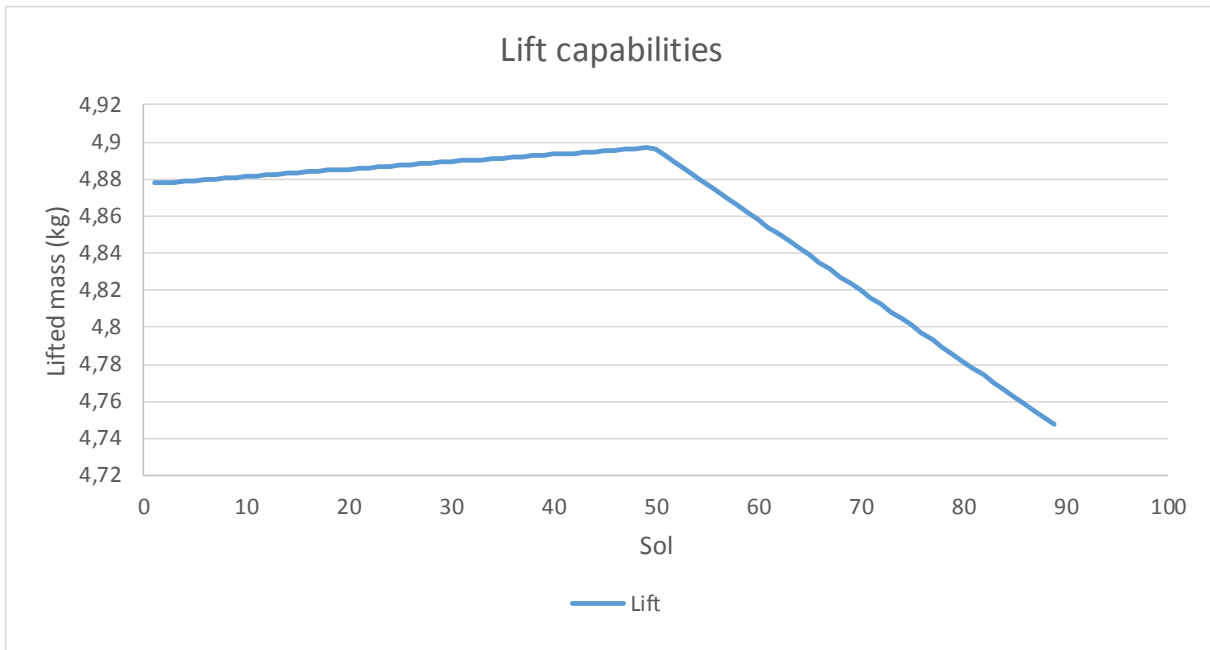


Figure 4-31 Lift capabilities of the balloon and the lift necessary to keep the balloon floating (total mass lifted).

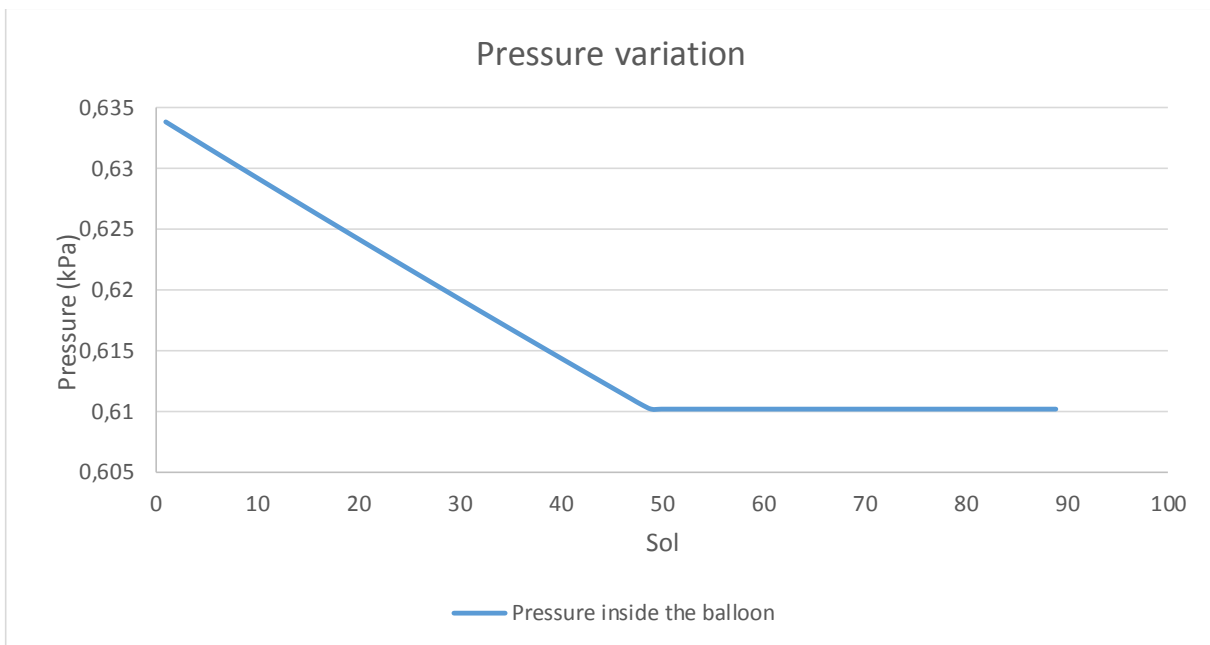


Figure 4-32 Pressure inside the balloon and atmospheric pressure during the balloon lifespan.

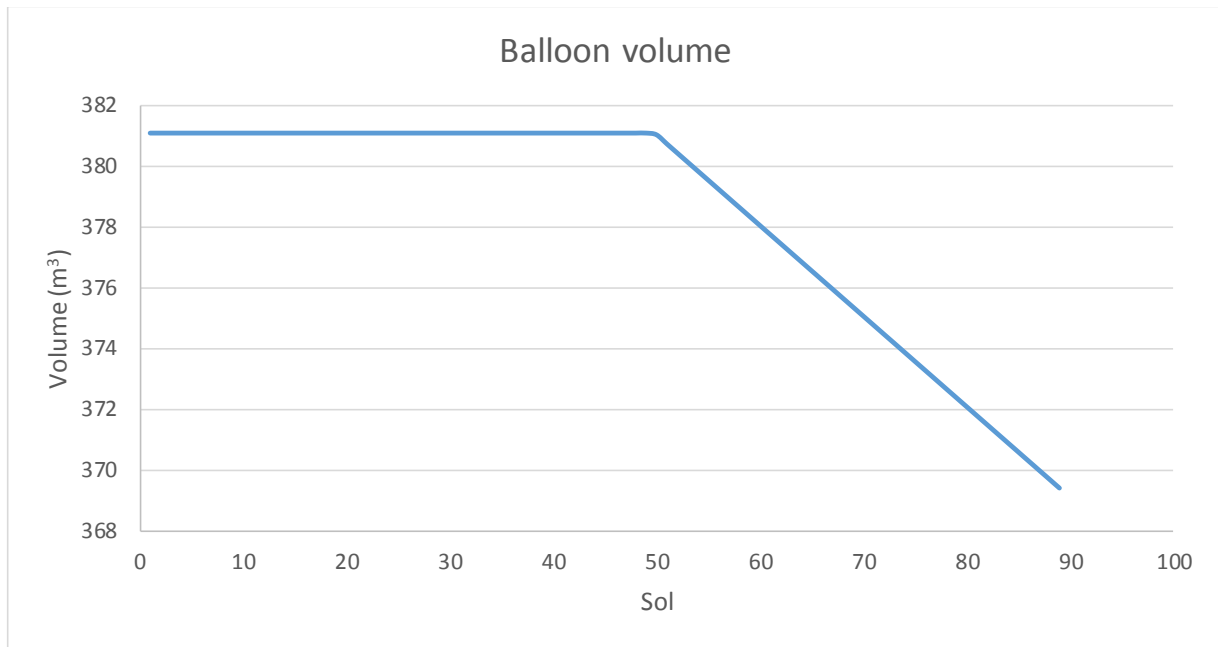


Figure 4-33 Balloon volume during its lifespan, notice the volume reduction once the gas in the interior reaches the atmospheric pressure.

Chapter 5

Further developments

As a technology demonstration and piggyback mission the objectives of the mission proposed here are humble compared to what a fully focused and developed mission based in balloons can offer, as the estimated mass for payload of the mission is below the 4 kg.

One of the logical next steps would be to increase the capabilities of the instruments on board, as well as introducing new ones such as spectrometers to study in detail the atmosphere composition at different altitudes. Another option would be to improve the lifespan of the mission by changing the balloon once it is near the end of its operational life. As the basket and all its instruments are designed to endure longer, this would only require a larger Helium tank, several envelopes (as much as desired) and a system capable to collect again the tether cable and exchange the balloon.

A different approach would be to use a tether balloon to deploy distant instruments or large ground structures, and once in the designated position deflate the balloon to locate the instrument or the end of the structure. With this approach and using the changing winds of Mars it might be possible for example to situate a net of sensors around a lander or gather soil samples from distant points by using a system to recover the tether cable.

When thinking in increasing the capabilities of the balloons to study mars, being tethered to a fixed point or a slow moving object in the surface is a major drawback, as their nature could allow them to float freely driven by the wind and therefore study wide areas of the surface in a level of detail only possible from their position. To perform this type of mission their dimensions will need to increase as they will need to be able to allocate the communication systems and power generation that in this proposal have been located in the rover.

This type of mission are already in study and several flight test have been performed simulating the characteristics of the Martian atmosphere [19] [27]. One of the biggest challenges for this kind of mission is to provide a solid solution to establish accurately enough the balloon position in the planet. This will allow to give the correct context to the information they collect and to communicate with the spacecraft in orbit that serve as a communication link to Earth, which may be difficult if the communication windows are not accurate enough.

The systems in development for this type of balloons include not only the flyover of the surface, but using the great range of possibilities that balloons offer to imagine different mission profiles. For example, balloons capable to place several small ground stations capable to create a network of seismographs on the Mars surface or balloons using the difference in the atmosphere temperature during the day and the night to land every night in different locations and acquire information from all those distant locations.

But letting the balloons soar with the wind is not only the only possibility to increase their capabilities. By providing the balloons with propulsion methods they will be capable to control their flight and therefore control their position. With this capability, locations that are nowadays unreachable by any other method used in Mars exploration will become accessible, and for example studying the Valles Marineris geological stratum (or any other geological accident) can open the door to study in detail the pass of the planet. This type of development will require an accurate positioning control as well as highly developed autonomous capabilities for flight.

In both cases the obstacle to save are great, from high performance energy storage and production systems to materials lightweight and capable to reduce as much as possible the permeability of the buoyant gas, while being capable to resist the stress produced during the balloon inflation. As Mars does not have a global magnetic field the navigation problem will be difficult to resolve, as there aren't enough satellites to generate a rudimentary positioning system, solutions as the seen in [37] can prove useful.

Nowadays it exists a lot of developments on several branches of science and engineer which if implemented in this type of mission could represent a leap forward in its feasibility, from supercapacitors to high efficiency solar cells and lightweight materials capable to shape a resistant and light structure.

Chapter 6

Conclusions

One of the objectives of this Master Thesis has been to confirm the viability of using balloons on Mars, by consulting different literature about it and performing the necessary calculations, it has been proven that the use of balloons in Mars is viable. Not all the configurations, sizes or lifting methods are capable to provide the necessary buoyancy to lift payload or to lift even their own mass, but nevertheless the suitable balloons can serve as a platform to perform scientific exploration for a wide range of different equipment, allowing a great variety in the type of missions balloons can carry out being a great deal of them impossible to implement in other platforms.

Balloons can become a great ally in the exploration of Mars, both by obtaining detailed information of great areas of the planet surface or as a complement to the type of missions carried out until these days, by for example increasing the range of sensors or allowing the study of zones that are not reachable by other means. In particular case of the mission proposed in this Master Thesis it has been studied the use of a balloon tethered to a base (a rover to be specifics) and the different methods of interaction regarding communications or energy among other things.

The mission proposal explained in these pages have several points that might deserve some reconsideration. The altitude of operation established for the balloon has been decided by using the maximum altitude than the capabilities of the POF system allowed to cover the maximum surface with the cameras as possible, but is quite probable than in a real scenario this altitude might become excessive as it does not provide the same level of detail than a lower position might.

A similar situation occurs with the orientation of some of the other sensors, that are probably not in the best position or orientation to develop their functionality to their maximum capabilities. A more detailed and specific analysis of all the factors affecting these elements might be capable to improve the expected performance of the systems listed in this Master Thesis. It is important to remark as well that most of the different components used for the systems of the mission proposal are elements designed for other missions or COTS, none of them designed with an airborne mission located in a balloon. For this reason, it is easy to estimate that specifically designed instruments and components could offer a much better response than the estimated here, improving the quality and the quantity obtained by this type of balloon mission.

Balloons lifespan is one of the factors that could be considered problematic in a planetary exploration mission, especially after the great performance of the last scientific missions to Mars but the objectives of a ground mission are different from the ones on an airborne one and the comparison of their lifespan does not have a lot of sense. Even so, the development of more resistant materials, improved methodologies and new designs will help to increase the lifespan of the balloons before a balloon mission is programmed to Mars.

Using a tethered balloon as a piggyback mission to Mars can prove to be a good test field to all the technologies that in the future can serve to send balloons as standalone missions to Mars, while providing a more controlled environment and lower risk of failure of a mission, as the rover will be able to perform normally its main mission not matter what is the fate of the balloon.

In conclusion, balloons can prove to be a good platform to explore those parts of Mars that otherwise might remain unreachable by more traditional methods, being possible to use them in conjunction with other mission configurations used to increase their capabilities, offering some of the advantages that airborne platforms can provide without the energy demands that airplanes or helicopters have.

Chapter 7

References

- [1] 'List of missions to minor planets', 2015. [Online]. Available: http://en.wikipedia.org/wiki/List_of_missions_to_minor_planets.
- [2] 'Missions - Mars Exploration Rover - Opportunity - NASA Science.' [Online]. Available: <http://science.nasa.gov/missions/mars-rovers/>. [Accessed: 09-Sep-2015].
- [3] 'Where is Curiosity?' [Online]. Available: <http://mars.nasa.gov/msl/mission/whereistherovernow/>. [Accessed: 09-Sep-2015].
- [4] 'ExoMars Rover.' [Online]. Available: <http://exploration.esa.int/mars/45084-exomars-rover/>. [Accessed: 02-Nov-2015].
- [5] R. Volpe, '2014 Robotics Activities at JPL', no. September, 2014.
- [6] 'ARES - A Proposed Mars Scout Mission.' [Online]. Available: <http://marsairplane.larc.nasa.gov/>. [Accessed: 08-Jun-2015].
- [7] H. Song and C. Underwood, 'A mars VTOL aerobot - preliminary design, dynamics and control', *IEEE Aerosp. Conf. Proc.*, 2007.
- [8] J. A. Jones, 'Inflatable Robotics for Planetary Applications 2 Inflatable Rovers', pp. 1–6, 2001.
- [9] N. Aeronautics and Nasa, 'Viking Mission to Mars', *NASA Facts*, p. 8, 1976.
- [10] P. I. J. Gómez-elvira and C. De Astrobiología, 'Rover Environmental Monitoring Station (REMS).' [Online]. Available: <http://mars.nasa.gov/msl/mission/instruments/environsensors/remss/>. [Accessed: 08-Jun-2015].
- [11] R. M. (Nasa A. R. C. Haberle, C. P. (Nasa A. R. C. McKay, J. B. (Nasa A. R. C. Pollack, O. E. (Seti I. Gwynne, D. H. (University of I. Atkinson, J. (Tel A. U.

- Appelbaum, G. a. (Sverdrup T. Landis, R. W. (Jet P. L. Zurek, and D. J. (Nasa L. R. C. Flood, 'Atmospheric Effects on the Utility of Solar Power on Mars', *Resources of Near Earth Space*. pp. 845–885, 1993.
- [12] A. Colozza, 'Airships for Planetary Exploration', *NASA/CR--2004-213345*, no. November, 2004.
- [13] S. Ravindran, S. E. Hobbs, and J. Jennings, 'Mars Magnus Aerobot Preliminary Design', *SpaceOps 2010 Conf.*, no. April, pp. 1–14, 2010.
- [14] J. S. M. Grant, A. Edgington, N. Rowe-?- Gurney and Department, 'Mars Airport', *J. Phys. Spec. Top.*, no. November, pp. 10–11, 2011.
- [15] B. F. O. R. M. Draft-, J. A. Jones, D. Fairbrother, G. Wff, and T. Lachenmcicr, 'Wind-driven montgolfjere balloons for mars - draft-.'
- [16] J. A. Cutts, V. V. Kerzhanovich, and J. A. Jones, 'Balloons for Planetary Exploration', *COSPAR 2000*, p. 9, 2000.
- [17] V. E. Lally and National Center for Atmospheric Research, *Superpressure Balloons for Horizontal Soundings of the Atmosphere*. NATIONAL CENTER FOR ATMOSPHERIC RESEARCH, 1967.
- [18] N. Yajima, N. Izutsu, T. Imamura, and T. Abe, *Scientific Ballooning; Technology and Applications of Exploration Balloons Floating in the Stratosphere and the Atmospheres of Other Planets*. Springer Science+Business Media, 2004.
- [19] H. Cathey and D. Pierce, 'Duration Flight of the NASA Super Pressure Balloon', *AIAA Balloon Syst. Conf.*, no. May, pp. 1–15, 2009.
- [20] H. M. Cathey and D. L. Pierce, 'Development of the NASA Ultra-Long Duration Balloon', *Pap. C3P3 - NASA Sci. Technol. Conf.*, pp. 1–14, 2007.
- [21] J. A. Jones, J. A. Cutts, J. L. Hall, J.-J. Wu, D. A. Fairbrother, and T. Lanchenmeier, 'Montgolfiere Balloon Missions from Mars and Titan', *Proc. 3rd Int. Planet. Probe Work.*, 2005.
- [22] J. A. Jones, 'Innovative balloon buoyancy techniques for atmospheric exploration', *2000 IEEE Aerosp. Conf. Proc. (Cat. No.00TH8484)*, vol. 7, 2000.
- [23] J. A. Jones, P. Mahaffy, W. Farrell, and C. Webster, 'Sampling of Trace Atmospheric Constituents Above the Surface of Mars from a Montgolfiere

- Balloon', no. Reference 1, pp. 2–5, 2001.
- [24] J. A. Jones and J. J. Wu, 'Solar Montgolfiere balloons for Mars', *Int. Balloon Technol. Conf.*, pp. 1–7, 1999.
- [25] V. V. Kerzhanovich, J. a. Cutts, and J. L. Hall, 'Low-cost balloon missions to mars and venus', *Eur. Sp. Agency, (Special Publ. ESA SP, no. 530, pp. 285–291, 2003.*
- [26] M. Conner, 'Could This Become The First Mars Airplane?' 29-Jun-2015.
- [27] J. L. Hall, M. T. Pauken, V. V Kerzhanovich, G. J. Walsh, D. Fairbrother, C. Shreves, and T. Lachenmeier, 'Flight Test Results for Aerially Deployed Mars Balloons', *AIAA Balloon Syst. Conf.*, no. May, pp. 21–24, 2007.
- [28] W. V Jones, D. Pierce, D. Gregory, M. Said, D. Fairbrother, D. Stuchlik, and J. Reddish, 'Ultra Long Duration Ballooning Technology Development', *29th Int. Cosm. Ray Conf. Pune*, vol. 3, pp. 405–408, 2005.
- [29] D. Barnes, 'Mars Tethered Balloon Case Study', *ExoMars Rover Phase-A study*, p. 10, 2004.
- [30] V. V. Kerzhanovich, J. a. Cutts, H. W. Cooper, J. L. Hall, B. a. McDonald, M. T. Pauken, C. V. White, a. H. Yavrouian, a. Castano, H. M. Cathey, D. a. Fairbrother, I. S. Smith, C. M. Shreves, T. Lachenmeier, E. Rainwater, and M. Smith, 'Breakthrough in Mars balloon technology', *Adv. Sp. Res.*, vol. 33, no. 10, pp. 1836–1841, 2004.
- [31] M. Design, D. Staff, and M. Field, 'Small Spacecraft Technology State of the Art', no. February, pp. 1–197, 2014.
- [32] 'Solar Radiation on a Tilted Surface | PVEducation.' [Online]. Available: <http://www.pveducation.org/pvcdrom/properties-of-sunlight/solar-radiation-on-tilted-surface>. [Accessed: 02-Nov-2015].
- [33] 'Power over Fiber.' [Online]. Available: <http://laser motive.com/products/power-over-fiber/>. [Accessed: 28-Jun-2015].
- [34] 'Encyclopedia of Laser Physics and Technology - power over fiber, optical delivery of power, photonic power, optical power isolator.' [Online]. Available: http://www.rp-photonics.com/power_over_fiber.html. [Accessed: 28-Jun-2015].

- [35] 'Optical power-over-fiber cable provides total electrical isolation - Laser Focus World.' [Online]. Available: <http://www.laserfocusworld.com/articles/2012/01/optical-power-over-fiber-cable-provides-total-electrical-isolation.html>. [Accessed: 28-Jun-2015].
- [36] N. N. Gandilo, M. Amiri, S. J. Benton, J. J. Bock, J. R. Bond, S. A. Bryan, H. C. Chiang, C. R. Contaldi, B. P. Crill, M. J. Devlin, B. Dober, M. Farhang, J. P. Filippini, L. M. Fissel, A. A. Fraisse, Y. Fukui, N. Galitzki, A. E. Gambrel, S. Golwala, J. E. Gudmundsson, M. Halpern, M. Hasselfield, G. C. Hilton, W. A. Holmes, V. V. Hristov, K. D. Irwin, W. C. Jones, Z. D. Kermish, J. Klein, A. L. Korotkov, C. L. Kuo, C. J. Mactavish, P. V. Mason, T. G. Matthews, K. G. Megerian, L. Moncelsi, T. A. Morford, T. K. Mroczkowski, J. M. Nagy, C. B. Netterfield, G. Novak, D. Nutter, E. Pascale, F. Poidevin, A. S. Rahlin, C. D. Reintsema, J. E. Ruhl, M. C. Runyan, G. Savini, D. Scott, J. A. Shariff, J. D. Soler, N. E. Thomas, A. Trangsrud, M. D. Truch, C. E. Tucker, G. S. Tucker, R. S. Tucker, A. D. Turner, A. C. Weber, D. V. Wiebe, E. Y. Young, T. Physics, L. Laguna, L. Laguna, and C. Gables, 'Attitude determination for balloon-borne experiments.'
- [37] D. Barnes, a. Shaw, P. Summers, M. Woods, R. Ward, M. Evans, G. Paar, and M. Sims, 'Autonomous image based localisation for a martian aerobot', *Rev. Fr. Photograph. Teledetect.*, no. 185, pp. 45–50, 2007.
- [38] 'HiRISE.' [Online]. Available: <http://mars.jpl.nasa.gov/mro/mission/instruments/hirise/>. [Accessed: 30-Jun-2015].
- [39] A. Griffiths, A. Coates, R. Jaumann, J.-L. Josset, H. Michaelis, G. Paar, D. Barnes, and J. Muller, 'The Panoramic Camera (Pancam) Instrument For The Exomars Rover', pp. 1–17, 2007.
- [40] D. Pullan, M. R. Sims, I. P. Wright, C. T. Pillinger, and R. Trautner, 'Beagle 2: The exobiological lander of mars express', *Eur. Sp. Agency, (Special Publ. ESA SP)*, no. 1240, pp. 165–204, 2004.
- [41] N. T. Bridges, P. E. Geissler, A. S. McEwen, B. J. Thomson, F. C. Chuang, K. E. Herkenhoff, L. P. Keszthelyi, and S. Martínez-Alonso, 'Windy Mars: A dynamic planet as seen by the HiRISE camera', *Geophys. Res. Lett.*, vol. 34, p. L23205, 2007.
- [42] K. Schwingenschuh, H. Feldhofer, W. Koren, I. Jernej, M. Stachel, W. Riedler, H. Slamanig, H. U. Auster, J. Rustenbach, H. K. Fornacon, H. J. Schenk, O. Hillenmaier, G. Haerendel, Y. Yeroshenko, V. Styashkin, A. Zaroutzky, A. Best, G. Scholz, C. T. Rusell, J. Means, D. Pierce, and J. G. Luhmann, 'A balloon-borne experiment to investigate the martian magnetic field', *Adv. Sp. Res.*, vol.

- 17, no. 9, pp. 81–85, 1996.
- [43] C. A. Raymond, V. V. Kerzhanovich, K. Leschly, J. A. Cutts, C. T. Russell, and J. Blamont, 'Mars Magnetometer Balloon Mission', p. 1.
- [44] 'Curiosity Detects Methane Spike on Mars - NASA Science.' [Online]. Available: http://science.nasa.gov/science-news/science-at-nasa/2014/16dec_methanespike/. [Accessed: 01-Jul-2015].
- [45] V. V. Kerzhanovich, 'Recent Progress In Planetary Balloons.' Pasadena, p. 1.
- [46] 'How Do You Drive NASA's Mars Rover Curiosity?' [Online]. Available: <http://www.space.com/17220-mars-rover-curiosity-martian-driving.html>. [Accessed: 04-Jul-2015].
- [47] 'JPL | News | NASA'S Mars Curiosity Debuts Autonomous Navigation.' [Online]. Available: <http://www.jpl.nasa.gov/news/news.php?release=2013-259>. [Accessed: 04-Jul-2015].
- [48] 'Rear Hazard Avoidance Camera Left String B.' [Online]. Available: https://pds.jpl.nasa.gov/ds-view/pds/viewContext.jsp?identifier=urn%3Anasa%3Apds%3Acontext%3Ainstrument%3Ainstrument.rhaz_left_b__msl&version=1.0. [Accessed: 06-Jul-2015].
- [49] 'Navigation Camera.' [Online]. Available: https://pds.jpl.nasa.gov/ds-view/pds/viewContext.jsp?identifier=urn%3Anasa%3Apds%3Acontext%3Ainstrument%3Ainstrument.navcam__msl&version=1.0. [Accessed: 06-Jul-2015].
- [50] NASA, 'Mars Exploration Rover Mission: The Mission', *NASA, Jet Propulsion Laboratory, California Institute of Technology*, 2010. [Online]. Available: http://marsrovers.jpl.nasa.gov/mission/sc_rover_temp_aerogel.html. [Accessed: 04-Jul-2015].
- [51] J. F. Bell, 'Mars Exploration Rover Athena Panoramic Camera (Pancam) investigation', *J. Geophys. Res.*, vol. 108, no. E12, 2003.
- [52] J. Maki, D. Thiessen, a. Pourangi, P. Kobzeff, T. Litwin, L. Scherr, S. Elliott, a. Dingizian, and M. Maimone, 'The Mars Science Laboratory engineering cameras', *Space Sci. Rev.*, vol. 170, no. 1–4, pp. 77–93, 2012.
- [53] 'The ExoMars Rover Instrument Suite.' [Online]. Available: <http://exploration.esa.int/mars/45103-rover-instruments/?fbodylongid=2127>.

- [Accessed: 07-Jul-2015].
- [54] 'DLR Institute of Planetary Research - The ExoMars PanCam High Resolution Camera (PanCam-HRC).' [Online]. Available: http://www.dlr.de/pf/en/desktopdefault.aspx/tabid-168/223_read-37586/. [Accessed: 07-Jul-2015].
- [55] 'PanCam Mounted on the Rover.' [Online]. Available: <http://exploration.esa.int/mars/47863-pancam-mounted-on-the-rover/>. [Accessed: 07-Jul-2015].
- [56] J. Gómez-Elvira, C. Armiens, L. Castañer, M. Domínguez, M. Genzer, F. Gómez, R. Haberle, a. M. Harri, V. Jiménez, H. Kahanpää, L. Kowalski, a. Lepinette, J. Martín, J. Martínez-Frías, I. McEwan, L. Mora, J. Moreno, S. Navarro, M. a. De Pablo, V. Peinado, a. Peña, J. Polkko, M. Ramos, N. O. Renno, J. Ricart, M. Richardson, J. Rodríguez-Manfredi, J. Romeral, E. Sebastián, J. Serrano, M. De La Torre Juárez, J. Torres, F. Torrero, R. Urquí, L. Vázquez, T. Velasco, J. Verdasca, M. P. Zorzano, and J. Martín-Torres, 'REMS: The environmental sensor suite for the Mars Science Laboratory rover', *Space Sci. Rev.*, vol. 170, no. 1–4, pp. 583–640, 2012.
- [57] O. Karatekin, W. Schmidt, and U. Kingdom, 'DREAMS for the ExoMars 2016 mission: a suite of sensors for the characterization of Martian environment', vol. 8, no. January, pp. 2013–2014, 2013.
- [58] E. Millour, 'ExoMars 2016 and 2018 programme', 2016.
- [59] P. Science, D. Survey, and M. G. Network, 'Mission Concept Study Planetary Science Decadal Survey Mars Geophysical Network', no. June, 2010.
- [60] D. V. Titov, W. J. Markiewicz, N. Thomas, and H. U. Keller, 'WATER VAPOR IN THE ATMOSPHERE OF MARS: FROM PATHFINDER TO MARS POLAR LANDER.', pp. 1–2.
- [61] 'Sensor de humedad Sensor fotoeléctrico.' [Online]. Available: <http://www.todopic.com.ar/utiles/hs1100es.pdf>. [Accessed: 05-Jul-2015].
- [62] 'Mars Water-Ice Clouds Are Key to Odd Thermal Rhythm', 25-Jun-2013. [Online]. Available: https://www.nasa.gov/mission_pages/MRO/news/mro20130612.html. [Accessed: 05-Jul-2015].
- [63] 'Sensor de Luz.' [Online]. Available: <http://cab.inta-csic.es/remes/es/descripcion->

- del-instrumento/sensor-de-presion-ps/. [Accessed: 05-Jul-2015].
- [64] B. Greenwood and T. Mutabingwa, 'Insight Introduction', *Nature*, 2002. [Online]. Available: <http://insight.jpl.nasa.gov/home.cfm>. [Accessed: 08-Jul-2015].
- [65] B. P. Weiss, C. T. Russell, B. J. Anderson, J. L. Kirschvink, M. P. Golombek, C. A. Raymond, and N. Murphy, 'MARS COMPASS: A MAGNETOMETER FOR THE MARS 2020 ROVER.', *45th Lunar Planet. Sci. Conf.*, pp. 12–13, 2014.
- [66] 'Magnetometer - DTU Space.' [Online]. Available: <http://www.space.dtu.dk/english/Research/Projects/ExoMars/Magnetometer>. [Accessed: 17-Jul-2015].
- [67] 'Micro Fabricated Atomic Magnetometer (MFAM) by Geometrics.' [Online]. Available: <http://mfam.geometrics.com/>. [Accessed: 08-Jun-2015].
- [68] L. G. Blomberg, G. T. Marklund, P. Lindqvist, F. Primdahl, and P. Brauer, 'The EMMA instrument on the Astrid-2 micro -satellite', pp. 0–20, 2003.
- [69] Y. Chen, A. Abushakra, and J. Lee, 'Vision-based horizon detection and target tracking for UAVs', *Lect. Notes Comput. Sci. (including Subser. Lect. Notes Artif. Intell. Lect. Notes Bioinformatics)*, vol. 6939 LNCS, no. PART 2, pp. 310–319, 2011.
- [70] 'Sector Aeroespacial - Sun Sensors | SOLAR MEMS.' [Online]. Available: <http://www.solar-mems.com/es/productos/aeroespacio>. [Accessed: 18-Jul-2015].
- [71] 'ESA preparing "sugar-cube" gyro sensors for future missions / Space Engineering & Technology / Our Activities / ESA'. [Online]. Available: http://www.esa.int/Our_Activities/Space_Engineering_Technology/ESA_preparing_sugar-cube_gyro_sensors_for_future_missions. [Accessed: 19-Jul-2015].
- [72] 'QRS11 | Systron Donner.' [Online]. Available: <http://www.systron.com/gyroscopes/qrs11-single-axis-analog-gyroscope>. [Accessed: 19-Jul-2015].
- [73] 'Command & Data Handling', 2006. [Online]. Available: http://www.cubesatshop.com/index.php?option=com_virtuemart&Itemid=75. [Accessed: 28-Jul-2015].
- [74] 'Cubesat and nano-satellite solutions.' [Online]. Available:

- <http://www.gomspace.com/>. [Accessed: 27-Jul-2015].
- [75] AGI, 'STK | Software to model, analyze, and visualize space, defense and intelligence systems', 2014. [Online]. Available: <http://www.agi.com/products/stk/>. [Accessed: 25-Oct-2015].
- [76] 'Windform XT 2.0. Polyamide based material carbon filled.' [Online]. Available: <http://www.windform.com/windform-xt-2-0.html>. [Accessed: 17-Aug-2015].
- [77] K. S. Bernstein and G. F. Galbreath, 'Structural design requirements and factors of safety for spaceflight hardware for human spaceflight', no. October, 2011.
- [78] 'Toyobo Zylon® AS Poly(p-phenylene-2,6-benzobisoxazole) Fiber.' [Online]. Available: <http://www.matweb.com/search/datasheet.aspx?matguid=b28dd4a356744320b3d7e38fe6f2b101&ckck=1>. [Accessed: 19-Aug-2015].
- [79] 'LLDPE | Matbase: the independent online material selection resource.' [Online]. Available: <http://www.matbase.com/material-categories/natural-and-synthetic-polymers/commodity-polymers/material-properties-of-linear-low-density-polyethylene-lldpe.html#properties>. [Accessed: 10-Sep-2015].
- [80] 'Earth and Martian Magnetic Fields', 06-Jun-2013. [Online]. Available: https://www.nasa.gov/mission_pages/msl/multimedia/hassler02.html. [Accessed: 09-Sep-2015].
- [81] 'File:Mars topography (MOLA dataset) with poles HiRes.jpg - Wikipedia, the free encyclopedia.' [Online]. Available: [https://en.wikipedia.org/wiki/File:Mars_topography_\(MOLA_dataset\)_with_poles_HiRes.jpg](https://en.wikipedia.org/wiki/File:Mars_topography_(MOLA_dataset)_with_poles_HiRes.jpg). [Accessed: 16-Sep-2015].
- [82] 'NASA - New NASA Balloon Successfully Flight-Tested Over Antarctica.' Brian Dunbar.

ANNEX I: Atmospheric model values

H (km)	T (K)	P (kPa)	ρ (kg/m ³)
0	238.74	0.6627	0.01469
0.1	235.63	0.6490	0.01458
0.2	233.13	0.6372	0.01447
0.3	231.15	0.6269	0.01435
0.4	229.64	0.6179	0.01424
0.5	228.50	0.6101	0.01413
0.6	227.70	0.6032	0.01402
0.7	227.16	0.5972	0.01392
0.8	226.84	0.5917	0.01381
0.9	226.71	0.5868	0.01370
1	226.71	0.5823	0.01359
1.1	226.83	0.5781	0.01349
1.2	227.02	0.5741	0.01339
1.3	227.26	0.5703	0.01328
1.4	227.54	0.5665	0.01318
1.5	227.83	0.5629	0.01308
1.6	228.11	0.5593	0.01298
1.7	228.39	0.5556	0.01288
1.8	228.64	0.5520	0.01278
1.9	228.86	0.5482	0.01268
2	229.04	0.5445	0.01258
2.25	229.32	0.5347	0.01234
2.5	229.31	0.5245	0.01211
2.75	229.03	0.5139	0.01188
3	228.52	0.5031	0.01165
3.25	227.84	0.4921	0.01143
3.5	227.04	0.4811	0.01122
3.75	226.18	0.4702	0.01100
4	225.29	0.4596	0.01080
4.25	224.42	0.4492	0.01060
4.5	223.58	0.4391	0.01040
4.75	222.78	0.4294	0.01020
5	222.02	0.4200	0.01001
5.25	221.28	0.4108	0.00983
5.5	220.55	0.4019	0.00964
5.75	219.81	0.3931	0.00947
6	219.03	0.3845	0.00929
6.25	218.19	0.3760	0.00912
6.5	217.28	0.3675	0.00895
6.75	216.30	0.3592	0.00879
7	215.26	0.3509	0.00863
7.5	213.04	0.3348	0.00832
8	210.88	0.3194	0.00802
8.5	209.03	0.3053	0.00773
9	207.56	0.2923	0.00745
9.5	205.88	0.2796	0.00719
10	202.16	0.2647	0.00693

Table I.0.1 Values obtained using the atmospheric model in 1.3.1 and used for **Figure 1-7, Figure 1-8 and Figure 1-9.**

ANNEX II: Mars solar flux

The solar flux in the Mars surface is obtained by the formulas included in [11]. S is the irradiance of solar radiation at the top of Martian atmosphere, μ is the cosine of the solar zenith “ z ” (II.2), S_0 is the solar irradiance at Mars mean solar distance, which is \bar{r} and r is the distance for a specific moment.

$$S = \mu S_0 \left(\frac{\bar{r}}{r} \right)^2 \quad (II.1)$$

$$\mu = \cos(z) = \sin \theta \sin \delta + \cos \theta \cos \delta \cos h \quad (II.2)$$

In (II.2), θ is the solar latitude and δ the solar declination while h is the hour angle. The value of h is obtained with (II.3), being t the time measured from local noon and P the length of a Martian day with a value $P = 88775 \text{ s}$. The solar declination angle (θ) value is function of the Mars’ obliquity ($\epsilon = 25. \text{s}$) and the planet orbital position L_s as can be observed in (II.4).

$$h = \frac{2\pi t}{P} \quad (II.3)$$

$$\sin \delta = \sin \epsilon \sin L_s \quad (II.4)$$

The distance between Mars and the Sun can be found with (II.5), being the orbit eccentricity $e = 0.0934$, the aerocentric longitude at perihelion $L_s^p = 250^\circ$.

$$\left(\frac{\bar{r}}{r} \right) = \frac{1 + e \cos(L_s - L_s^p)}{1 - e^2} \quad (II.5)$$

Time measured from local noon (s)	Orbital position (°)												
	0	30	60	90	120	150	180	210	240	270	300	330	360
3551	545	486	439	430	471	545	619	657	653	633	616	591	545
7102	493	439	397	389	425	493	560	595	592	574	558	535	493
10653	410	365	329	322	352	409	466	496	494	479	466	446	410
14204	301	267	240	235	257	300	342	366	366	355	345	329	301
17755	174	152	136	132	145	171	197	213	215	209	202	192	174
21306	35	28	23	21	24	31	40	47	51	51	48	43	35
24857	-105	-99	-93	-92	-99	-111	-120	-121	-115	-110	-109	-109	-105
28408	-239	-219	-202	-200	-217	-246	-272	-282	-274	-263	-258	-253	-239
31959	-358	-326	-300	-295	-321	-366	-407	-424	-415	-399	-391	-381	-358
35510	-455	-413	-378	-373	-406	-463	-517	-540	-529	-509	-498	-485	-455
39061	-523	-474	-434	-428	-465	-532	-594	-621	-609	-587	-574	-558	-523
42612	-558	-505	-463	-456	-496	-567	-634	-663	-651	-627	-613	-596	-558
46163	-558	-505	-463	-456	-496	-567	-634	-663	-651	-627	-613	-596	-558
49714	-523	-474	-434	-428	-465	-532	-594	-621	-609	-587	-574	-558	-523
53265	-455	-413	-378	-373	-406	-463	-517	-540	-529	-509	-498	-485	-455
56816	-358	-326	-300	-295	-321	-366	-407	-424	-415	-399	-391	-381	-358
60367	-239	-219	-202	-200	-217	-246	-272	-282	-274	-263	-258	-253	-239
63918	-105	-99	-93	-92	-99	-111	-120	-121	-115	-110	-109	-109	-105
67469	35	28	23	21	24	31	40	47	51	51	48	43	35
71020	174	152	136	132	145	171	197	213	215	209	202	192	174
74571	301	267	240	235	257	300	342	366	366	355	345	329	301
78122	410	365	329	322	352	409	466	496	494	479	466	446	410
81673	493	439	397	389	425	493	560	595	592	574	558	535	493
85224	545	486	439	430	471	545	619	657	653	633	616	591	545
88775	562	502	454	444	486	563	639	678	674	653	635	610	562

Table II.0.1 Values of solar flux at the Martian upper atmosphere during a day for different orbital positions used in Figure 3-3.

Latitude (θ)	Orbital position ($^{\circ}$)												
	0	30	60	90	120	150	180	210	240	270	300	330	360
-90	0	-110	-183	-213	-196	-124	0	147	264	302	249	132	0
-80	98	-21	-100	-131	-107	-23	111	262	376	410	354	235	98
-70	192	69	-14	-45	-15	78	219	368	476	504	448	331	192
-60	281	157	72	42	77	177	320	464	561	583	529	417	281
-50	362	241	156	128	167	270	411	545	630	645	594	491	362
-40	431	317	235	210	252	355	490	610	680	687	640	549	431
-30	487	383	307	285	329	430	554	657	708	708	668	591	487
-20	529	438	370	352	396	491	601	683	716	708	674	614	529
-10	554	479	421	408	452	538	630	689	701	686	661	620	554
0	563	506	460	452	493	568	639	674	666	643	627	606	563
10	554	517	485	482	520	581	630	638	610	581	574	574	554
20	529	513	495	498	530	576	601	583	535	501	504	524	529
30	487	493	490	498	525	554	554	510	444	405	419	459	487
40	431	458	470	483	503	514	490	422	340	298	321	379	431
50	362	409	436	454	467	460	411	321	226	181	213	288	362
60	281	348	388	410	416	391	320	210	104	59	98	189	281
70	192	277	329	355	352	310	219	92	-20	-64	-19	83	192
80	98	196	260	288	278	220	111	-28	-144	-186	-136	-25	98
90	0	110	183	213	196	124	0	-147	-264	-302	-249	-132	0

Table II.0.2 Values of maximum solar flux (Wh/m²) at Mars upper atmosphere in different latitudes at different orbital moments used for in Figure 3-2.

ANNEX III: Balloon buoyancy

<i>Altitude</i>	<i>0 m</i>
<i>Temperature</i>	238,74 K
<i>Pressure</i>	0,662739967 kPa
<i>Density</i>	0,014694 kg/m ³
<i>Altitude</i>	<i>500 m</i>
<i>Temperature</i>	228,5031486 K
<i>Pressure</i>	0,610106472 kPa
<i>Density</i>	0,014133037 kg/m ³
<i>Altitude</i>	<i>750 m</i>
<i>Temperature</i>	226,9768904 K
<i>Pressure</i>	0,59436932 kPa
<i>Density</i>	0,013861072 kg/m ³
<i>Balloon</i>	
<i>Helium density at 0 m</i>	0,001334611 kg/m ³
<i>Helium density at 500 m</i>	0,001394401 kg/m ³
<i>Helium density at 750 m</i>	0,001403777 kg/m ³

Altitude 750 m

Balloon diameter (m)	Balloon radius [a] (m)	[c] (m)	Balloon volume (m ³)	Balloon surface (m ²)	Envelope thickness (m)	Envelope mass spheroid (kg)	Envelope mass pumpkin (kg)	Helium mass (kg)	Payload mass (kg)	Balloon total mass (kg)
1	0,5	0,320707	0,335844	2,876164	4,70106E-07	0,001232	0,001417	0,00045	0,002767	0,004183704
1,5	0,75	0,481061	1,133472	6,471369	7,05159E-07	0,004157	0,004781	0,00151	0,009339	0,01412
2	1	0,641414	2,686749	11,50466	9,40212E-07	0,009854	0,011332	0,00359	0,022137	0,033469629
2,5	1,25	0,801768	5,247558	17,97603	1,17527E-06	0,019246	0,022133	0,007	0,043237	0,065370369
3	1,5	0,962121	9,067779	25,88548	1,41032E-06	0,033258	0,038246	0,0121	0,074714	0,112959998
3,5	1,75	1,122475	14,3993	35,23301	1,64537E-06	0,052812	0,060734	0,01922	0,118643	0,179376293
4	2	1,282828	21,494	46,01862	1,88042E-06	0,078833	0,090658	0,02869	0,177099	0,267757032
4,5	2,25	1,443182	30,60376	58,24232	2,11548E-06	0,112245	0,129081	0,04084	0,252159	0,381239993
5	2,5	1,603535	41,98046	71,9041	2,35053E-06	0,153971	0,177066	0,05603	0,345897	0,522962954
5,5	2,75	1,763889	55,87599	87,00396	2,58558E-06	0,204935	0,235675	0,07457	0,460389	0,696063692
6	3	1,924243	72,54224	103,5419	2,82064E-06	0,266061	0,30597	0,09682	0,59771	0,903679985
6,5	3,25	2,084596	92,23107	121,5179	3,05569E-06	0,338273	0,389015	0,12309	0,759935	1,14894961
7	3,5	2,24495	115,1944	140,932	3,29074E-06	0,422495	0,48587	0,15374	0,949141	1,435010346
7,5	3,75	2,405303	141,6841	161,7842	3,5258E-06	0,519651	0,597599	0,18909	1,167401	1,76499997
8	4	2,565657	171,952	184,0745	3,76085E-06	0,630664	0,725263	0,22949	1,416793	2,14205626
8,5	4,25	2,72601	206,25	207,8028	3,9959E-06	0,756458	0,869926	0,27526	1,699391	2,569316993
9	4,5	2,886364	244,83	232,9693	4,23095E-06	0,897957	1,03265	0,32675	2,01727	3,049919948
9,5	4,75	3,046717	287,944	259,5738	4,46601E-06	1,056085	1,214497	0,38429	2,372506	3,587002902
10	5	3,207071	335,8437	287,6164	4,70106E-06	1,231765	1,41653	0,44822	2,767174	4,183703632
10,5	5,25	3,367424	388,781	317,0971	4,93611E-06	1,425922	1,63981	0,51887	3,20335	4,843159917
11	5,5	3,527778	447,0079	348,0158	5,17117E-06	1,639479	1,885401	0,59658	3,683108	5,568509534
11,5	5,75	3,688132	510,7763	380,3727	5,40622E-06	1,873361	2,154365	0,68169	4,208525	6,362890261
12	6	3,848485	580,3379	414,1676	5,64127E-06	2,12849	2,447764	0,77453	4,781676	7,229439876
12,5	6,25	4,008839	655,9447	449,4006	5,87633E-06	2,405791	2,76666	0,87543	5,404636	8,171296156
13	6,5	4,169192	737,8486	486,0717	6,11138E-06	2,706188	3,112116	0,98474	6,079481	9,19159688
13,5	6,75	4,329546	826,3014	524,1809	6,34643E-06	3,030604	3,485195	1,10279	6,808285	10,29347982
14	7	4,489899	921,5551	563,7281	6,58149E-06	3,379963	3,886958	1,22992	7,593125	11,48008277
14,5	7,25	4,650253	1023,861	604,7135	6,81654E-06	3,75519	4,318468	1,36646	8,436075	12,75454349
15	7,5	4,810606	1133,472	647,1369	7,05159E-06	4,157207	4,780788	1,51274	9,339211	14,11999976

15,5	7,75	4,97096	1250,64	690,9984	7,28664E-06	4,586939	5,27498	1,66912	10,30461	15,57958936
16	8	5,131314	1375,616	736,298	7,5217E-06	5,04531	5,802106	1,83591	11,33434	17,13645008
16,5	8,25	5,291667	1508,652	783,0357	7,75675E-06	5,533243	6,363229	2,01346	12,43049	18,79371968
17	8,5	5,452021	1650	831,2114	7,9918E-06	6,051662	6,959411	2,20211	13,59512	20,55453594
17,5	8,75	5,612374	1799,912	880,8252	8,22686E-06	6,601491	7,591715	2,40218	14,83032	22,42203665
18	9	5,772728	1958,64	931,8771	8,46191E-06	7,183654	8,261202	2,61402	16,13816	24,39935958
18,5	9,25	5,933081	2126,436	984,3671	8,69696E-06	7,799075	8,968936	2,83796	17,52071	26,48964251
19	9,5	6,093435	2303,552	1038,295	8,93202E-06	8,448677	9,715978	3,07435	18,98004	28,69602321
19,5	9,75	6,253788	2490,239	1093,661	9,16707E-06	9,133384	10,50339	3,3235	20,51825	31,02163947
20	10	6,414142	2686,749	1150,466	9,40212E-06	9,854121	11,33224	3,58576	22,13739	33,46962906
20,5	10,25	6,574495	2893,335	1208,708	9,63717E-06	10,61181	12,20358	3,86148	23,83955	36,04312975
21	10,5	6,734849	3110,248	1268,388	9,87223E-06	11,40738	13,11848	4,15097	25,6268	38,74527934
21,5	10,75	6,895203	3337,74	1329,507	1,01073E-05	12,24174	14,078	4,45458	27,50121	41,57921558
22	11	7,055556	3576,064	1392,063	1,03423E-05	13,11583	15,08321	4,77265	29,46487	44,54807627
22,5	11,25	7,21591	3825,469	1456,058	1,05774E-05	14,03057	16,13516	5,10551	31,51984	47,65499918
23	11,5	7,376263	4086,21	1521,491	1,08124E-05	14,98689	17,23492	5,4535	33,6682	50,90312209
23,5	11,75	7,536617	4358,537	1588,362	1,10475E-05	15,98569	18,38355	5,81695	35,91204	54,29558277
24	12	7,69697	4642,703	1656,67	1,12825E-05	17,02792	19,58211	6,1962	38,25341	57,83551901
24,5	12,25	7,857324	4938,959	1726,417	1,15176E-05	18,11449	20,83167	6,59159	40,6944	61,52606858
25	12,5	8,017677	5247,558	1797,603	1,17527E-05	19,24633	22,13328	7,00345	43,23709	65,37036925
25,5	12,75	8,178031	5568,75	1870,226	1,19877E-05	20,42436	23,48801	7,43211	45,88355	69,37155881
26	13	8,338384	5902,789	1944,287	1,22228E-05	21,6495	24,89693	7,87793	48,63585	73,53277504
26,5	13,25	8,498738	6249,925	2019,786	1,24578E-05	22,92269	26,36109	8,34122	51,49607	77,8571557
27	13,5	8,659092	6610,411	2096,724	1,26929E-05	24,24483	27,88156	8,82233	54,46628	82,34783859
27,5	13,75	8,819445	6984,499	2175,099	1,29279E-05	25,61686	29,45939	9,32159	57,54857	87,00796147
28	14	8,979799	7372,441	2254,913	1,3163E-05	27,03971	31,09566	9,83934	60,745	91,84066213
28,5	14,25	9,140152	7774,487	2336,164	1,3398E-05	28,51428	32,79143	10,3759	64,05765	96,84907834
29	14,5	9,300506	8190,892	2418,854	1,36331E-05	30,04152	34,54775	10,9317	67,4886	102,0363479
29,5	14,75	9,460859	8621,905	2502,982	1,38681E-05	31,62234	36,36569	11,5069	71,03992	107,4056085
30	15	9,621213	9067,779	2588,548	1,41032E-05	33,25766	38,24631	12,102	74,71369	112,9599981

Table III.0.1 Balloon properties for a neutral buoyancy altitude of 750 m.

Altitude 500 m

Balloon diameter (m)	Balloon radius [a] (m)	[c] (m)	Balloon volume (m ³)	Balloon surface (m ²)	Envelope thickness (m)	Envelope mass spheroid (kg)	Envelope mass pumpkin (kg)	Helium mass (kg)	Payload mass (kg)	Balloon total mass (kg)
1	0,5	0,320707	0,335844	2,876164	4,70106E-07	0,001232	0,001417	0,00045	0,002862	0,004278191
1,5	0,75	0,481061	1,133472	6,471369	7,05159E-07	0,004157	0,004781	0,00151	0,009658	0,014438893
2	1	0,641414	2,686749	11,50466	9,40212E-07	0,009854	0,011332	0,00359	0,022893	0,034225525
2,5	1,25	0,801768	5,247558	17,97603	1,17527E-06	0,019246	0,022133	0,007	0,044713	0,066846728
3	1,5	0,962121	9,067779	25,88548	1,41032E-06	0,033258	0,038246	0,0121	0,077265	0,115511147
3,5	1,75	1,122475	14,3993	35,23301	1,64537E-06	0,052812	0,060734	0,01922	0,122694	0,183427422
4	2	1,282828	21,494	46,01862	1,88042E-06	0,078833	0,090658	0,02869	0,183146	0,273804199
4,5	2,25	1,443182	30,60376	58,24232	2,11548E-06	0,112245	0,129081	0,04084	0,260769	0,389850119
5	2,5	1,603535	41,98046	71,9041	2,35053E-06	0,153971	0,177066	0,05603	0,357708	0,534773826
5,5	2,75	1,763889	55,87599	87,00396	2,58558E-06	0,204935	0,235675	0,07457	0,476109	0,711783963
6	3	1,924243	72,54224	103,5419	2,82064E-06	0,266061	0,30597	0,09682	0,618119	0,924089172
6,5	3,25	2,084596	92,23107	121,5179	3,05569E-06	0,338273	0,389015	0,12309	0,785884	1,174898097
7	3,5	2,24495	115,1944	140,932	3,29074E-06	0,422495	0,48587	0,15374	0,98155	1,46741938
7,5	3,75	2,405303	141,6841	161,7842	3,5258E-06	0,519651	0,597599	0,18909	1,207263	1,804861664
8	4	2,565657	171,952	184,0745	3,76085E-06	0,630664	0,725263	0,22949	1,46517	2,190433593
8,5	4,25	2,72601	206,25	207,8028	3,9959E-06	0,756458	0,869926	0,27526	1,757417	2,627343809
9	4,5	2,886364	244,83	232,9693	4,23095E-06	0,897957	1,03265	0,32675	2,086151	3,118800956
9,5	4,75	3,046717	287,944	259,5738	4,46601E-06	1,056085	1,214497	0,38429	2,453516	3,668013676
10	5	3,207071	335,8437	287,6164	4,70106E-06	1,231765	1,41653	0,44822	2,861661	4,278190612
10,5	5,25	3,367424	388,781	317,0971	4,93611E-06	1,425922	1,63981	0,51887	3,31273	4,952540407
11	5,5	3,527778	447,0079	348,0158	5,17117E-06	1,639479	1,885401	0,59658	3,80887	5,694271704
11,5	5,75	3,688132	510,7763	380,3727	5,40622E-06	1,873361	2,154365	0,68169	4,352228	6,506593147
12	6	3,848485	580,3379	414,1676	5,64127E-06	2,12849	2,447764	0,77453	4,94495	7,392713377
12,5	6,25	4,008839	655,9447	449,4006	5,87633E-06	2,405791	2,76666	0,87543	5,589181	8,355841039
13	6,5	4,169192	737,8486	486,0717	6,11138E-06	2,706188	3,112116	0,98474	6,287069	9,399184774
13,5	6,75	4,329546	826,3014	524,1809	6,34643E-06	3,030604	3,485195	1,10279	7,040759	10,52595323
14	7	4,489899	921,5551	563,7281	6,58149E-06	3,379963	3,886958	1,22992	7,852397	11,73935504
14,5	7,25	4,650253	1023,861	604,7135	6,81654E-06	3,75519	4,318468	1,36646	8,72413	13,04259885
15	7,5	4,810606	1133,472	647,1369	7,05159E-06	4,157207	4,780788	1,51274	9,658105	14,43889331

15,5	7,75	4,97096	1250,64	690,9984	7,28664E-06	4,586939	5,27498	1,66912	10,65647	15,93144706
16	8	5,131314	1375,616	736,298	7,5217E-06	5,04531	5,802106	1,83591	11,72136	17,52346875
16,5	8,25	5,291667	1508,652	783,0357	7,75675E-06	5,533243	6,363229	2,01346	12,85494	19,218167
17	8,5	5,452021	1650	831,2114	7,9918E-06	6,051662	6,959411	2,20211	14,05934	21,01875048
17,5	8,75	5,612374	1799,912	880,8252	8,22686E-06	6,601491	7,591715	2,40218	15,33671	22,92842781
18	9	5,772728	1958,64	931,8771	8,46191E-06	7,183654	8,261202	2,61402	16,68921	24,95040765
18,5	9,25	5,933081	2126,436	984,3671	8,69696E-06	7,799075	8,968936	2,83796	18,11896	27,08789863
19	9,5	6,093435	2303,552	1038,295	8,93202E-06	8,448677	9,715978	3,07435	19,62813	29,34410941
19,5	9,75	6,253788	2490,239	1093,661	9,16707E-06	9,133384	10,50339	3,3235	21,21886	31,72224861
20	10	6,414142	2686,749	1150,466	9,40212E-06	9,854121	11,33224	3,58576	22,89329	34,22552489
20,5	10,25	6,574495	2893,335	1208,708	9,63717E-06	10,61181	12,20358	3,86148	24,65357	36,85714689
21	10,5	6,734849	3110,248	1268,388	9,87223E-06	11,40738	13,11848	4,15097	26,50184	39,62032326
21,5	10,75	6,895203	3337,74	1329,507	1,01073E-05	12,24174	14,078	4,45458	28,44026	42,51826262
22	11	7,055556	3576,064	1392,063	1,03423E-05	13,11583	15,08321	4,77265	30,47096	45,55417363
22,5	11,25	7,21591	3825,469	1456,058	1,05774E-05	14,03057	16,13516	5,10551	32,5961	48,73126494
23	11,5	7,376263	4086,21	1521,491	1,08124E-05	14,98689	17,23492	5,4535	34,81783	52,05274517
23,5	11,75	7,536617	4358,537	1588,362	1,10475E-05	15,98569	18,38355	5,81695	37,13828	55,52182299
24	12	7,69697	4642,703	1656,67	1,12825E-05	17,02792	19,58211	6,1962	39,5596	59,14170702
24,5	12,25	7,857324	4938,959	1726,417	1,15176E-05	18,11449	20,83167	6,59159	42,08394	62,91560591
25	12,5	8,017677	5247,558	1797,603	1,17527E-05	19,24633	22,13328	7,00345	44,71345	66,84672831
25,5	12,75	8,178031	5568,75	1870,226	1,19877E-05	20,42436	23,48801	7,43211	47,45027	70,93828285
26	13	8,338384	5902,789	1944,287	1,22228E-05	21,6495	24,89693	7,87793	50,29655	75,19347819
26,5	13,25	8,498738	6249,925	2019,786	1,24578E-05	22,92269	26,36109	8,34122	53,25443	79,61552296
27	13,5	8,659092	6610,411	2096,724	1,26929E-05	24,24483	27,88156	8,82233	56,32607	84,20762581
27,5	13,75	8,819445	6984,499	2175,099	1,29279E-05	25,61686	29,45939	9,32159	59,5136	88,97299538
28	14	8,979799	7372,441	2254,913	1,3163E-05	27,03971	31,09566	9,83934	62,81918	93,91484031
28,5	14,25	9,140152	7774,487	2336,164	1,3398E-05	28,51428	32,79143	10,3759	66,24494	99,03636924
29	14,5	9,300506	8190,892	2418,854	1,36331E-05	30,04152	34,54775	10,9317	69,79304	104,3407908
29,5	14,75	9,460859	8621,905	2502,982	1,38681E-05	31,62234	36,36569	11,5069	73,46563	109,8313137
30	15	9,621213	9067,779	2588,548	1,41032E-05	33,25766	38,24631	12,102	77,26484	115,5111465

Table III.0.2 Balloon properties for a neutral buoyancy altitude of 500 m.

ANNEX IV: Balloon Lifespan

Atmosphere

<i>Temperature</i>	228,5031486	K
<i>Pressure</i>	0,610106472	kPa
<i>Density</i>	0,014133037	kg/m ³

Helium

<i>R</i>	2,08	kJ/(kg·K)
<i>Molar mass</i>	4,002602	g/mol

Balloon Characteristics

<i>Initial density inside balloon</i>	0,001394401	kg/m ³
<i>Initial Partial pressure</i>	0,662739967	kPa
<i>Total mass lifted</i>	4,750810385	kg
<i>surface</i>	312,8962295	m ²
<i>Volume</i>	381,0809236	m ³
<i>Initial quantity of gas</i>	0,508594719	kg
<i>Film thickness</i>	4,93611E-06	m
<i>Permeability</i>	8,68056E-14	(m ³ ·m)/(KPa·m ² ·s)

Sol	Rate of loss	Percentage of loss (%)	Balloon Volume (m ³)	Helium mass (kg)	Helium density (kg/m ³)	Helium pressure (kPa)	Lift capacity (kg)	Free lift (kg)
1	3,64675E-06	0,000848048	381,0809236	0,508163	0,001333	0,633785	4,877668	0,126857
2	3,48742E-06	0,000810996	381,0809236	0,507751	0,001332	0,633271	4,87808	0,127269
3	3,48459E-06	0,000810339	381,0809236	0,50734	0,001331	0,632757	4,878491	0,127681
4	3,48177E-06	0,000809682	381,0809236	0,506929	0,00133	0,632245	4,878902	0,128091
5	3,47895E-06	0,000809026	381,0809236	0,506519	0,001329	0,631734	4,879312	0,128502
6	3,47614E-06	0,000808372	381,0809236	0,506109	0,001328	0,631223	4,879721	0,128911
7	3,47333E-06	0,000807718	381,0809236	0,505701	0,001327	0,630713	4,88013	0,12932
8	3,47052E-06	0,000807066	381,0809236	0,505293	0,001326	0,630204	4,880538	0,129728
9	3,46772E-06	0,000806415	381,0809236	0,504885	0,001325	0,629696	4,880946	0,130135
10	3,46492E-06	0,000805764	381,0809236	0,504478	0,001324	0,629188	4,881353	0,130542
11	3,46213E-06	0,000805115	381,0809236	0,504072	0,001323	0,628682	4,881759	0,130948
12	3,45934E-06	0,000804467	381,0809236	0,503667	0,001322	0,628176	4,882164	0,131354
13	3,45656E-06	0,00080382	381,0809236	0,503262	0,001321	0,627671	4,882569	0,131759
14	3,45378E-06	0,000803174	381,0809236	0,502858	0,00132	0,627167	4,882973	0,132163
15	3,45101E-06	0,000802529	381,0809236	0,502454	0,001318	0,626664	4,883377	0,132567
16	3,44824E-06	0,000801884	381,0809236	0,502051	0,001317	0,626161	4,88378	0,132969
17	3,44547E-06	0,000801241	381,0809236	0,501649	0,001316	0,62566	4,884182	0,133372
18	3,44271E-06	0,000800599	381,0809236	0,501247	0,001315	0,625159	4,884584	0,133773
19	3,43996E-06	0,000799959	381,0809236	0,500846	0,001314	0,624659	4,884985	0,134174
20	3,4372E-06	0,000799319	381,0809236	0,500446	0,001313	0,624159	4,885385	0,134575
21	3,43446E-06	0,00079868	381,0809236	0,500046	0,001312	0,623661	4,885785	0,134974
22	3,43171E-06	0,000798042	381,0809236	0,499647	0,001311	0,623163	4,886184	0,135373
23	3,42898E-06	0,000797405	381,0809236	0,499249	0,00131	0,622666	4,886582	0,135772
24	3,42624E-06	0,000796769	381,0809236	0,498851	0,001309	0,62217	4,88698	0,13617
25	3,42351E-06	0,000796134	381,0809236	0,498454	0,001308	0,621675	4,887377	0,136567
26	3,42079E-06	0,0007955	381,0809236	0,498057	0,001307	0,62118	4,887774	0,136963
27	3,41806E-06	0,000794868	381,0809236	0,497661	0,001306	0,620686	4,88817	0,137359
28	3,41535E-06	0,000794236	381,0809236	0,497266	0,001305	0,620193	4,888565	0,137754
29	3,41263E-06	0,000793605	381,0809236	0,496871	0,001304	0,619701	4,888959	0,138149
30	3,40993E-06	0,000792975	381,0809236	0,496477	0,001303	0,61921	4,889353	0,138543
31	3,40722E-06	0,000792346	381,0809236	0,496084	0,001302	0,618719	4,889747	0,138936
32	3,40452E-06	0,000791719	381,0809236	0,495691	0,001301	0,618229	4,89014	0,139329
33	3,40183E-06	0,000791092	381,0809236	0,495299	0,0013	0,61774	4,890532	0,139721
34	3,39914E-06	0,000790466	381,0809236	0,494908	0,001299	0,617252	4,890923	0,140113
35	3,39645E-06	0,000789841	381,0809236	0,494517	0,001298	0,616764	4,891314	0,140504
36	3,39377E-06	0,000789217	381,0809236	0,494126	0,001297	0,616278	4,891704	0,140894
37	3,39109E-06	0,000788594	381,0809236	0,493737	0,001296	0,615792	4,892094	0,141284
38	3,38841E-06	0,000787972	381,0809236	0,493348	0,001295	0,615306	4,892483	0,141673
39	3,38574E-06	0,000787352	381,0809236	0,492959	0,001294	0,614822	4,892872	0,142061
40	3,38308E-06	0,000786732	381,0809236	0,492571	0,001293	0,614338	4,893259	0,142449
41	3,38042E-06	0,000786113	381,0809236	0,492184	0,001292	0,613855	4,893647	0,142836
42	3,37776E-06	0,000785495	381,0809236	0,491798	0,001291	0,613373	4,894033	0,143223
43	3,37511E-06	0,000784878	381,0809236	0,491412	0,00129	0,612892	4,894419	0,143609
44	3,37246E-06	0,000784262	381,0809236	0,491026	0,001289	0,612411	4,894805	0,143994
45	3,36981E-06	0,000783647	381,0809236	0,490641	0,001287	0,611931	4,895189	0,144379
46	3,36717E-06	0,000783032	381,0809236	0,490257	0,001286	0,611452	4,895574	0,144763
47	3,36453E-06	0,000782419	381,0809236	0,489874	0,001285	0,610974	4,895957	0,145147
48	3,3619E-06	0,000781807	381,0809236	0,489491	0,001284	0,610496	4,89634	0,14553

49	3,35927E-06	0,000781196	381,0809236	0,489108	0,001283	0,610106	4,896723	0,145912
50	3,35713E-06	0,00078081	381,0262877	0,488726	0,001283	0,610106	4,896332	0,145522
51	3,35713E-06	0,00078142	380,7287788	0,488345	0,001283	0,610106	4,89251	0,141699
52	3,35713E-06	0,000782031	380,4312698	0,487963	0,001283	0,610106	4,888687	0,137876
53	3,35713E-06	0,000782643	380,1337608	0,487581	0,001283	0,610106	4,884864	0,134054
54	3,35713E-06	0,000783256	379,8362519	0,487199	0,001283	0,610106	4,881041	0,130231
55	3,35713E-06	0,00078387	379,5387429	0,486817	0,001283	0,610106	4,877218	0,126408
56	3,35713E-06	0,000784485	379,2412339	0,486435	0,001283	0,610106	4,873396	0,122585
57	3,35713E-06	0,000785101	378,943725	0,486053	0,001283	0,610106	4,869573	0,118762
58	3,35713E-06	0,000785718	378,646216	0,485671	0,001283	0,610106	4,86575	0,11494
59	3,35713E-06	0,000786335	378,348707	0,485289	0,001283	0,610106	4,861927	0,111117
60	3,35713E-06	0,000786954	378,0511981	0,484907	0,001283	0,610106	4,858104	0,107294
61	3,35713E-06	0,000787574	377,7536891	0,484526	0,001283	0,610106	4,854281	0,103471
62	3,35713E-06	0,000788195	377,4561801	0,484144	0,001283	0,610106	4,850459	0,099648
63	3,35713E-06	0,000788816	377,1586712	0,483762	0,001283	0,610106	4,846636	0,095825
64	3,35713E-06	0,000789439	376,8611622	0,48338	0,001283	0,610106	4,842813	0,092003
65	3,35713E-06	0,000790063	376,5636532	0,482998	0,001283	0,610106	4,83899	0,08818
66	3,35713E-06	0,000790688	376,2661443	0,482616	0,001283	0,610106	4,835167	0,084357
67	3,35713E-06	0,000791313	375,9686353	0,482234	0,001283	0,610106	4,831345	0,080534
68	3,35713E-06	0,00079194	375,6711263	0,481852	0,001283	0,610106	4,827522	0,076711
69	3,35713E-06	0,000792568	375,3736174	0,48147	0,001283	0,610106	4,823699	0,072889
70	3,35713E-06	0,000793196	375,0761084	0,481088	0,001283	0,610106	4,819876	0,069066
71	3,35713E-06	0,000793826	374,7785994	0,480707	0,001283	0,610106	4,816053	0,065243
72	3,35713E-06	0,000794457	374,4810905	0,480325	0,001283	0,610106	4,812231	0,06142
73	3,35713E-06	0,000795088	374,1835815	0,479943	0,001283	0,610106	4,808408	0,057597
74	3,35713E-06	0,000795721	373,8860725	0,479561	0,001283	0,610106	4,804585	0,053775
75	3,35713E-06	0,000796355	373,5885636	0,479179	0,001283	0,610106	4,800762	0,049952
76	3,35713E-06	0,000796989	373,2910546	0,478797	0,001283	0,610106	4,796939	0,046129
77	3,35713E-06	0,000797625	372,9935456	0,478415	0,001283	0,610106	4,793117	0,042306
78	3,35713E-06	0,000798262	372,6960367	0,478033	0,001283	0,610106	4,789294	0,038483
79	3,35713E-06	0,000798899	372,3985277	0,477651	0,001283	0,610106	4,785471	0,034661
80	3,35713E-06	0,000799538	372,1010187	0,477269	0,001283	0,610106	4,781648	0,030838
81	3,35713E-06	0,000800178	371,8035098	0,476888	0,001283	0,610106	4,777825	0,027015
82	3,35713E-06	0,000800819	371,5060008	0,476506	0,001283	0,610106	4,774003	0,023192
83	3,35713E-06	0,000801461	371,2084919	0,476124	0,001283	0,610106	4,77018	0,019369
84	3,35713E-06	0,000802103	370,9109829	0,475742	0,001283	0,610106	4,766357	0,015547
85	3,35713E-06	0,000802747	370,6134739	0,47536	0,001283	0,610106	4,762534	0,011724
86	3,35713E-06	0,000803392	370,315965	0,474978	0,001283	0,610106	4,758711	0,007901
87	3,35713E-06	0,000804038	370,018456	0,474596	0,001283	0,610106	4,754889	0,004078
88	3,35713E-06	0,000804685	369,720947	0,474214	0,001283	0,610106	4,751066	0,000255
89	3,35713E-06	0,000805333	369,4234381	0,473832	0,001283	0,610106	4,747243	-0,00357

Table IV.1 Lifespan calculations for the balloon.